JUSCIMAR DA SILVA

EFFECTIVENESS AND STABILITY OF ALUMINIUM AND IRON OXIDES NANOPARTICLES FOR ARSENATE ADSORPTION

Tese apresentada à Universidade Federal de Viçosa, como parte das exigências do Programa de Pós-Graduação em Solos e Nutrição de Plantas, para obtenção do título de *Doctor Scientiae*.

VIÇOSA
MINAS GERAIS – BRASIL
2008

Ficha catalográfica preparada pela Seção de Catalogação e Classificação da Biblioteca Central da UFV

T
S586e
2008

Silva, Juscimar da, 1977-
Effectiveness and stability of aluminium and iron oxides nanoparticles for arsenate adsorption / Juscimar da Silva. – Viçosa, MG, 2008.
xiii, 80f.: il. ; 29cm.

Orientador: Jaime Wilson Vargas de Mello.
Tese (doutorado) - Universidade Federal de Viçosa.
Referências bibliográficas: f. 76-80.

1. Controle de qualidade da água. 2. Água - Purificação. 3. Água - Teor de arsênio. 4. Água - Óxido de ferro. 5. Água - Óxido de alumínio. 6. Arsênio - Adsorção. I. Universidade Federal de Viçosa. II. Título.

CDD 22.ed. 628.162

JUSCIMAR DA SILVA

EFFECTIVENESS AND STABILITY OF ALUMINIUM AND IRON OXIDES NANOPARTICLES FOR ARSENATE ADSORPTION

Tese apresentada à Universidade Federal de Viçosa, como parte das exigências do Programa de Pós-Graduação em Solos e Nutrição de Plantas, para obtenção do título de *Doctor Scientiae*.

APROVADA: 16 de junho de 2008.

D.Sc. Cláudia Lima Caldeira

Prof. Carlos Ernesto G. R. Schaefer

Prof. Massimo Gasparon

Prof. Maurício Paulo Ferreira Fontes

Prof. Jaime Wilson Vargas de Mello
(Orientador)

Aos meus pais, Amado e Maria, e à minha avó, Fabiana, pela educação e pelo amor.

À Ângela minha esposa, pelos momentos de companheirismo e pela convivência.

Ao Guilherme (in memoriam) e ao nosso filho(a), que ainda está para nascer, mas já é a motivação maior para continuar trabalhando.

Aos meus irmãos, Rita, Itamar e Gislene, pelo carinho e pela compreensão.

Aos meus sobrinhos, Gustavo, Isadora, Letícia, Bruno, Franciele e Gabriel.

À toda minha família e aos meus amigos.

"Never regard study as a duty, but as an enviable opportunity to learn to know the liberating influence of beauty in the realm of the spirit for your own joy and the profit of the community to which your later work belongs."

Albert Einstein

AGRADECIMENTOS

A Deus, pela vida e pela paz, nos momentos de dificuldade, pela calma na hora de decidir o que é certo ou errado e pela sabedoria, nas tomadas de decisões.

A minha esposa Ângela, pela constante companhia, carinho e incondicional dedicação.

À Universidade Federal de Viçosa, especialmente ao Departamento de Solos, pela oportunidade de realização do curso.

Ao CNPq, pela concessão da bolsas de Doutorado e Doutorado "Sandwich". À FAPEMIG pelo financiamento da pesquisa.

Aos professores Jaime Wilson Vargas de Mello e Walter Antônio Pereira Abrahão, pela amizade, experiência e ensinamentos compartilhados, pela colaboração e pelos incentivos em diversas etapas, desde a iniciação científica até o curso de Pós-Graduação.

Aos professores Massimo Gasparon e Paulo Vasconcelos da The University of Queensland, Austrália, pela amizade e experiência compartilhada, bem como pela recepção incondicional e utilização das dependências do Earth Science Department que proporcionaram o bom desenvolvimento de grande parte deste trabalho.

À professora Virgínia Ciminelli e suas colaboradoras Cláudia Lima Caldeira, Maria Sylvia Silva Dantas (Sica) e demais funcionários e alunos do Departamento de Engenharia Metalúrgica e Materiais da Universidade Federal de Minas Gerais, pelo auxílio, pela orientação e pelas trocas de experiência durante as análises de Espectroscopia Raman.

Aos membros da banca examinadora, D.Sc. Cláudia Lima Caldeira, Prof. Carlos Ernesto G. R. Schaefer, Prof. Massimo Gasparon, e Prof. Maurício Paulo Ferreira Fontes que contribuíram para o melhoramento deste trabalho.

Ao professor Victor Hugo Alvarez Venegas, pelo apoio, pelos ensinamentos e pelo exemplo de pessoa e profissionalismo.

Aos demais professores, colegas de curso e a todos os funcionários do Departamento de Solos, pela convivência, pelas críticas, pela colaboração e amizade.

A todos os amigos, de longa e de recente data, em especial ao Geraldo Robésio, Ítalo, Augusto, Mattiello, Maurão, Nilton, Cristiane Assis, Diego, Elton Valente, Pacheco, dentre tantos outros, pelo convívio e pela amizade.

Aos grandes amigos de Brisbane, Autrália, que fizeram mais fácil a adaptação e vida no exterior: Marinho (verdadeiro irmão que tomou conta de mim e minha esposa), Arne, Auk, Guia, Maurizio, Jia Jia, Ben, Felipe, Maria D'aguia, Fiona, Tony Jong, Frank, Peter, Emma, Ai e Eric.

A todos que, de alguma forma, contribuíram para realização deste trabalho.

BIOGRAFIA

JUSCIMAR DA SILVA, filho de Amado Francisco da Silva e Maria da Conceição Silva, nasceu em 4 de agosto de 1977, em Viçosa, Minas Gerias, Brasil.

Em maio de 2002, graduou-se em Agronomia, pela Universidade Federal de Viçosa e, em abril do mesmo ano, iniciou, nesta mesma instituição, o Programa de Pós-Graduação, em nível de Mestrado, em Solos e Nutrição de Plantas.

Em março de 2004, iniciou o Programa de Pós-Graduação, em nível de Doutorado, em Solos e Nutrição de Plantas, na Universidade Federal de Viçosa. De agosto de 2006 a agosto de 2007, participou do Programa Doutorado "Sandwich" do CNPq, onde efetuou trabalhos da presente Tese no Earth Science Department da The University of Queensland, Australia.

Em junho de 2008, concluiu o curso de Doutorado.

CONTENT

TABLE LIST

FIGURE LIST

CHAPTER 2

CHAPTER 3

RESUMO

SILVA, Juscimar, D.Sc., Universidade Federal de Viçosa, Junho de 2008. **Eficiência e estabilidade de nanopartículas de óxidos de alumínio e de ferro para adsorver arsênio**. Orientador: Jaime Wilson Vargas de Mello. Co-orientadores: Walter Antônio Pereira Abrahão e Virgínia Sampaio Teixeira Ciminelli.

A geoquímica do arsênio e do ferro estão intimamente correlacionadas, de modo que os métodos de remoção de As da água são baseados na alta afinidade deste metalóide por nanominerias de oxihidróxidos de ferro. No entanto, em ambientes anóxicos as bactérias redutoras de ferro desempenham papel crucial na catálise de transformações redox que, em última análise, controlam a mobilidade do As em ambientes aquáticos. Nanominerias de Al são comuns em solos e sedimentos e também apresentam grande afinidade por As. Além disso, sob condições redutoras, o Al é estável e sua presença na estrutura dos oxihidróxidos de Fe aumenta a establidade destes oxidos, conforme bem documentado na literatura. Desta maneira, a associação da alta afinidade dos oxihidróxidos de Fe por As com a estabilidade do Al sob condições anóxicas pode ser uma alternativa vantajosa para a remoção de As da água. Neste estudo, a espectroscopia Raman foi utilizada para investigar a influência do alumínio estrutural nos modos vibracionais de goethitas e das fases formadas entre arsenato e os diferentes oxihidróxidos de Al e Fe, bem como o potencial destes nanominerais para adsorção de As. A estabilidade do As retido por oxihidróxidos de Al e Fe sob condições anóxicas, na presença da bacteria *Shevanella putrefaciens* e anions competidores, fosfato ou carbonato, também foi investigada. Hidróxido de Al de baixa cristalinidade [$Al(OH)_3$], gibisita (Gb), ferrihidrita 2 linhas (Fh), hematita (Hm), goethita (Gt) e três goethitas com substituição por alumínio (AlGt), contendo 13, 20 e 23 cml mol^{-1} de Al, foram sintetizados e caracterizados química e fisicamente. Estes adsorventes sem e com

arsenato foram caracterizados por difração de raios-X, reflectância difusa e espectroscopia Raman. A cinética de adsorção em duas diferentes relações solido:solução, 2,0 e 5,0 g L^{-1}, e as isotermas de adsorção foram obtidas após equilibrar as amostras com soluções de arsenato sob agitação constante. A adsorção máxima de As(V) foi medida em diferentes valores de pH, variando de 3 até 9. Os adsorventes foram incubados anaerobicamente, sob atmosfera de N_2, e os sobrenadantes foram periodicamente amostrados para avaliar as concentrações de As solúvel. A presença de alumínio estrutural aumentou a área superficial específica e a capacidade de adsorção de As da goethita. Os efeitos gerais da presença do Al estrutural foram diminuir a cristalinidade e deslocar as linhas espectrais da goethita. Tal desordem estrutural foi claramente identificada por espectroscopia Raman e difração de raios-X. As alterações nas frequências vibracionais e largura de bandas devido ao Al estrutural resultou em perdas e sobreposição de muitas bandas ativas da goethita. Esses efeitos aumentaram com o grau de substituição. A técnica Raman também confirmou a ocorrência de magnetita na amostra de goethita com menor grau de substituição, conforme identificado por difração de raios-X. Bandas vibracionais da ligações As-O foram observadas em todos os espectros Raman, exceto para goethita não substituída, provavelmente devido ao seu menor carregamento de As. As posições das bandas vibracionais As-O sugerem que o As(V) foi fortemente retido na superfície dos minerais como complexos de esfera interna. A despeito do rápido equilíbrio, a aumento na concentração de sólido, limitou a eficiência e a velocidade da adsorção de As. A adsorção máxima de As(V) diminuiu na seguinte ordem: $Al(OH)_3$ > Fh > $AlGt_{13}$ > $AlGt_{20}$ > $AlGt_{23}$ > Gb > Hm > Gt. No entanto, calculando as capacidades de adsorção por área superficial, Gb, Gt e Hm mostraram valores mais altos. Isto sugere que os sítios reativos não foram completamente ocupados por arsenato em goethitas com substituição por Al e oxihidróxidos mal cristalisados. Não foi observada relação entre tamanho médio das partículas e adsorção máxima. Isto sugere reagregação das partículas durante a análise ou imperfeições na superfície das partículas com aumento de sua carga líquida, resultando em alta densidade de adsorção. O comportamento de todas as amostram foi fortemente depente do pH e a adsorção máxima foi obtida em condições levemente ácidas. De modo geral os hidróxidos de Al foram mais eficientes do que os de oxihidróxidos de Fe para remover As(V) da água. A presença de alumínio estrutural aumentou consideravelmente a eficiência das goehitas, as quais se mostraram promissoras como adsorventes para remoção de arsênio de águas contaminadas. Verificou-se que as células de *S. putrefaciens*

foram capazes de se ligar nas superficies minerais e utilizar os oxihidróxidos de Fe, tanto cristalinos quanto mal cristalisados, como aceptores finais de elétrons, mobilizando arsenio em solução. Goethitas substituidas por Al apresentaram decrescimo na fração de ferro solúvel e As mobilizado com o aumento do Al estrutural. A relação entre área surperficial específica e dissolução redutiva de Fe e As também foi afetada pelo aumento do Al estrutural, conforme esperado. O fosfato e o carbonato afetaram a cinética de redução do Fe devido à precipitação do ferro em solução como fases minerais metaestáveis (por exemplo vivianita e siderita). Parece que fases minerais análogas de fosfatos serviram como sumidouro para o arsênio, limitando sua mobilização. Fosfato competiu fortemente com o arsenato e sua eficiência parece ter sido governada pela natureza da ligação entre o As e a surperfície adsorvente. Uma maior fração de As foi dessorvido por fosfato na gibbsita, seguida pelas goethitas substituidas por Al. Por outro lado, apenas a gibbsita mostrou quantidades significativas de arsenato deslocado por carbonato. Não obstante a baixa cristalinidade, o $Al(OH)_3$ foi mais eficiente para reter arsenato na sua superfície seguido por ferrihidrita e hematita.

ABSTRACT

SILVA, Juscimar, D.Sc., Universidade Federal de Viçosa, June 2008. **Effectiveness and stability of aluminium and iron oxides nanoparticles for arsenate adsorption**. Adviser: Jaime Wilson Vargas de Mello. Co-advisers: Walter Antônio Pereira Abrahão and Virgínia Sampaio Teixeira Ciminelli.

The geochemical fates of arsenic and iron are closely correlated that methods of arsenic removal from water are based on the high affinity of this metalloid with Fe (hydr)oxides nanominerals. Nevertheless, in anoxic environment dissimilatory iron reducing bacteria play a fundamental role in catalysing the redox transformations that ultimately control the mobility of As in aquatic environment. Aluminium nanominerals are ubiquitous and also have great affinity for arsenic. Additionally, under reducing conditions, Al is rather stable and its presence in the Fe (hydr)oxides framework enhance their stability, as well reported in the literature. Thus, by associating the higher binding affinity of Fe (hydr)oxides for arsenic and the higher stability of Al under anoxic conditions can be an advantageous alternative for removing arsenic from water. In this study, we investigated the influence of structural Al in the Raman vibrational stretching modes of goethite and arsenate phases formed on its surface and on other Al and Fe (hydr)oxides, as well as their potential in adsorbing arsenic. The stability of arsenic retained by aluminium and iron (hydr)oxides under anoxic conditions in the presence of *S. putrefaciens* cells, and phosphate or carbonate competing anions was also investigated. Poorly crystalline aluminium hydroxide [$Al(OH)_3$], gibbsite (Gb), 2-line ferrihydrite (Fh), hematite (Hm), goethite (Gt), and three Al-substituted goethites (AlGt) containing 13, 20, and 23 cmol mol^{-1} of Al were synthesised and characterised chemically and physically. These adsorbents without and with arsenate were investigated by X-ray diffraction, diffuse reflectance, and Raman spectroscopy. Adsorption kinetics at two

different solid:solution ratios, 2.0 and 5.0 g L^{-1}, and adsorption isotherms were obtained after equilibrating the samples with arsenate solution under constant shaking. As(V) adsorption maxima was measured at different pH ranging from 3 to 9. The adsorbents were anaerobically incubated under N_2 atmosphere and supernatants were periodically sampled to evaluate the contents of soluble As. Presence of structural Al increased the specific surface area and the As adsorption capacity of the Gt. The general effects of the structural Al were to reduce Gt crystallinity and displace spectral lines. Such structural disorder was clearly identified by Raman spectroscopy and X-Ray diffraction. Changes in vibrational frequencies and linewidths due to structural Al resulted in loss and overlap of many Gt active bands. These effects increased as the degree of substitution increased. Raman technique also confirmed the co-occurrence of magnetite in $AlGt_{13}$ sample, as indicated by XRD. As-O vibrational bands were visualised on all Raman spectra, except for pure Gt probably due to its lowest content of adsorbed As(V). Positions of As-O vibrational band suggested that As(V) was strongly retained on the minerals as inner-sphere surface complexes. In spite of the fast equilibrium, the increase in solid concentration limited the efficiency and velocity of arsenic adsorption. The As(V) adsorption maxima decreased in the following order: $Al(OH)_3$ > Fh > $AlGt_{13}$ > $AlGt_{20}$ > $AlGt_{23}$ > Gb > Hm > Gt. Nevertheless, by calculating adsorption capacities in terms of surface area, Gb, Gt, and Hm showed higher As(V) loading capacity. This suggest that available reactive sites were not fully occupied by arsenate on the amorphous and Al-substituted (hydr)oxides. No relationship was observed between medium particle size and maxima adsorption. This suggests re-aggregation of the particles during the particle size measurement, or imperfections on the surface of the particles increasing their net charge, resulting in high adsorption density. The behaviour of all samples was strongly dependent on pH, and the maximum adsorption was achieved in slightly acidic conditions. In general, Al hydroxides were more efficient than Fe (hydr)oxides to remove As(V) from water. The presence of structural Al enhanced considerably the efficiency of the goethites which showed to be promising as adsorbents to remove arsenic from contaminated water. We found that *S. putrefaciens* cells were able to bind on mineral surfaces and utilise both noncrystalline and crystalline iron (hydr)oxides as electron acceptor releasing arsenic into solution. Al-substituted goethites presented a decrease in the fraction of soluble iron and mobilised arsenic as structural Al increased. The expected relationship between specific surface area and reductive dissolution of Fe and As was also affected by the increment in structural Al. Phosphate and carbonate

affected the kinetics of iron reduction due to precipitation of soluble iron as metastable mineral phases (e.g. vivianite and siderite). It seems that analogous mineral phases of phosphates served as a sink for As limiting its mobilisation. Phosphate competed strongly with arsenate and its efficiency seemed to be governed by the nature of the binding mechanism between As and adsorbent surface. Higher fraction of arsenic was desorbed by phosphate from gibbsite followed by AlGts. Conversely, only Gb showed significant amounts of arsenate displaced by carbonate. In spite of low crystallinity, $Al(OH)_3$ was the most efficient in retaining arsenate on its surface followed by Fh and Hm.

INTRODUCTION

Arsenic is a waterborne contaminant and its occurrence in groundwater is a public health concern. The long term exposure to arsenic can lead to critical problems, mainly cancers. Following the recommendation of the World Health Organization (WHO) many countries worldwide, including Brazil, have adopted the threshold of 10 μg L^{-1} of As in drinking water, as safer for consumption.

Among the heavy metalloids and oxianions-forming elements (e.g. As, Se, Sb, Mo, V, Cr, U, Re), arsenic is perhaps unique to mobilise at the pH values typically found in groundwaters (pH 6.5 – 8.5) and under both oxidising and reducing conditions. The geodistribution of As depends on parental rock, and its global average in soil is about 5 mg kg^{-1}. Mudstones, shales and slates have the highest concentrations among the common rocks, although extremely high concentrations can be found in some coals. As the chemistry of arsenic follows closely that of S, the greatest concentration of the element tend to occur in sulphide minerals, of which arsenopyrite (FeAsS) is the most abundant mineral followed by orpiment (As_2S_3) and realgar (AsS) (Matschullat, 2000; Smedley and Kinniburg, 2002; O'Day, 2006). Then, the natural input of arsenic in the environment is closely related to weathering of As-bearing rocks and minerals. Anthropogenic source, i.e. mining and smelting activity and pesticides and wood preservative uses, has also contributed to such addition.

In the environment arsenic can be found as inorganic and organic compounds, in several valence states, i.e. -3, -1, 0, +3, and +5. In natural water arsenic occurs mainly in inorganic forms as trivalent arsenite [As(III)] (as H_3AsO_3) or pentavalent arsenate [As(V)] (as $H_2AsO_4^-$ and $HAsO_4^{2-}$). In addition, in marine waters and lakes arsenic can undergo microbial methylation and both As(III) and As(V) can coexist with monomethilarsonic acid (MMA) and dimethilarsinic acid (DMA). According to Matschullat (2000), the methylated species account for up to ~10% of the total As in the

euphotic zone of many oceanic regions. Furthermore, redox potential (Eh) and pH control the toxicity, mobility, and bioavailability of arsenic as well as the distribution of its species. Therefore, arsenite is expected to be the stable aqueous form under moderately reducing conditions, roughly from Eh of about +300 mV at pH 4 to -200 mV at pH 9, whilst arsenate is the dominant species in oxidising aqueous solutions (O'Day, 2006). Because of relatively slow transformation on the redox conditions, both species, As(III) or As(V), can be often found in either redox environment.

Nanominerals of aluminium and iron (hydr)oxides are ubiquitous and play a crucial role on geochemical and biogeochemical reactions and kinetics of arsenic in the environment. Sorption reactions on the surface of these nanoparticles have been extensively investigated in order to elucidate the mechanisms associated with arsenic mobility and bioavailability, as an attempt to improve the methods of water treatment which are still based on coagulation/precipitation processes. Problems with regard to addition of undesirable anions, such as sulphate, nitrate, and chloride into the water are the major limitation of this method as well as the safe separation, handling, and disposal of the contaminated sludge (Driehaus et al., 1998; Banerjee et al., 2008). Several adsorbent materials have been assessed, i.e. aluminium hydroxide (Anderson et al., 1976; Ladeira et al., 2001), activated alumina (Mortazavi et al., 1999), natural (hydr)oxides (Deschamps et al., 2003, 2005; Vithanage et al., 2007), clay minerals (Manning and Goldberg, 1996a, 1997; Garcia-Sanchez et al., 2002), granular ferric hydroxides (Driehaus et al., 1998; Wilkie and Hering, 1996), ferrihydrite (Waychunas et al., 1993; Jain et al., 1999; Jia and Demopoulos, 2005; Jia et al., 2006), goethite (Grossl et al., 1997; Hongshao and Stanford, 2001; Gimenez et al., 2007), and others.

Even though Al and Fe (hydr)oxides have great affinity for arsenic, attention concerning the stability of these nanoparticle should be taken into account. As well known, the solubility of aluminium hydroxides are much higher than of ferric ones. For instance, stability diagrams developed by Lindsay (1979), show that at the same pH activity of Al^{3+} is roughly $10^{6.12}$ times higher than the activity of Fe^{3+}, both controlled by their poorly crystalline hydroxide phases, under oxidising conditions. Then, soluble arsenic in equilibrium with Al nanominerals can be a matter of greater concern. On the other hand, changes in redox status affect considerably the stability of the Fe (hydr)oxides nanoparticles.

Dissimilatory iron reduction is an important geomicrobial process in soils, sediments, and aquifers, where it depends primarily on Fe(III) (hydr)oxide minerals as

terminal electron acceptors (Bonneville et al., 2006). In addition to being an important oxidation pathway of organic matter and generating soluble ferrous iron, microbial iron reduction can have a major impact on the persistence and mobility of arsenic, toxic metals, radionuclides, and organic contaminants under anoxic conditions (Lovley et al., 1993; Cummings et al., 1999; Zachara et al., 2001; Behrends and Van Cappellen, 2005). Many authors have reported arsenic release as a result of dissimilatory reduction of Fe(III) to Fe(II) (Cummings et al., 1999; Zobrist et al., 2000; Islam et al., 2004; Burnol et al., 2007). Microbially mediated reduction of assemblages comprising arsenic sorbed to ferric (hydr)oxides is gaining consensus as the dominant mechanism for the mobilization of arsenic into the West Bengal and Bangladesh aquifers (Smedley and Kinniburg 2002; Islam et al., 2004; O'Day 2006).

Several of the iron (hydr)oxide nanoparticles have isostructural equivalents in which cations other than Fe occupy the interstices of the oxygen framework. Therefore, the existence of these isostructural compounds suggests that solid solutions could be formed between end members via isomorphous substitution for Fe(III) by other cations (Cornell and Schwertmann, 2003). Al is 17% smaller than iron, and, even though it is separated from Fe by forming Al-silicates (clay minerals), a significant proportion is always also incorporated into Fe(III) (hydr)oxides. Goethite is one of the thermodynamically most stable iron oxides (Cornell and Schwertmann, 2003) in soil and sediments and the full range of substitution in natural sample of up to 33 cmol mol^{-1} is found.

Aluminium is stable under anoxic conditions, since it does not participates of the electron transferring reactions. For this reason, the presence of structural Al enhance the stability of the iron (hydr)oxides, as already reported. Slower rate of reductive dissolution (chemical or microbiological) in the presence of Al substituting Fe in the iron (hydr)oxides structure was reported by Schwertmann (1984), Jeanroy et al. (1991), and reference therein. Torrent et al. (1987) observed that Al substitution depressed the reductive dissolution of synthetic goethite and hematite by dithionite/citrate/bicarbonate solution. Bousserrhine et al. (1999) also demonstrated that biological reduction of Al, Cr, Mn, and Co-substituted goethites was decreased as substitution increased. Al-goethite was more resistant to reductive dissolution than other substituted goethites. Thus, by associating the higher binding affinity of Fe (hydr)oxides for arsenic and the higher stability of Al under anoxic conditions can be an advantageous alternative for removing arsenic from water.

Natural attenuation of arsenic by adsorption on (hydr)oxides nanominerals may be also limited due to competing oxyanions, in which one anion will normally be competing for the sorption sites (Hongshao and Stanforth, 2001; Sahai et al., 2007; Zang et al.; 2008). Due to similar acid dissociation constants phosphate (pK_{a1} = 2.1, pK_{a2} = 7.2, pK_{a3} = 12.3) behaves much like arsenate (pK_{a1} = 2.2, pK_{a2} = 6.9, pK_{a3} = 11.4). Therefore, they should have similar effects on the surface of the (hydr)oxides nanoparticles. Hongshao and Stanforth (2001) found that under acidic conditions the quantity of arsenate that is replaced with phosphate from goethite increases with contact time before phosphate is added, but the amount of arsenate that can not be replaced with phosphate is independent of contact time at an initial molar ratio of phosphate to arsenate of 1, and vice versa. Zang et al. (2008) verified that the density of irreplaceable phosphate or arsenic on goethite decreases to a limit with an increase in the initial concentration of the other anion. Liu et al. (2001) reported that more arsenate is replaced by phosphate from goethite as the initial molar ratio of phosphate to arsenate increases. Manning and Goldberg (1996) suggested that there were sites on the surface that were specific for each ion as well as some nonspecific sites on which both ions could adsorb.

In addition to phosphate, carbonate may also, to a lesser extent, limit the arsenate sorption reactions. The displacement of adsorbed As with dissolved carbonate was recently examined theoretically by Appelo et al. (2002), and this mechanism was proposed to be potentially one of the major reasons for high As concentrations in groundwater. In Bangladesh, the mobilization of As by carbonate has been used to explain the occurrence of high levels of As in groundwaters (Anawar et al., 2003).

Thus, it is worthwhile to investigate the adsorption and replacement of one anion from mineral nanoparticles by another. In addition, investigations of the competition between the anions can provide insight into the reactions occurring on the surface.

Spectroscopy investigations show that arsenic is strongly bonded on the surface of the Al and Fe (hydr)oxide nanoparticles due to ligand exchange with hydroxyl groups (OH or OH_2), and the formation of inner-sphere binuclear monodentate-bidentate surface complexes is the principal binding mechanism (Waychunas et al., 1993; Sun and Donner, 1996 and 1998; Manning et al., 1998; Goldberg et al., 2001; Ladeira et al., 2001; Ona-Nguema et al., 2005; Makris et al., 2007). Nevertheless, Catalano et al. (2008) reported outer- and inner-sphere arsenate complexation on the surface of corundum and hematite. In the past few years, Raman spectroscopy has also been

applied to assess arsenic coordination in a variety of geologic and synthetic material with environmental remediation purpose (Myneni et al., 1998; Frost and Kloprogge, 2003; Frost et al., 2003; Frost et al., 2006). Raman spectroscopy is a scattering technique that provides information on vibrational modes of molecules. When photons of visible light are scattered with the emission or absorption of phonons, the energy (or frequency) shifts are very small, but they can be measured. The process is referred to as Raman Scattering when the phonon emitted or absorbed is optical. Otherwise, they are acoustical and the process is referred to a Brilhonin scattering. The resulting differences between scattered and incident energy correspond to specific energy-level differences for the substance under study and such yield insights into its molecular structure. It can distinguish, unambiguously, between minerals with the same stoichiometry but different crystal structure. Unlike FTIR, the Raman spectroscopy in aqueous system is straightforward because water is a weak Raman scatter. In addition, this technique is non-destructive, requires minimal sample preparation, and can be used on massive specimens from lump or to fine powder and liquid (Hope et al., 2001).

Vibrational spectroscopy studies have shown that the symmetry of the AsO_4^{3-} tetrahedron is strongly distorted by the protonation, cation presence, and water coordination (Myneni et al., 1998a and 1998b). The vibrational spectra of Ca, Mn, Fe, Co, Ni, Cu, and Zn AsO_4^{3-} complexes in crystalline hydrated solids indicate that the As-O_{Metal} symmetric stretching vibrations shifted to different energies when compared to the aqueous AsO_4^{3-}. For example, the transition metal arsenates, such as those of Mn, Fe, Co, Ni, Cu, and Zn exhibit a red shift for symmetric stretching vibrations, whilst the vibrational Al-arsenate spectra shifted to a lower wavenumber, as predicted by theoretical studies (Myneni et al. 1998). Among all tetrahedral oxyanions, the position of the arsenate vibrations occurs at lower wavenumbers than the other naturally occurring mineral oxyanions (Frost et al., 2006).

Accordingly, this work aimed to investigate experimentally the effectiveness of synthetic poorly crystalline aluminium hydroxide, gibbsite, ferrihydrite, hematite, goethite, and Al-substituted goethites for adsorbing arsenic from contaminated water and evaluate the stability of the sorption products face to dissimilatory iron reduction and competing anions. The results presented herein are divided in three chapters: in the chapter 1, we investigated the Raman stretching spectra of these synthetic nanominerals without and with loaded As(V) and identified the arsenate phases associated with by adsorption process; the chapter 2 presents the results of arsenate adsorption process onto

the surface of the samples assessed by kinetics, isotherm and envelope of adsorption. Finally, in the chapter 3, we report the effect of bacterial iron reduction and competing anion, phosphate and carbonate, on arsenic mobilisation.

Chapter 1

RAMAN SPECTROSCOPY OF As(V) LOADED Al AND Fe (HYDR)OXIDES

ABSTRACT

Raman spectroscopy has been widely used to characterise Al and Fe (hydr)oxides features. Nowadays, that technique has also been applied to the study of contaminants in soils, sediments, and waters. Most of investigations involve identification of arsenate phase in connection with Al and Fe (hydr)oxides since they are ubiquitous and play a key role in controlling As mobility and bioavailability. However, these investigations have been carried out on pure minerals, and little is known about the vibrational stretching modes of the Fe (hydr)oxides containing structural Al. Thus, the objective of this work was to investigate the influence of structural Al in the vibrational stretching modes of goethite as well as identify the arsenate phase formed on its surface and on other Al and Fe (hydr)oxides. Hematite (Hm), goethite (Gt), 2-line ferrihydrite (Fh), gibbsite (Gb), poorly crystalline aluminium hydroxide [$Al(OH)_3$], and Al-substituted goethites (AlGts) were synthesised, and characterised chemically and physically. These adsorbents without and with adsorbed arsenate were investigated by means of X-Ray diffraction, diffuse reflectance, and Raman spectroscopy. Presence of structural Al increased the specific surface area of the Gt, and its As adsorption capacity. The general effects of the structural Al were to reduce Gt crystallinity and displace spectral lines. Such structural disorder was clearly identified by Raman spectroscopy and X-Ray diffraction. Changes in vibrational frequencies and linewidths due to structural Al resulted in loss and overlap of many Gt active bands. These effects increased as the degree of substitution increased. Raman technique also confirmed the co-occurrence of magnetite in $AlGt_{13}$ sample, as indicated by XRD. As(V) loading adsorbents caused changes or no additional phases in the XRD and diffuse reflectance patterns. On the other hand, As-O vibrational bands were visualised on all Raman spectra, except for pure Gt probably due to its lowest content of adsorbed As(V). Positions of As-O vibrational band suggested that As(V) was strongly retained on the minerals as inner-sphere surface complexes, except for Gb and Hm where a lesser stable complex seems to predominate due to evidence of surface precipitation. After thermal treatment, magnetite transformed completely into Hm which presented a red shift on the spectral line evidencing the presence of Al in the magnetite lattice.

Keywords: Raman spectroscopy, arsenic, Al-substituted goethite, iron and aluminium (hydr)oxides, contamination.

1. INTRODUCTION

The groundwater and surface water contamination by arsenic around the world is a very sensitive issue which has concerned the scientific community. The most serious problems related to arsenic contamination have been reported in Bengal Basin (West Bengal and Bangladesh, mainly) where more than 40 million people have been drinking water with excessive arsenic (Smedley and Kinniburg, 2002). In Brazil, some areas of the Iron Quadrangle mineral province in Minas Gerais State revealed a naturally high As background due to arsenopyrite mineralization in either disseminated veins or fractures, with average As concentrations above 100 mg kg^{-1} in soils and 100 μg L^{-1} in local water (Mello et al., 2006; Deschamps et al., 2005; Matschullat et al., 2000). On the basis of chronic toxicological effect of As, currently WHO recommends the threshold of 10 μg L^{-1} in drinking water.

Arsenic in the environment can exist either as organic or as inorganic forms, and its toxicity depends primarily on its valence states (-3, 0, -1, +3, or +5). Redox potential (Eh) and pH control As speciation, and then its toxicity, mobility, and bioavailability in terrestrial environment. In addition, arsenic can be methylated and both As(III) and As(V) can coexist with monomethylarsonic acid (MMA), and dimethylarsinic acid (DMA). Because of relatively slow transformation on the environmental redox conditions, both species, As(III) or As(V), can be often found in either redox environment.

The most common technique for removing arsenic from water is coagulation with ferric salts, followed by filtration (Driehaus et al., 1998). However, due to the difficulties to handle the waste generated by coagulation technique, the attempt to seek for more efficient methods have propelled the investigation of different adsorptive materials. Adsorptive process have been assessed and materials such as activated alumina, poorly crystalline ferric hydroxides and granular ferric hydroxides, have been shown to be more promising due to their high affinity for arsenate (USEPA 2000, and references therein).

The main surface complexes formed between arsenic and Al and Fe (hydr)oxides are inner-sphere mono and, or, binuclear, involving ligand exchanges with surface OH and OH_2 groups. These linking mechanisms have been confirmed by different techniques, i.e. EXAFS (Waychunas et al., 1993; Manning et al., 1998; Ladeira et al., 2001; Ona-Nguema et al., 2005; Makris et al., 2007), ATR-FTIR (Sun and Donner, 1996 and 1998), nuclear magnetic resonance (NMR) (Goldberg et al., 2001).

Raman spectroscopy has also been a useful tool to identify arsenic compounds with environmental remediation purpose (Frost and Kloprogge, 2003; Frost et al., 2003; Frost et al., 2006), since its mobility and availability is mostly controlled by Al and Fe (hydr)oxides. Raman spectroscopy is a scattering technique that provides information on vibrational modes of molecules. When photons of visible light are scattered with the emission or absorption of phonons, the energy (or frequency) shifts are very small, but they can be measured. The process is referred to as Raman Scattering when the phonon emitted or absorbed is optical. Otherwise, they are acoustical and the process is referred to a Brilhouin scattering. The resulting differences between scattered and incident energy correspond to specific energy-level differences for the substance under study and such yield insights into its molecular structure. It can distinguish, unambiguously, between minerals with the same stoichiometry but different crystal structure. Unlike FTIR, the Raman spectroscopy in aqueous system is straightforward because water is a weak Raman scatter. In addition, this technique is non-destructive, requires minimal sample preparation, and can be used on massive specimens from lump or to fine powder and liquid (Hope et al., 2001).

Vibrational spectroscopy studies have shown that the symmetry of the AsO_4^{3-} tetrahedron is strongly distorted by the protonation, cation presence, and water coordination (Myneni et al., 1998a and 1998b). The vibrational spectra of Ca, Mn, Fe, Co, Ni, Cu, and Zn AsO_4^{3-} complexes in crystalline hydrated solids indicate that the As-O_{Metal} symmetric stretching vibrations shifted to different energies when compared to the aqueous AsO_4^{3-}. For example, the transition metal arsenates, such as those of Mn, Fe, Co, Ni, Cu, and Zn exhibit a red shift for symmetric stretching vibrations, whilst the vibrational Al-arsenate spectra shifted to a lower wavenumber, as predicted by theoretical studies (Myneni et al. 1998b). Among all tetrahedral oxyanions, the position of the arsenate vibrations occurs at lower wavenumbers than the other naturally occurring mineral oxyanions (Frost et al., 2006).

Although several spectroscopy investigations have confirmed the strong attachment of arsenic onto Al or Fe (hydr)oxide surfaces, no spectroscopic studies have been related to As adsorbed onto Al-substituted goethites. Therefore, this work aimed to investigate the Raman stretching spectra of Al-substituted goethites, hematite, goethite, gibbsite, poorly crystalline aluminium hydroxide, 2-line ferrihydrite pure, and loaded with As(V) and identify the arsenate phases associated with by adsorption process.

2. MATERIAL AND METHODS

2.1. Synthesis of Al and Fe (Hydr)oxides

2.1.1. Iron (Hydr)oxides Synthesis. Hematite (Hm), Goethite (Gt), and 2-line Ferrihydrite (Fh) were synthesised by neutralizing $Fe(NO_3)_3$ solution with KOH following the procedure described in Schwertmann and Cornell (2000). A series of Aluminium substituted goethite was also synthesised following the methods therein. Three Al-substituted goethites with different Al:Fe ratio (15:50, 25:50, and 35:50) were prepared from a ferrous solution and aluminium chloride by precipitation with potassium hydroxides and aged in a plastic bottle during 90 days. Slow oxidation of Fe^{2+} to Fe^{3+} and incorporation of Al^{3+} in the goethite structure were achieved by opening the bottle daily and vigorously stirring the suspensions during 5 minutes. In order to remove the excess of Al^{3+}, the precipitates were washed twice with 0.01 mol L^{-1} KOH solution. All (hydr)oxides were washed with Milli-Q water, centrifuged, and dried at 50 ^{o}C at an oven with air circulation, except for Ferrihydrite which was freeze-dried.

2.1.2. Aluminium Hydroxides Synthesis. Gibbsite was prepared following procedures outlined in Kyle et al. (1975). An $Al(NO_3)_3$ solution was titrated with 4 mol L^{-1} NaOH solution to a pH of 4.6 ± 0.2. The gelatinous precipitate was heated for two hours at 40 ^{o}C, then washed twice, dialyzed against Milli-Q water for 36 days, and dried at 50 ^{o}C. Poorly crystalline aluminium hydroxide was prepared from an aluminium nitrate solution by precipitation with 4 mol L^{-1} NaOH solution. The procedure was similar to that followed for the synthesis of gibbsite, but the heating was suppressed step to preserve a low crystallinity. Similarly to ferrihydrite, poorly crystalline aluminium hydroxide was freeze-dried in order to prevent further crystallization.

2.2. Characterisation Analyses. Particle size distribution was obtained by laser particle size analyser (Micromeritics Saturn Digisizer model 5200). Prior to particle measurement, samples were externally dispersed in a sodium metaphosphate medium for 1 h. The content of Al and Fe were determined by wet chemistry methods. Thus, 0.1000 g of dried sample was mixed with 3 mL of HCl and 1 mL of HNO_3 (both double-distilled) into a conical Teflon digestion vessels (10 mL) with screw caps. After 10 min the vessels were closed and placed on a hot-plate. The digestion was carried out

at 120 ^{o}C for about 4h, and after that, the samples were left digesting overnight at 70 ^{o}C constant temperature. After cooling to room temperature, the digested samples were transferred to 25 mL volumetric flask, filled with Milli-Q water. Aliquots were transferred to 10 ml plastic bottles and stored until measurements. Total Al and Fe were determined by inductively coupled plasma optical emission spectroscopy (ICP-OES), using a perking Elmer Optima 3300 DV. The degree of Al^{3+} substitution in the Gt was determined by the Al:Fe molar ratio, i.e. cmol mol^{-1} = $Al^{3+}/(Al^{3+}+Fe^{3+})*100$.

The specific surface area was determined by N2 adsorption (BET method) using multiple point technique (Quantachrome model NOVA 1000). The sample was previously degassed at 110 ^{o}C for 2 h with vacuum a continual stream of N_2 prior to the surface area determination.

2.3. As(V) Loaded (Hydr)oxides. Al and Fe (hydr)oxides were loaded with arsenate by supplying As(V) to one gram of each sample in 10 mmol L^{-1} $CaCl_2$ solutions at pH 5.0 ±0.2. Suspensions were left reacting in a horizontal shaker for one week, and after that, the tubes were centrifuged (3000 rpm, 30 min.), the supernatants were filtered through 0.22 μm membrane filters (Millipore Millex-GV, USA) and stored for further As analyses. The As-rich (hydr)oxides were freeze-dried and stored for further spectroscopic studies. Amounts of adsorbed As(V) were calculated by the difference between the initial and final As concentration in solution. Arsenic adsorbed by the reaction vessels were measured in blanks containing arsenic solution but no adsorbent materials. Contents of As in solution were measured by inductively coupled plasma optical emission spectroscopy (ICP-OES), using a Perkin Elmer Optima 3300 DV. Scandium was used as internal standard to correct for instrumental instabilities and matrix effect. Solution of this element was added to the solution to reach a final concentration of 44.5 μmol L^{-1}. Typical detection limits (3σ) of 0.42 μmol L^{-1} of As were obtained. All assays were carried out in triplicates.

2.4. X-ray diffraction (XRD) and diffuse reflectance (DR). These techniques were used to characterise the synthesised adsorbents and to investigate the influence of structural Al in the Gt properties. Self-supporting mounts were prepared by adding powdered samples (<53 μm) into rectangular holes of glass slides and Al sample holders for further analyses on XRD diffractometer and diffuse reflectance

spectrometer, respectively. XRD was performed using a cobalt Kα radiation at 40 kV and 30 mA in a Rigaku diffractometer with graphite monochromator. Acquisition time for the XRD patterns in the 4-80^{o} 2θ interval was set at 10 sec per 0.05^{o} 2θ step. For DR, samples were gently pressed against aluminium paper to minimise preferred orientation. Holders were placed into the sphere, and the spectra were recorded from 300 to 900 nm in 0.5 nm steps at 52 nm min^{-1} using a double cluster GBC, model CINTRA 20, equipped with an $MgSO_4$-coated integrating sphere 10 cm in diameter. The diffuse reflectance spectra of each adsorbent were treated mathematically in order to eliminate imperfections and noises. From this process, the data were smoothed following the method stated by Barrón et al. (2000). The graphics of the second derivative of the Kubelka-Munk function [f(KM) = $(1 - R)^2/2R$, where R is the reflectance in percentage] were obtained from the percentage of the spectra of the smoothed reflectance.

2.5. Raman Spectroscopy. Analyses were performed on dried samples in a Jobin Yvon/Horiba model LabRam HR 800. The detector was 1024 x 256 pixel liquid nitrogen cooler charge coupled device (CCD). A He-Ne laser 632.8 nm wavelength and power output of 20 mW measured at the laser head was used as the excitation force. In order to avoid sample degradation, the laser power was always kept below 0.08 mW on the sample, except for Gb and $Al(OH)_3$. Samples were targeted by the laser beam through microscope objective (Olympus 100X, 0.9 NA), and the scattered light was collected through the same objective in a back scattering configuration. The entrance slits to the spectrograph were 100 micrometers with a correspondent resolution of 2.0 cm^{-1}. Holographic grating was of 600 g mm^{-1}. Frequency calibration was achieved using the 520 cm^{-1} line silicon. The sample was pressed on a glass slide on the microscope stage. Acquisition time was at 30 s per scan (≅ 10). Collected Raman spectra were analysed and optimised with Origin 7.0 software, and the collected spectra were normalised and background corrected.

As magnetite was shown to co-precipitate with the smallest degree of Al substitution, laser-induced thermal effect was also investigated in order to observe the crystal stability and feasible phase transformation. Firstly, a darker crystal (magnetite) was selected, and a spectrum was obtained at 0.08 mW. Secondly, the filter was removed and so the crystal was directly irradiated by the laser beam at 8 mW per three

seconds. After that, the power of the laser beam was decreased to the initial value (0.08 mW), and a second run was carried out upon the modified sample.

3. RESULTS AND DISCUSSION

3.1. Characterisation Analyses. Assuming the theoretical formula for each mineral, the recovering percentage by wet digestion was higher than 90%. Trace amounts of Al in Hm, Gt, and Fh, as well as Fe in Gb and poorly crystalline $Al(OH)_3$ were, in general, lower than standard error of the mean, and so attributed to analytical error. The Al-goethites end products presented 0.13, 0.20, and 0.23 cmol mol^{-1} of Al (Table 1). According to these substitution degrees in the Al-goethite structures, they will be henceforth referred to as $AlGt_{13}$, $AlGt_{20}$, and $AlGt_{23}$.

Ferrihydrite exhibited the highest surface area followed by AlGts. Specific surface area of the Al-substituted goethites slightly increased as the aluminium incorporation increased from 13 to 20 cmol mol^{-1}, but decreased with further increase of Al content. No trend between Al content and surface area was observed, as also previously reported by Schulze and Schwertmann (1987), Strauss et al. (1997), and Gonzales et al. (2002). According to Gonzales et al. (2002) the crystal size of goethite became smaller as Al substitution increased, but no clear trend between Al content and surface area was observed.

Particle size distribution obtained for samples passed through < 53 μm sieve decreased in the following order: Fh > Gb > $Al(OH)_3$ > $AlGt_{13}$ > $AlGt_{20}$ > $AlGt_{23}$ > Gt > Hm. Since specific surface area is related to the particle size, the negative correlation between these characteristics was expected. However, no trend was observed between this variable and specific surface area (Table 1). An explanation is occurrence of aggregation processes, affecting the particle size measurement, in spite of ultrasonic dispersion before and during analysis, mainly for ferrihydrite. According to Cornell and Schwertmann (2003) the small and spherical particles of ferrihydrite often pack together to form aggregates. Analytical limitation of the laser particle size analysis could be also argued to explain the lack of correlation. Transformation of diffraction patterns to grain size is based on matrixes, which are calculated for spheres (Konert and Vandenberghe, 1997). In that case, the volume of platy particles (e.g. gibbsite) may be overestimated because such particles are larger than their equivalent spherical diameter (Pye and Blott, 2004). Conversely, the volume of elongated or very angular particles might be underestimated.

Table 1 – Surface area (SA), mean particle size (MPS), content of Al and Fe, recovered (Rc), degree of Al substitution in the goethites, and adsorbed As(V). Data are represented as means ± standard error of the mean (n=3)

ADSORBENT	SA	MPS	Total Al and Fe content		Rc[a/]	Al for Fe substitution[b/]	$As_{adsorb.}$[c/]
			Al	Fe			
	-- $m^2\ g^{-1}$ --	------- μm -------	---------- g kg^{-1} ----------		-- % --	-- cmol mol^{-1}--	--------- μmol g^{-1} -----
Hm (α-Fe_2O_3)	34.8	0.20 ± 0.001[d]	0.03 ± 0.04	656.85 ± 0.93	93.91		159.97 ± 2.68
Fh ($Fe_5HO_8 . 4H_2O$)	260.4	23.47 ± 0.31	0.55 ± 0.54	528.63 ± 3.61	90.93		1,063.45 ± 45.10
Gt (α-FeOOH)	20.6	0.97 ± 0.02	0.74 ± 0.07	575.19 ± 0.02	91.52		77.92 ± 2.33
$AlGt_{13}$	119.4	11.33 ± 3.87	69.06 ± 0.82	456.42 ± 1.45		13	412.44 ± 1.90
$AlGt_{20}$	124.7	3.25 ± 0.47	97.75 ± 1.50	404.62 ± 0.62		20	407.75 ± 0.73
$AlGT_{23}$	113.2	2.55 ± 2.71	113.81 ± 1.12	380.97 ± 1.79		23	386.68 ± 3.02
Gb $Al(OH)_3$	45.7	21.01 ± 0.46	334.06 ± 2.75	0.80 ± 1.02	96.58		215.88 ± 0.60
$Al(OH)_3$ [$Al(OH)_3\ 3H_2O$]	8.3	12.60 ± 1.31	214.08 ± 0.03	0.27 ± 0.39	104.77		1,541.22 ± 5.89

[a/] calculated considering the theoretical formula for each material;
[b/] calculated from the following molecular relation: Al for Fe substitution = (Al / Fe + Al)*100;
[c/] calculated by the difference between the initial and final As(V) concentration in solution.

In addition, the technique does not take into account imperfections on the mineral structure which can significantly contribute to increase the reactive adsorption sites. For instance, ionic substitution of Al for Fe in the goethite lattice has a marked effect on goethite properties, such as variations in crystal size, shape and surface area, and structural OH content (Murad and Schwertmann, 1983; Schwertmann, 1984; Schulze and Schwertmann, 1987; Torrent et al., 1987; Jeanroy et al., 1991) which account for great structural disorder. The amount of adsorbed arsenate calculated herein indicates that all adsorbents were fully loaded, as indicated by maximum capacities measurements (Silva et al., 2008).

3.2. XRD spectra. In general, the XRD patterns revealed well defined sharp peaks, characteristics of well crystallised minerals for Hm, Gt, and Gb (Figure 1). The main peaks corresponds to d(104), d(110), and d(002), as previously reported by Dixon and Weed (1989) and Cornell and Schwertmann (2003). Ferrihydrite spectrum exhibited high degree of structural disorder with two broad peaks at ~38 and ~74 2θ corresponding to d(110) and d(300), typical of 2-line ferrihydrite. Aluminium hydroxide [$Al(OH)_3$] also showed typical spectrum with no diffraction pattern confirming its poor crystallinity. XRD peaks for Al-substituted goethites fairly agree with the pure goethite, but with shifts on the diffraction lines towards higher angles due to the presence of structural aluminium. It is well known that the size at the unit cell decreases when Al replaces Fe in the goethite structure, because the Al^{3+} ion is slightly smaller than the Fe^{+3} ion, i.e. 0.053 vs 0.065 nm respectively (Schulze and Schertmann, 1984). The higher is the degree of Al substitution the greater are the shifts, as observed herein. In addition, a narrow peak at ~42° 2θ (d = 0.2532 nm) was detected on the $AlGt_{13}$ XRD spectrum, which can be ascribed to magnetite. The presence of magnetite as coprecipitated with $AlGt_{13}$ was confirmed by attraction to a magnet. Magnetite formation is feasible at low Al/(Al + Fe) ratio due to the slow oxidation of ferrous ions. As the aluminium concentration is low, the excess of Fe^{3+} can encapsulate part of the soluble Fe^{2+} ions, leading to formation of magnetite rather than goethite. At an Al/O_4 molar ratio close to 0.4, substitution of aluminium for iron tetrahedrically coordinated in the magnetite structure is expected (Cornell and Schwertmann, 2003).

3.3. DR spectra. The second derivative of the Kubleka-Munk function [f(KM)] from the fitted diffusion reflectance spectra showed typical observation bands for hematite,

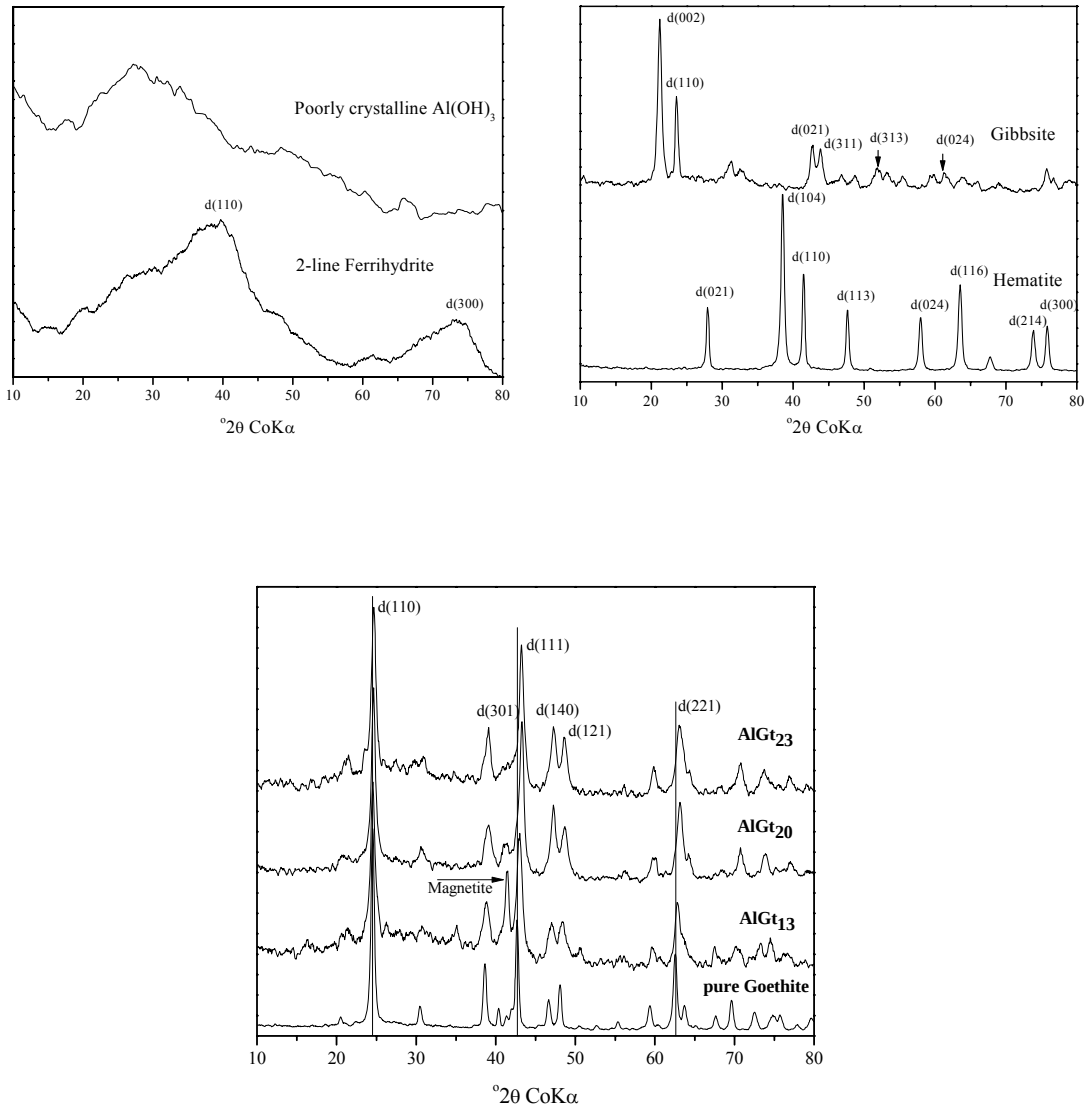

Figure 1 – X-ray powder diffraction of hematite, goethite, gibbsite, Al-substituted goethite, 2-line ferrihydrite, and poorly crystalline aluminium hydroxide.

ferrihydrite, and goethite (Figure 2), as reported in the literature (Sherman and Waite, 1985; Scheinost et al., 1999; Torrent and Barrón, 2003). Al-substituted goethites showed reflectance pattern similar to pure goethite, but with slight shifts of the ~430 nm band to shorter wavelengths (blue shift), as Al-substitution increased. In addition, absorption bands close to 360-380 nm were pronounced for Al-goethites, which this band is ascribed to the $^6A_1 \longrightarrow {}^4E(^4D)$ ligand field transition of Fe^{3+} (Sherman and Waite, 1985). Therefore, it can be surmised that this behaviour is due to structural disorder in the Gt framework caused by the presence of Al. The effects of Al substitution in goethite

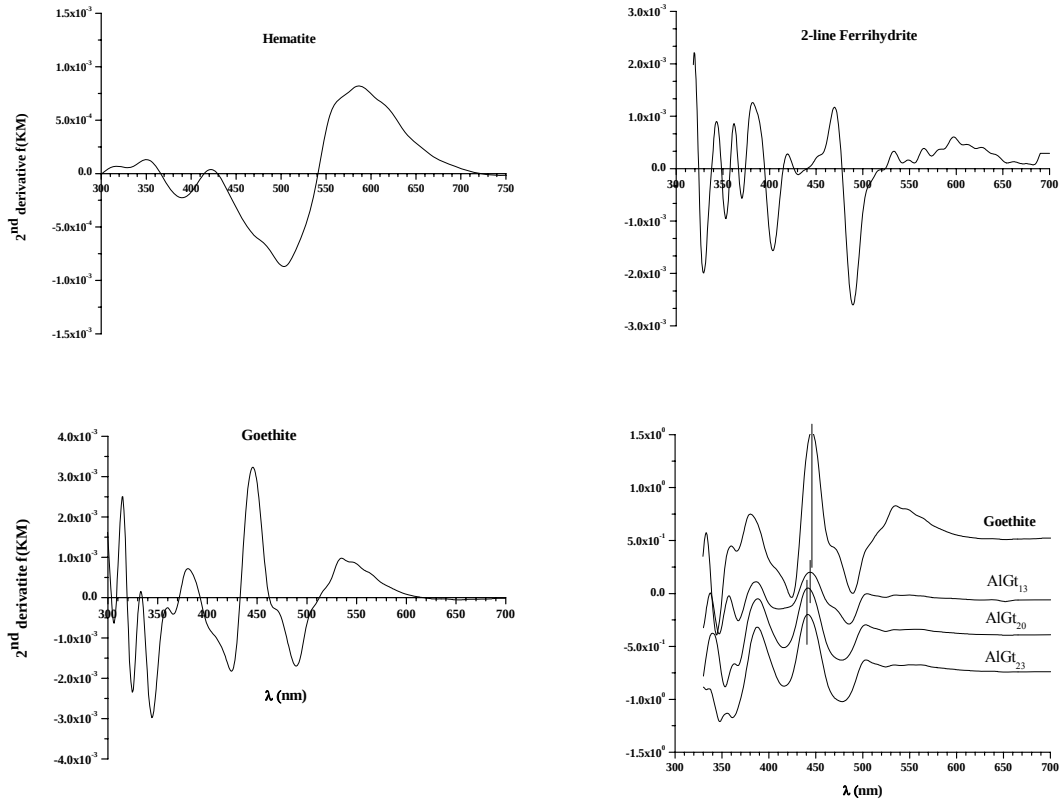

Figure 2 – Second derivative of the Kubelka-Munk (KM) function of the hematite, ferrihydrite, goethite, and Al-substituted goethite samples.

can be also seen in the logarithmic function of the diffuse reflectance spectra against wavelength (Figure 3). The blue shift of the main absorption edge (towards higher energy), represented by the electron pair transition (EPT_1 and EPT_2), is in line with Kosmas et al. (1986) and Scheinost et al. (1999). Malengreau et al. (1996) also observed such blue shift, but they were not able to establish a quantitative relationship between band shift and Al substitution. We also failed to evidence that relation because the $AlGt_{13}$ reflectance spectrum is quite different from the other goethites. It exhibited a higher light absorption capacity due to its darker colour as a resulted of the co-occurrence of the magnetite.

The reflectance spectra of the sample loaded with arsenate exhibited no difference in relation to the samples without arsenic. Then, it can be assumed that the surface complexes formed between arsenate and iron (hydr)oxides surface groups do not substantially affected the ligand field transition property of the ferric minerals.

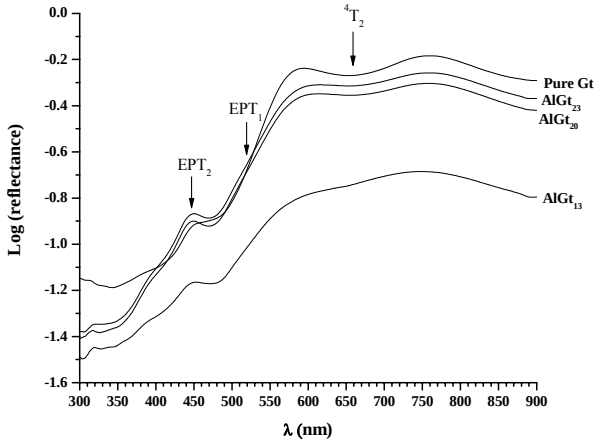

Figure 3 – Diffuse reflectance spectra of unsubstituted and substituted goethites in the near ultra violet-visible-near infra-red regions

3.4. Raman spectroscopy. The As-O stretching vibration is very sensitive to its environment and it has been used to identify different arsenate phases (Goldberg and Johnston, 2001; Frost et al., 2006; Jia et al., 2006). It can be observed that the Raman spectra of crystalline (hydr)oxides showed sharp peaks whilst the poorly crystalline minerals exhibited a noise broad peaks due to high degree of structural distortion.

3.4.1. Raman spectra for Gb and poorly crystalline Al(OH)$_3$. Hydroxyl stretching bands are related to the structural surface of the aluminium minerals and this feature is widely used to distinguish similar aluminium phases. For gibbsite the Raman spectrum in the high frequency region exhibited four strong sharp peaks at 3358, 3431, 3522, and 3615 cm^{-1} (Figure 4b) which is ascribed to OH gibbsite groups. This result is in line with Huneke et al. (1980) and Ruan et al. (2002). In addition, Gb spectrum reveals several picks in the low-medium frequency region (150 – 1050 cm^{-1}) with strong doublet at 541/572 cm^{-1} and a narrow intense peak at 324 cm^{-1} followed by weak bands between 200 and 450 cm^{-1} frequency. Three shoulders can be also observed at ~308, ~360, and ~507 cm^{-1} (Figure 4a). Probably, the main peaks are due to Al-O vibration group, and the minor bands in the low-frequency regions arise from vibrational motions of hydroxyls, lattice modes, and vibrations of hydrogen bonds as argued by Rogers (1993), and references therein.

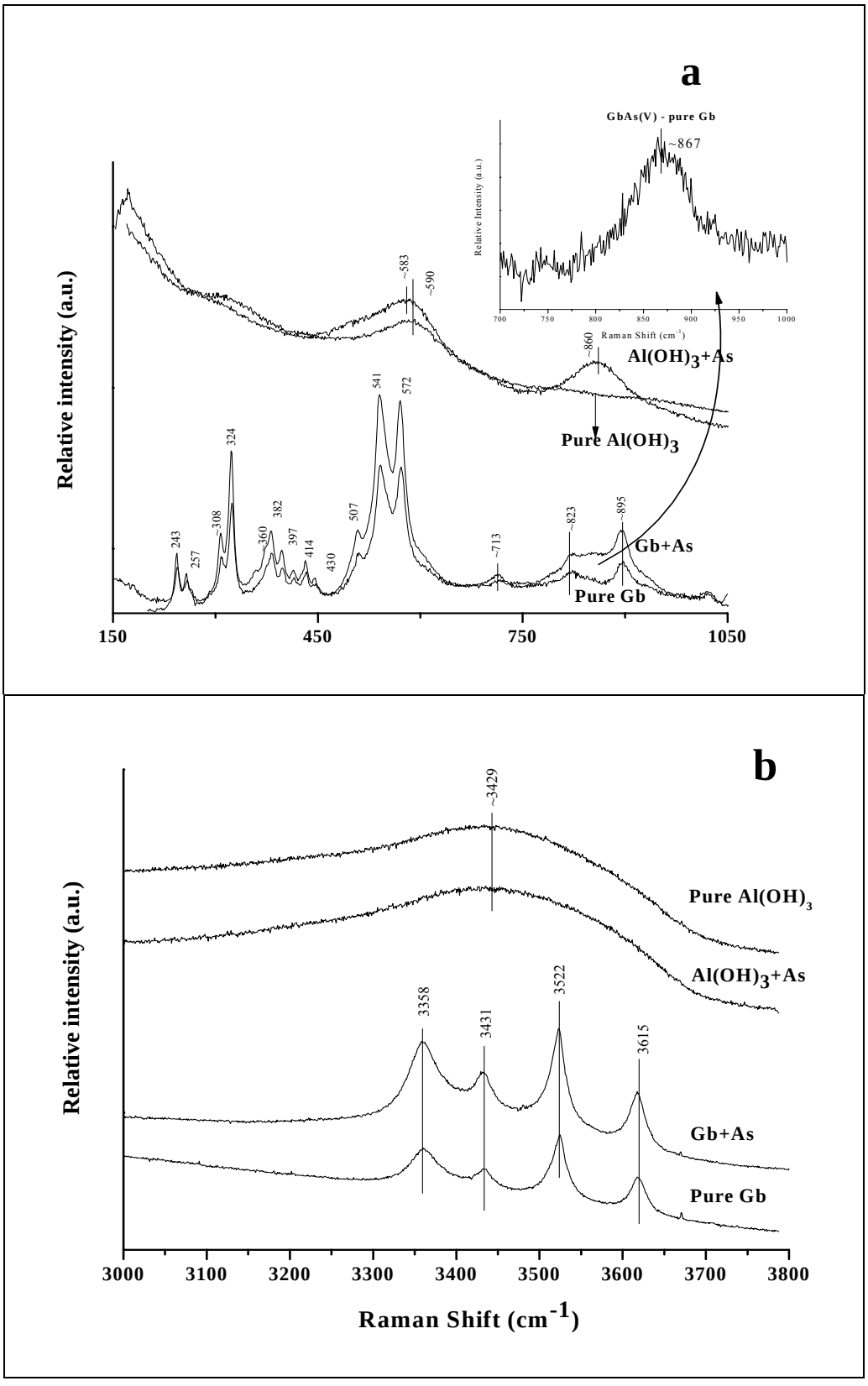

Figure 4 – Raman spectra of gibbsite (Gb) and aluminium hydroxide [$Al(OH)_3$] with and without As(V). a, Gb and $Al(OH)_3$ spectra in the 150 – 1050 region; b, Gb and $Al(OH)_3$ spectra in the 3000 – 3800 region. Inset in panel a represents the remaining band after subtraction of the Raman spectrum of Gb with and without As loaded.

By subtracting the Raman spectrum of pure gibbsite from As(V)-gibbsite sorption product one, a broad band at ~867 cm^{-1} was obtained (Figure 4a, inset) . This band positions lay close to that reported by Goldberg and Johnston (2001) which observed vibrational band in the 874 cm^{-1} frequency region for As(V) aqueous solution. These authors argued that at pH 5.0 the dominant arsenate species is $H_2AsO_4^{2-}$ with symmetry of C2v, and addressed that band position to As-O vibrational group. Theoretical studies have indicated that Al may strongly distort arsenate tetrahedron and the As-O_{Al} vibrations should shift to low wavenumbers when compared to the uncomplexed arsenate. FTIR spectra of arsenate in poorly crystalline Al-arsenate supported this statement and showed that the As-O_{Al} vibrations shifted to 740 cm^{-1}, whilst the As-$O_{uncomplexed}$ exhibited a broad band at 887 cm^{-1} (Myneni et al., 1998, and reference therein). The presence of adsorbed As(V) enhanced the vibrational stretching of the OH units and seems to have slightly contributed to diminish the luminescence of the pure Gb spectrum.

Raman spectrum of the poorly crystalline $Al(OH)_3$ exhibits a broad peak at ~590 cm^{-1} which is very close to that reported to Gb at 572 cm^{-1}. Then, it also can be assigned to Al-O stretching vibration unit. The presence of adsorbed arsenate is clearly resolved by the strong As-O stretching vibration band at ~860 cm^{-1} (Figure 4a). A band displaced of 7 cm^{-1} is also observed in the As(V)-$Al(OH)_3$ sorption product in relation to pure $Al(OH)_3$ spectra. This finding is also in line with Goldberg and Johnston (2001). These authors pointed out that the infrared and Raman-active As-O bands in the 844 – 865 cm^{-1} region are ascribed to As-O vibration of an inner-sphere Al-O-As complex. In our investigation the As-O vibration band lay between this range (~860 cm^{-1}), therefore, we can infer that arsenic is strongly retained on $Al(OH)_3$ surface as a very stable surface complex.

For poorly crystalline aluminium hydroxide of empirical formula $Al(OH)_3.3H_2O$, two types of OH groups maybe assumed, one from the OH units and another from interlamellar water (OH_{H2O}). Bands at ~3429 cm^{-1} is assigned to OH stretching vibration of the hydroxyl unit. The enlargement observed on the pure $Al(OH)_3$ line which starts from ~1250 up to ~3200 cm^{-1} may be ascribed to OH_{H2O} units due to water stretching bands (Figure 4b). This OH_{H2O} stretching vibrational bands on arsenate-$Al(OH)_3$ sorption products spectrum depleted notably, evidencing that the adsorption of As(V) detached water molecules. It has been shown that the water can be reversibly lost and the number of water molecules per formula unit can vary up to 3 (Frost et al., 2006).

Then, considering the high structural disorder of the poorly crystalline $Al(OH)_3$, the exchange of protons between water molecules and arsenate ions is feasible.

3.4.2. Raman spectra for Hm and Fh. Hematite spectrum exhibited narrow peaks characteristic of a well crystalline mineral (Figure 5). The positions of the Raman-active bands are in good agreement with previous studies (de Faria et al., 1997; Bouchard and Smith, 2003; Chamritski and Burns, 2005). Sharp peaks can be observed at 228, 247, 294, 412, 498, 614, and 1315 cm^{-1}. The band at 660 cm^{-1} can be attributed to structural defects on hematite making it appears as a prohibited line on the Raman spectrum. This band is active on infrared spectrum. The weak broad band at ~840 cm^{-1} could be better observed on the subtracted As(V)-loaded hematite spectrum (Figure 5, inset). This band is assigned to As-O stretching vibration. Low resolution of this band can be attributed to the relative low As(V) adsorption capacity of the Hm in comparison with Fh. This band position also lay close that one addressed by Jia et al. (2006) probably as product of surface adsorption. No shift was observed on the spectral line due to the presence of adsorbed As(V), indicating that the sample remained unchanged evenupon the laser beam.

Similarly to Hm, all diagnostic peaks on the Raman spectrum of the 2-line ferrihydrite can be observed at ~368, ~508, ~717, and 1377 cm^{-1}. A shoulder is also observed at ~676 cm^{-1} (Figure 5). These positions of the Raman-active bands agree with previous studies carried out by Mazetti and Thistlethwaite (2002). Nevertheless, our results differ from that reported by Jia et al. (2006). These authors reported three strong narrow peaks at 222, 289, and 407 cm^{-1}. Such pattern would not be expected for poorly crystalline minerals which usually exhibit broad and unresolved bands due to their high degree of structural disorder. Therefore, this discrepancy may be due to the laser power used in the experiment. Laser-induced thermal effect on mineral phases was shown by de Faria et al. (1996) who argued that the laser power magnitude is an important consideration when interpreting Raman.

The presence of adsorbed arsenate is clearly resolved by the strong As-O stretching vibration band at ~843 cm^{-1} (Figure 5) and it is in agreement with that observed for As(V)-hematite spectra (Figure 5, inset). Arsenic vibration band at 845 cm^{-1} for inner-sphere As(V) complex on ferrihydrite surface was reported by Jia et al. (2006). They attributed such binding mechanism to that complex since the adsorption of As(V) at pH 8 is assumed to be via binuclear complexation. Thus, the same inference may match for these results.

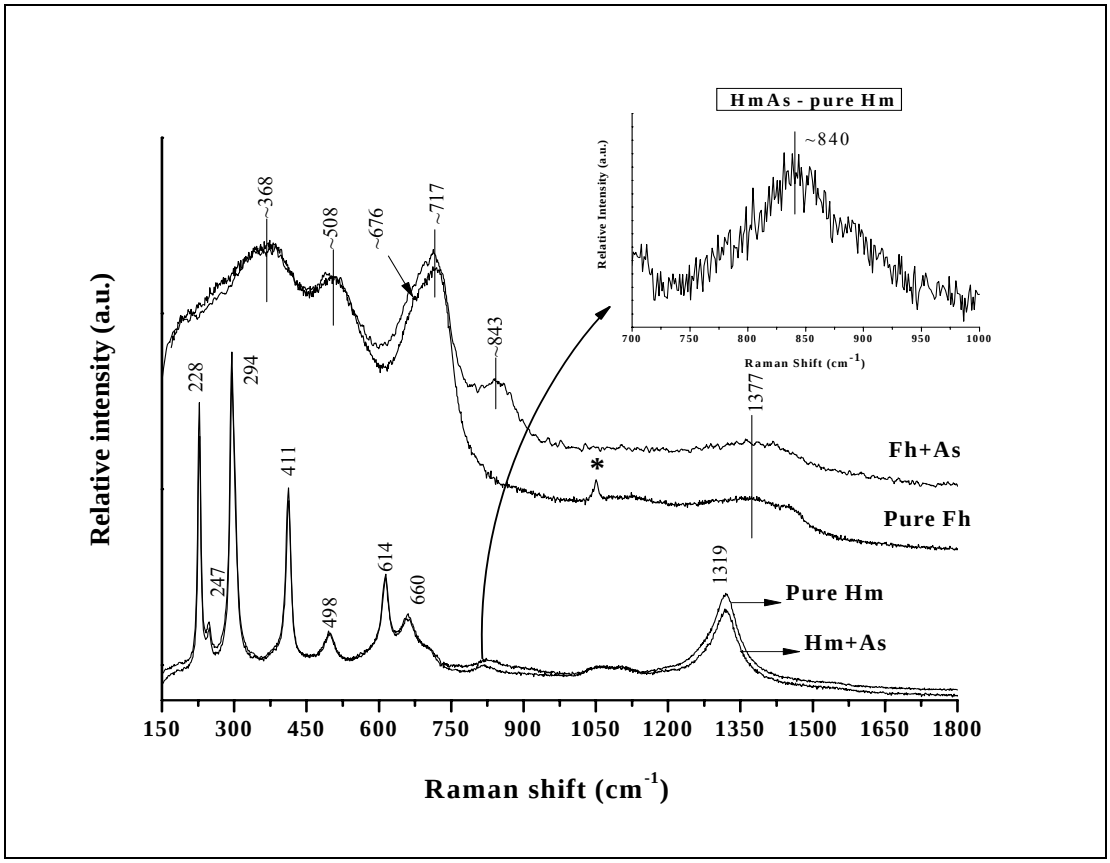

Figure 5 – Raman spectra of the hematite (Hm) and 2-line ferrihydrite (Fh) with and without As(V). The symbol * indicates residual bands of the reagent (NO_3^-) used in the synthesis. Inset in the panel represents the remaining band after subtraction of the Raman spectrum of Hm with and without As loaded.

3.4.3. Raman spectra for Gt and Al-substituted goethites. Pure Gt spectrum shows narrow peaks characteristic of a well crystalline mineral (Figure 6). Two strong can be visualised at 303 and 389 cm^{-1} followed by other peaks at 248, 485, 549, 687, and 1003 cm^{-1} and two shoulder at 403 and 420 cm^{-1}. A weak peak was also observed at 205 cm^{-1} frequency. These peaks position are in perfect agreement with previous investigations (de Faria et al., 1997; Oh et al., 1998; Bouchard and Smith, 2003) confirming the synthesised goethite. We have not found references to the small peaks at low frequencies in the literature, i.e. 169 and 208 cm^{-1}, and that one located at 614 cm^{-1}. Consequently, these peaks are probably due to some ambiguous variations in the goethite lattice. No arsenate stretching vibrational bands were observed on the As(V)-loaded goethite (spectrum not shown), which can be ascribed to the lowest As(V) adsorption capacity of goethite.

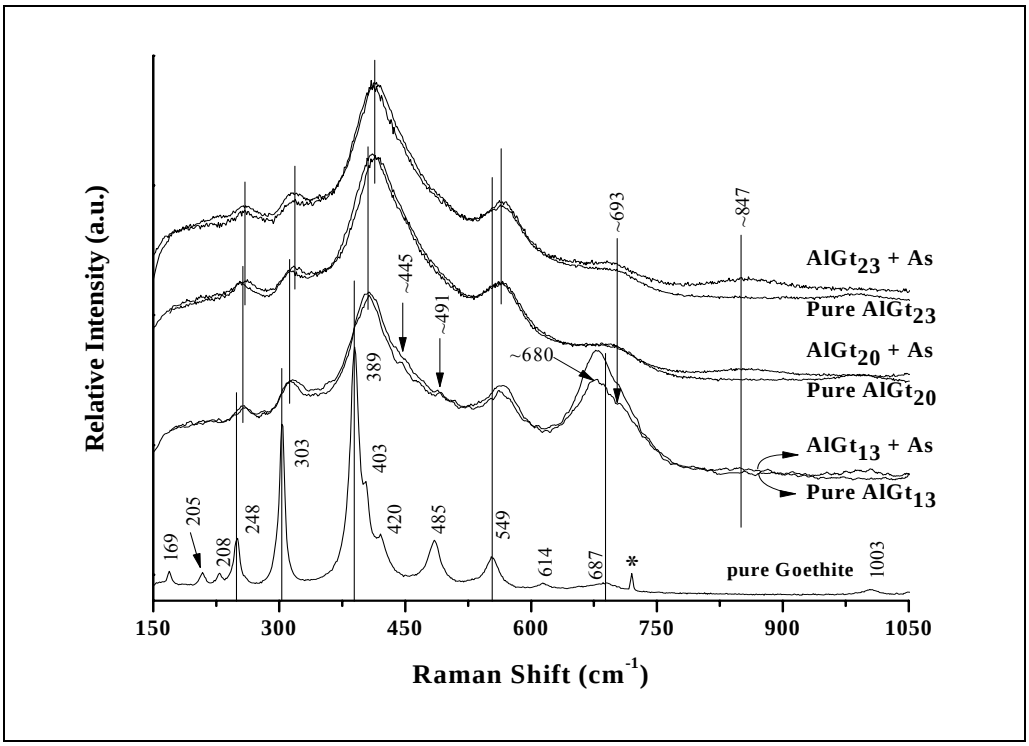

Figure 6 – Raman spectra of the goethite and Al-substituted goethites ($AlGt_{13}$, $AlGt_{20}$, and $AlGt_{23}$) with and without As(V). The symbol * indicates residual bands of the reagent (NO_3^-) used in the synthesis.

Aluminium substitution in the goethite structure affected considerably its vibrational features, especially the resolution of the Raman spectrum. In general, Al had a major influence under the degree of crystallinity and under the frequency of the spectral bands of the goethite. The main sharp peaks observed on pure Gt spectrum were broadened and shifted towards the high frequency region (red shift), as indicated by vertical bars in Figure 6. For goethites with higher Al content, the lines are broader and the shifts are less pronounced. For instance, the vibrational frequency of the main Gt peak at 389 cm^{-1} shifted to ~406 cm^{-1}, and then to 414 cm^{-1} as the Al content increased to 13 and to 20 cmol mol^{-1}, respectively.

The relative intensity was also influenced by the presence of structural Al. Reduction on the intensity along with the red shift and linewidth resulted in loss and overlap of many peaks, especially those observed in the low frequency region of the pure Gt spectrum. Iron is a strongly polarising atom and when it is incorporated into another mineral lattice it modifies the vibrational properties of the crystal. For example, the presence of a small amount of iron in the structure of spharelite enhanced the intensity of its second-order Raman spectrum (Mernagh and Trudu, 1993). Hence, a

counter effect, i.e. substitution of iron in the (hydro)xide lattices by other ions (e.g. Al), should result in intensity depletion. The scope of this process occurs gradually as suggested by the two shoulders at 445 and 491 cm^{-1} on the $AlGt_{13}$ spectrum, probably product of the Raman band alterations at 420 and 485 cm^{-1} on pure Gt spectrum.

In general, the presence of arsenate phase adsorbed on Al-substituted goethites can be visualised at ~847 cm^{-1} frequency on the As(V)-AlGt Raman spectra (Figure 6). Even though arsenate band on the As(V)-AlGt Raman spectrum is more pronounced as structural Al increase, arsenate seems to be more associated with iron than aluminium, since the As(V)-AlGt band positions are much closer to those verified for Hm (~840) and Fh (~843) than those observed for Gb (~867 cm^{-1}) and poorly crystalline $Al(OH)_3$ (~860 cm^{-1}). Similar to other Raman spectra analysed herein , these bands are also ascribed to As-O stretching vibrational group.

The Raman technique also revealed that $AlGt_{13}$ sample is rather heterogeneous. The well resolved Raman-active band at ~680 cm^{-1} is characteristic of magnetite, formed during the synthesis, as argued earlier. This band appears wider and somewhat shifted concerning to that one observed at 670 cm^{-1} for pure magnetite (Gasparov et al., 2000; Chamritski and Burns, 2005). Fe_3O_4 has an inverse spinel, cubic unit cell, and there are two iron position in the magnetite structure: *A* positions characterised by tetrahedral oxygen surrounding the Fe ions, which is occupied only by Fe^{3+}; whereas the octahedral *B* positions can be occupied by Fe^{2+} and Fe^{3+} (Gasparov et al., 2000). Thus, substitution of Al^{3+} for tetrahedral Fe^{3+} is feasible to occur, as discussed previously (section 3.2.1). As these modifications are the same of those verified for AlGts, i.e. increase in frequency and linewidth, we infer that Al is also incorporated in the magnetite lattice.

3.4.4. Raman spectra for Magnetite and phase transformation. In order to confirm the presence of co-precipitated magnetite and to investigate the laser-induced thermal effect giving rise to magnetite phase transformation, the laser was set at a darker region on the sample. The Raman-active bands observed at 190, 315, and 680 cm^{-1} confirmed the co-occurrence of magnetite with $AlGt_{13}$. The peak at ~670 cm^{-1} is assigned to A_{1g} mode which has a higher frequency than *Eg* mode and is addressed to the stretching vibrations of the oxygen atoms along the Fe(*A*)-O bonds (Gasparov et al., 2000). Similarly to that observed on the $AlGt_{13}$ spectrum, the main magnetite Raman-active peak at ~680 cm^{-1} present a red shift of approximately ~10 cm^{-1} as well as a broad shape (Figure 7). The main peaks that should appear at 400 to 550 cm^{-1} on typical

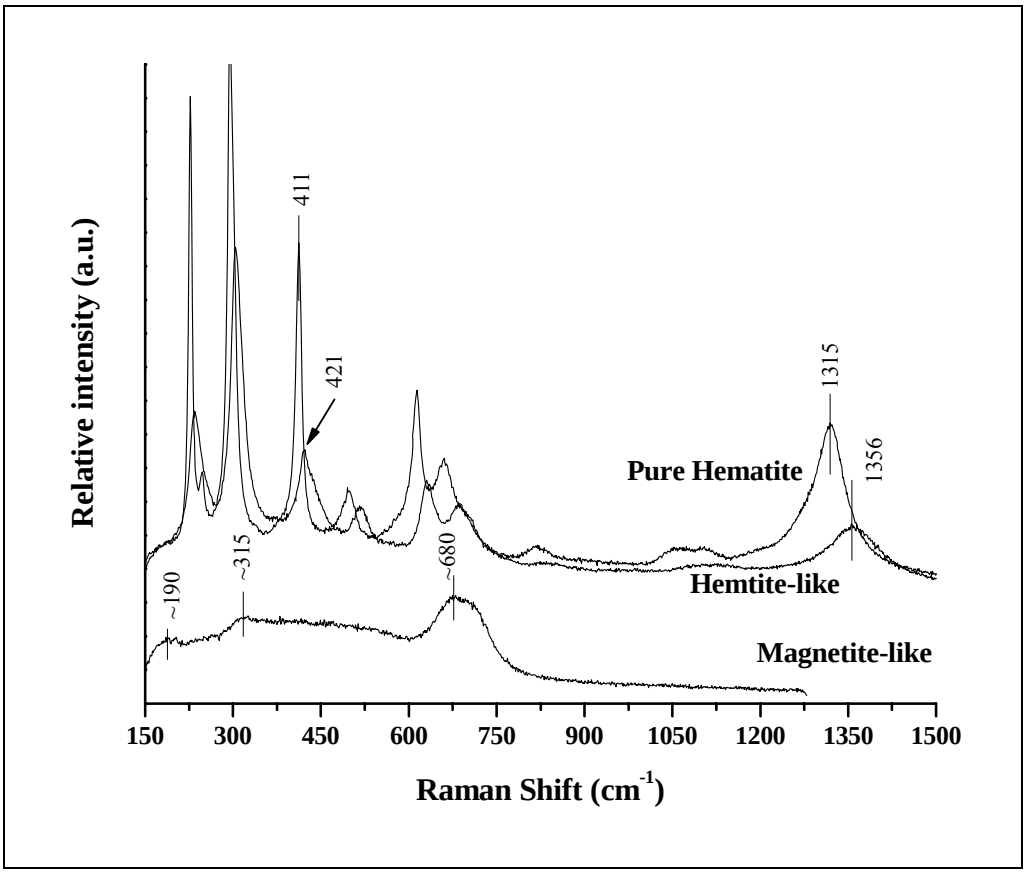

Figure 7 – Raman spectra of magnetite before and after thermal treatment. Pure hematite spectrum was plotted in order to compare with heated magnetite spectrum.

magnetite spectrum (Gasparov et al., 2000; Chamritski and Burns, 2005) were lost due to spectral modifications on the linewidth. This lack can be ascribed to the presence of Al in the magnetite lattice.

In relation to thermal treatment, magnetite showed to be very sensitive. After three seconds of higher laser irradiation, magnetite transformed completely into hematite-like phase, as shown in Figure 7. Nevertheless, the hematite-like spectrum obtained after heating the magnetite crystal differs from that recorded for pure hematite. All Raman-active bands on the hematite-like spectrum presented a red shift as well as a decrease in relative intensity. Considering that Al is not lost during the heat process, these changes can be also ascribed to the presence of structural Al replacing iron. Hematite-like spectrum presented a red shift (40 cm^{-1}) in the higher frequency region (>1300 cm^{-1}) in comparison with pure Hm one (Figure 7). For natural and synthetic Hm, the band at 411 cm^{-1} is particularly sensitive to variations caused by hydration, by ion substitution, or by the temperature of the sample (Bouchard and Smith, 2003).

Indeed, this band is displaced on Hm-like spectra, but our data suggest that the band at the higher frequency region seems to be most sensitive to such variations.

4. SUMMARY AND CONCLUSIONS

Raman spectroscopy and complementary XRD and diffuse reflectance were used to characterise different Al and Fe (hydr)oxides, to investigate the influence of structural Al in the goethite vibrational features as well as to identify the arsenate phase formed on the mineral surfaces. Spectroscopic results of the synthesised mineral phases fairly agreed with previous data reported in the literature. The presence of aluminium increased greatly the specific surface area of the goethite and improved its efficiency in adsorbing As(V). In addition, aluminium distorted considerably the spectroscopic patterns of the goethite mostly displacing its spectral lines due to change in its unit cell parameters. Raman spectroscopy was the major technique to reveal the structural disorder caused by Al in the Gt properties. Furthermore, this technique was sensible to detect As(V) adsorbed on the mineral surfaces, mainly on poorly crystalline Al(OH3) and ferrihydrite. Raman spectra in general revealed well resolved bands between 800 and 915 cm^{-1} frequencies, addressed to As-O stretching vibrational groups. The presence of arsenate was not visualised for Gt and rather slightly observed for Hm probably due to their lower As(V) adsorption capacities. As a general observation, our results agree that arsenic is retained as inner-sphere complex on poorly crystalline $Al(OH)_3$, Fh, and AlGts. But for Gb and Hm a lesser stable complex seems to predominate due to evidence of precipitation on their surface. The presence of coprecipitated magnetite was confirmed by Raman spectroscopy and X-Ray diffraction. Evidence of aluminium replacing iron even in the magnetite lattice was supported by modifications on its main spectral band along with the laser-induced Hm-like Raman spectrum.

In soils, goethite is the most stable ferric mineral and generally present appreciable amount of incorporated Al in its lattice, then, the immobilisation of contaminants, i.e. arsenate, may to a certain extent to be more associated with Al-substituted goethites than to other pure crystalline Fe (hydr)oxides. Although poorly crystalline Fe hydroxides participates more efficiently in sorption processes due to their larger surface area and consequently higher number of reactive surface sites, they are primarily dissolved via bioreduction reactions under anoxic conditions (low Eh),

resulting in arsenic mobilisation. In contrast, the presence of structural Al is expected to enhance the stability of goethites face to reductive dissolution. Consequently, the dissolution-desorption mechanisms is limited in Al-substituted goethite, contributing to prevent the arsenic dispersion. Nevertheless, further studies are warranted to better understand the role of aluminium in the sorption mechanisms and in the stability of the binding complex formed between arsenic and goethite surface under environmental conditions.

Raman spectroscopy in association with other techniques figures as an important tool to identify and characterise individual minerals. This is relevant in environmental sciences, which deal with complex matrixes, generally composed by an assemblage of minerals. Especially Al and Fe (hydr)oxides and their anion sorption products which can be assessed since each anion has its own vibrational stretching bands. Additionally, it is possible to detect the occurrence of ion substitutions that contribute to modify the mineral features.

5. REFERENCE

Barrón, V., Mello, J.W.V., and Torrent, J. Caracterização de oxidos de ferro em solos por espectroscopia de reflectância difusa. In: Novais, R. F., Venegas, V. H. A, Schaefer, C. E. R. G. (Eds). Tópicos em Ciência do Solo. Viçosa, 139-162, SBCS, 2000.

Bouchard, M. and Smith, D.C., 2003. Catalogue of 45 reference Raman spectra of minerals concerning research in art history or archaeology, especially on corroded metals and coloured glass. Spectrochimica Acta Part a-Molecular and Biomolecular Spectroscopy 59, 2247-2266.

Chamritski, I. and Burns, G., 2005. Infrared- and Raman-active phonons of magnetite, maghemite, and hematite: A computer simulation and spectroscopic study. Journal of Physical Chemistry B 109, 4965-4968.

Cornell, R.M. and Schwertmann, U., 2003. The iron oxides: structure, properties, reactions, occurences and uses. Wiley-VCH, Weinheim; Cambridge.

deFaria, D.L.A., Silva, S.V., and deOliveira, M.T., 1997. Raman microspectroscopy of some iron oxides and oxyhydroxides. Journal of Raman Spectroscopy 28, 873-878.

Deschamps, E., Ciminelli, V.S.T., and Holl, W.H., 2005. Removal of As(III) and As(V) from water using a natural Fe and Mn enriched sample. Water Research 39, 5212-5220.

Dixon, J.B. and Weed, S.B., 1989. Minerals in soil environments. Soil Science Society of America, Madison, Wisconsin.

Driehaus, W., Jekel, M., Hildebrandt, U., 1998. Granular ferric hydroxide - a new adsorbent for the removal of arsenic from natural water. J. Water Supply Res. Technol. 47, 30 - 35.

Frost, R.L. and Kloprogge, J.T., 2003. Raman spectroscopy of some complex arsenate minerals - implications for soil remediation. Spectrochimica Acta Part a-Molecular and Biomolecular Spectroscopy 59, 2797-2804.

Frost, R.L., Kloprogge, T., Weier, M.L., Martens, W.N., Ding, Z., and Edwards, H.G.H., 2003. Raman spectroscopy of selected arsenates - implications for soil

remediation. Spectrochimica Acta Part a-Molecular and Biomolecular Spectroscopy 59, 2241-2246.

Frost, R.L., Weier, M., and Martens, W., 2006. Using Raman spectroscopy to identify mixite minerals. Spectrochimica Acta Part a-Molecular and Biomolecular Spectroscopy 63, 60-65.

Gasparov, L.V., Tanner, D.B., Romero, D.B., Berger, H., Margaritondo, G., and Forró, L., 2000. Infrared and Raman studies of the Verwey transition in magnetite. Physical Review B 62, 7939.

Goldberg, S. and Johnston, C.T., 2001. Mechanisms of arsenic adsorption on amorphous oxides evaluated using macroscopic measurements, vibrational spectroscopy, and surface complexation modeling. Journal of Colloid and Interface Science 234, 204-216.

Goldberg, S., Lebron, I., Suarez, D.L., and Hinedi, Z.R., 2001. Surface Characterization of Amorphous Aluminum Oxides. Soil Sci Soc Am J 65, 78-86.

Gonzalez, E., Ballesteros, M.C., and Rueda, E.H., 2002. Reductive dissolution kinetics of Al-substituted goethites. Clays and Clay Minerals 50, 470-477.

Hongshao, Z. and Stanforth, R., 2001. Competitive adsorption of phosphate and arsenate on goethite. Environ. Sci. Technol. 35, 4753-4757.

Hope, G.A., Woods, R., and Munce, C.G., 2001. Raman microprobe mineral identification. Minerals Engineering 14, 1565-1577.

Huneke, J.T., Cramer, R.E., Alvarez, R., and El-Swaify, S.A., 1980. The identification of gibbsite and bayerite by laser Raman spectroscopy. Soil Sci Soc Am J 44, 131-134.

Jeanroy, E., Rajot, J.L., Pillon, P., and Herbillon, A.J., 1991. Differential dissolution of hematite and goethite in dithionite and its implication on soil yellowing. Geoderma 50, 79-94.

Jia, Y.F., Xu, L.Y., Fang, Z., and Demopoulos, G.P., 2006. Observation of surface precipitation of arsenate on ferrihydrite. Environmental Science & Technology 40, 3248-3253.

Konert, M. and Vandenberghe, J., 1997. Comparison of laser grain size analysis with pipette and sieve analysis: A solution for the underestimation of the clay fraction. Sedimentology 44, 523-535.

Kosmas, C.S., Franzmeier, D.P., and Schulze, D.G., 1986. Relationship among derivative spectroscopy, color, crystallite dimensions, and Al substitution of synthetic goethites and hematites. Clays and Clay Minerals 34, 625-634.

Kyle J.H., Posner, A. M., and Quirk J.P. , 1975. Kinetics of isotopic exchange of phosphate adsorbed on gibbsite. Journal of Soil Science 26, 34-43.

L. Mazzetti, P.J.T., 2002. Raman spectra and thermal transformations of ferrihydrite and schwertmannite. Journal of Raman Spectroscopy 33, 104-111.

Ladeira, A.C.Q., Ciminelli, V.S.T., Duarte, H.A., Alves, M.C.M., and Ramos, A.Y., 2001. Mechanism of anion retention from EXAFS and density functional calculations: Arsenic (V) adsorbed on gibbsite. Geochimica Et Cosmochimica Acta 65, 1211-1217.

Makris, K.C., Sarkar, D., Parsons, J.G., Datta, R., and Gardea-Torresdey, J.L., 2007. Surface arsenic speciation of a drinking-water treatment residual using X-ray absorption spectroscopy. Journal of Colloid and Interface Science 311, 544-550.

Malengreau, N., Bedidi, A., Muller, J.P., and Herbillon, A.J., 1996. Spectroscopic control of iron oxide dissolution in two ferralitic soils. European Journal of Soil Science 47, 13-20.

Manning, B.A., Fendorf, S.E., and Goldberg, S., 1998. Surface structures and stability of arsenic(III) on goethite: spectroscopic evidence for inner-sphere complexes. Environ. Sci. Technol. 32, 2383-2388.

Matschullat, J., Perobelli Borba, R., Deschamps, E., Figueiredo, B.R., Gabrio, T., and Schwenk, M., 2000. Human and environmental contamination in the Iron Quadrangle, Brazil. Applied Geochemistry 15, 181-190.

Mello, J., Roy, W., Talbott, J., and Stucki, J., 2006. Mineralogy and arsenic mobility in arsenic-rich Brazilian soils and sediments. Journal of Soils and Sediments 6, 9-19.

Mernagh, T.P. and Trudu, A.G., 1993. A laser Raman microprobe study of some geologically important sulphide minerals. Chemical Geology 103, 113-127.

Murad, E. and Schwertmann, U., 1983. The influence of aluminum substitution and crystallinity on the Mossbauer-spectra of goethite. Clay Minerals 18, 301-312.

Myneni, S.C.B., Traina, S.J., Waychunas, G.A., and Logan, T.J., 1998a. Experimental and theoretical vibrational spectroscopic evaluation of arsenate coordination in aqueous solutions, solids, and at mineral-water interfaces. Geochimica et Cosmochimica Acta 62, 3285-3300.

Myneni, S.C.B., Traina, S.J., Waychunas, G.A., and Logan, T.J., 1998b. Vibrational spectroscopy of functional group chemistry and arsenate coordination in ettringite. Geochimica et Cosmochimica Acta 62, 3499-3514.

Oh, S., Cook, D.C., and Townsend, H.E., 1998. Characterization of iron oxides commonly formed as corrosion products on steel. Hyperfine Interactions 112, 59-66.

Ona-Nguema, G., Morin, G., Juillot, F., Calas, G., and Brown, G.E., 2005. EXAFS analysis of arsenite adsorption onto two-line ferrihydrite, hematite, goethite, and lepidocrocite. Environmental Science & Technology 39, 9147-9155.

Pye, K. and Blott, S.J., 2004. Particle size analysis of sediments, soils and related particulate materials for forensic purposes using laser granulometry. Forensic Science International 144, 19-27.

Rodgers, K.A., 1993. Routine identification of aluminium hydroxides polymorphs with the Laser Raman Microprobe. Clay Minerals 28, 85-99.

Ruan, H.D., Frost, R.L., Kloprogge, J.T., and Duong, L., 2002. Far-infrared spectroscopy of alumina phases. Spectrochimica Acta Part A: Molecular and Biomolecular Spectroscopy 58, 265-272.

Scheinost, A.C., Schulze, D.G., and Schwertmann, U., 1999. Diffuse reflectance spectra of Al substituted goethite: A ligand field approach. Clays and Clay Minerals 47, 156-164.

Schulze, D.G. and Schwertmann, U., 1984. The influence of aluminum on iron-oxides .10. Properties of Al-Substituted goethites. Clay Minerals 19, 521-539.

Schulze, D.G. and Schwertmann, U., 1987. The influence of aluminum on iron-oxides.13. Properties of goethites synthesized in 0.3-M KOH at 25-Degrees-C. Clay Minerals 22, 83-92.

Schwertmann, U., 1984. The influence of aluminum on iron-oxides.9. Dissolution of Al-Goethites in 6m HCl. Clay Minerals 19, 9-19.

Schwertmann, U. and Cornell, R.M., 2000. Iron oxides in the laboratory: preparation and characterization. Wiley-VCH, Weinheim; Chichester.

Shebanova, O. N., Lazor, P., 2003. Raman study of magnetite (Fe_3O_4): laser-induced thermal effects and oxidation. Journal of Raman Spectroscopy 34, 845-852.

Sherman, D.M. and Waite, T.D., 1985. Electronic-spectra of Fe^{3+} oxides and oxide hydroxides in the near IR to near UV. American Mineralogist 70, 1262-1269.

Silva, J., Mello, J.W.V., Gasparon, M., Abrahão, W.A.P., Jong, T. and Ciminelli, V.S.T., 2008. Arsenic adsorption onto aluminium and iron (hydr)oxides: kinetics, isotherm, and envelope of adsorption. (To be submitted)

Smedley, P.L. and Kinniburgh, D.G., 2002. A review of the source, behaviour and distribution of arsenic in natural waters. Applied Geochemistry 17, 517-568.

Strauss, R., Brummer, G.W. and Barrow, N.J., 1997. Effects of crystallinity of goethite: I. Preparation and properties of goethite of differing crystallinity. European Journal of Soil Science 48, 87-99.

Sun, X.H. and Doner, H.E., 1996. An investigation of arsenate and arsenite bonding structures on goethite by FTIR. Soil Science 161, 865-872.

Sun, X.H. and Doner, H.E., 1998. Adsorption and oxidation of arsenite on goethite. Soil Science 163, 278-287.

Torrent, J. and Barron, V., 2003. The visible diffuse reflectance spectrum in relation to the color and crystal properties of hematite. Clays and Clay Minerals 51, 309-317.

Torrent, J., Schwertmann, U., and Barron, V., 1987. The reductive dissolution of synthetic goethite and hematite in dithionite. Clay Minerals 22, 329-337.

USEPA. (2000). Technologies and costs for removal of arsenic from drinking water. Draft report, EPA-815-R-00-028, Washington, DC.

Waychunas, G.A., Rea, B.A., Fuller, C.C., and Davis, J.A., 1993. Surface-chemistry of ferrihydrite .1. EXAFS studies of the geometry of coprecipitated and adsorbed arsenate. Geochimica Et Cosmochimica Acta 57, 2251-2269.

Weerasooriya, R., Tobschall, H.J., Wijesekara, H.K.D.K., and Bandara, A., 2004. Macroscopic and vibration spectroscopic evidence for specific bonding of arsenate on gibbsite. Chemosphere 55, 1259-1270.

Chapter 2

ARSENIC ADSORPTION ONTO ALUMINIUM AND IRON (HYDR)OXIDES: KINETICS, ISOTHERM AND ENVELOPE OF ADSORPTION

ABSTRACT

The geochemical fates of iron and arsenic are so closely correlated that methods of arsenic removal from water are in general based on the high affinity of this metalloid with iron (hydr)oxides. Thus, the purpose of this study was to investigate the potential of Al-substituted goethites in adsorbing arsenic compared with other Fe and Al (hydr)oxides. Hematite (Hm), goethite (Gt), 2-line ferrihydrite (Fh), gibbsite (Gb), aluminium hydroxide [$Al(OH)_3$], and three Al-substituted goethites containing 13, 20, and 23 cmol mol of Al ($AlGt_{13}$, $AlGt_{20}$, and $AlGt_{23}$, respectively) were synthesised and used as adsorbent for As(V). Adsorption kinetics at two different solid:solution ratios, 2.0 and 5.0 g L^{-1}, and adsorption isotherms were obtained after equilibrating the samples with arsenate solution for respectively 96 and 24 hours under constant shaking. As(V) adsorption maxima was measured at different pH ranging from 3 to 9. In spite of the fast equilibrium, the increase in solid concentration limited the efficiency and velocity of arsenic adsorption. The As(V) adsorption maxima decreased in the following order: $Al(OH)_3$ > Fh > $AlGt_{13}$ > $AlGt_{20}$ > $AlGt_{23}$ > Gb > Hm > Gt. Nevertheless, by calculating adsorption capacities in terms of surface area, Gb, Gt, and Hm showed higher As(V) loading capacity than Fh. This suggest available reactive sites not fully occupied by arsenate on the amorphous and Al-substituted (hydr)oxides during the adsorption experiment. No relationship was observed between average particle size and adsorption maxima. This suggests re-aggregation of the particles during the particle size measurement, or imperfections on the surface of the particles increasing their net charge, resulting in high adsorption density. The behaviour of all samples was dependent on pH, and the maximum adsorption was achieved in slightly acidic conditions. In general, Al (hydr)oxides were more efficient than Fe (hydr)oxides to remove As(V). The presence of structural Al enhanced considerably the arsenic uptake capacity of the goethites which showed to be promising as an adsorbent to remove arsenic from water.

Keyword: arsenic, kinetics, adsorption envelope, Al-goethites, Al and Fe hydroxides.

1. INTRODUCTION

Arsenic contamination has been considered an important and very sensitive issue due to its high toxicity to man and other living organisms. The current World Health Organization (WHO) guideline for arsenic in drinking water is 10 μg L^{-1}. This limit is recommended by WHO based on toxicological test and was already adopted in many countries, such as Brazil, United State of America, Germany, and others. In Australia, the drink water guideline value for As is 7 μg L^{-1} (NHMRC & NRMMC, 2004). Nevertheless, the presence of arsenic in ground and surface water has been found in values higher than this threshold.

Some parts of Bangladesh, West Bengal, Inner Mongolia, Vietnam, India, Mexico, Argentina, Chile, and Brazil are well known regions with anomalous levels of As in drinking water (Matschullat et al., 2000; Smedley and Kinninburg, 2002; Smedley et al., 2003). Weathering of As-rich parental material and human activities, such as use of arsenical fertilizers and pesticides as well as industrial and mining activities are prominent contamination source. In Brazil, in the past, an estimated 3.1 million metric tons of tailing materials with average As content of 14,500 mg kg^{-1} have been deposited along valleys without adequate assessment of environmental impact (Deschamps et al., 2002). Moreover, previous studies in these areas revealed a naturally high As background, with average As concentrations above 100 mg kg^{-1} in soils and 100 μg L^{-1} in local water (Matschullat et al., 2000; Deschamps et al., 2002; Mello et al., 2006).

The biogeochemical cycle of arsenic has been reviewed by Anderson and Bruland (1991), Schnoor (1996), Matschullat (2000), Smedley and Kinniburg (2002), and others. The distribution of arsenic species in the environment depends primarily on redox potential (Eh) and pH (e.g. $H_3AsO_4/H_2AsO_4^-$ $pK_{a1} = 2.2$; $H_2AsO_4^-/HAsO_4^{2-}$ $pK_{a2} = 6.9$; $HAsO_4^{2-}/AsO_4^{3-}$ $pK_{a3} = 11.4$). In well-oxidised water, arsenate [As(V)] as $H_2AsO_4^-$ and $HAsO_4^{2-}$ is the predominant species while arsenite [As(III)] occur predominately in reduced environments mainly as H_3AsO_3. Nevertheless, both species can be often found in either redox environment due to relatively slow transformation on the redox conditions.

Sorption processes also play an important role on As behaviour controlling its mobility and bioavailability. Hydroxyl groups (OH and OH_2) in the coordination spheres of metals on the mineral surfaces are the most abundant and reactive adsorption sites. Consequently Al and Fe (hydr)oxides have a strong affinity for As(V) (Pierce and Moore, 1982; Stumm and Sulzberger, 1992). The strong retention of As(V) by oxides

and hydroxides is ascribed to inner-sphere mononuclear or binuclear monodentate-bidentate surface complexes (Waychunas et al., 1993; Sun and Doner, 1996; Fendorf et al., 1997).

There are many different technologies for removing arsenic from drinking water. Precipitation/coagulation or adsorption processes have been preferably considered at the water plant treatment. A number of investigation has focused on using aluminium and ferric salts (Jekel, 1994; Wickramasinghe et al., 2004) and natural or synthetic Fe or Al (hydr)oxides (Anderson et al., 1976; Driehaus et al., 1998; Ladeira et al., 2001; García-Sanchez et al., 2002; Deschamps et al., 2003; Ladeira and Ciminelli 2004; Deschamps et al., 2005). The use of aluminium or ferric salts as a coagulant can lead to parallels problems regards to the addition of undesirable anion, such as sulphate, nitrate, and chloride into the water. Other problems associated with this technique are the safe separation and the handling of the contaminated coagulant sludge (Driehaus et al., 1998).

The adsorption technique has secured a place in advanced methods of arsenic removal because of the easy handling of the sludge, free operation and regeneration capability. For this reason, metal (hydr)oxides have been studied by many researchers with regards to the developing technologies for arsenic removal from contaminated water. These materials include amorphous ferric hydroxides (Pierce and Moore, 1982), granular ferric hydroxides (GFH) (Driehaus et al., 1998), crystalline ferric hydroxide (Manna et al., 2003), amorphous aluminium hydroxides (Anderson et al., 1976), natural Fe and Mn minerals (Deschamps et al., 2003, 2005), activated alumina (Singh and Pant, 2004; Sierra-Alvarez et al., 2005). In general, methods using Fe (salt) are more effective than Al in removing As from water. Nevertheless, Fe (hydr)oxides used to remove As from water are rather unstable in low Eh environments. Thus, under reducing conditions, the mechanism of arsenic sorption may also depend on Fe reduction (Cummings et al., 1999).

The disposal of Fe-As-rich waste generated at water treatments plants is an environmental concern, and requires the development of methods to improve the stability of these compounds under anaerobic conditions. Previous investigations have suggested a positive correlation between goethite stability under reducing conditions and structural Al content (Schwertmann, 1991; Maurice et al., 2000; Gonzales et al., 2002). In this study we assessed the potential of Al-substituted goethites in adsorbing arsenate in comparison to other Al and Fe (hydr)oxides.

2. MATERIALS AND METHODS

2.1. Adsorbents

Aluminium and iron (hydr)oxides were synthesised, and the main characteristics of all adsorbents are in Table 1. Hematite, Goethite, and 2-line Ferrihydrite were synthesised following the procedure described in Schwertmann and Cornell (2000). A series of aluminium substituted goethites were also synthesised following the methods therein. The Al-goethites were prepared by precipitation of ferrous and aluminium chloride solution with potassium hydroxide solution and aged in a plastic bottle during 90 days. Slow oxidation of Fe^{2+} to Fe^{3+} and incorporation of Al^{3+} in the goethite structure were achieved by opening the bottle daily and stirring the suspension vigorously during five minutes. In order to remove the excess of Al, the precipitates were washed twice with 0.01 mol L^{-1} KOH solution. Precipitates of (hydr)oxides were washed several times with Milli-Q water, centrifuged and dried at 50 ^{o}C at an oven with air circulation, except for ferrihydrite which was freeze-dried Gibbsite was prepared following the procedures outlined in Kyle et al. (1975). An $Al(NO_3)_3$ solution was titrated with a 4 mol L^{-1} NaOH solution to a pH of 4.6 ±0.2. The gelatinous precipitate was heated for two hours at 40 ^{o}C, then washed twice, dialyzed against Milli-Q water for 36 days, and dried at 50 ^{o}C. Poorly aluminium hydroxide was also prepared from an aluminium nitrate solution by precipitation with 4 mol L^{-1} NaOH solution. The procedure was similar to that followed for the synthesis of gibbsite, but with the suppression of the heating step to preserve low crystallinity. Similarly to ferrihydrite, the aluminium hydroxide was freeze-dried in order to prevent its crystallization.

Prior to any analysis, all samples were passed through the < 53 μm sieve. The specific surface area was determined by N_2 adsorption, BET method, using multiple point technique (Quantachrome model NOVA 1000) and particle size was measured using a Micromeritics Saturn Digisizer model 5200. The identity of the desired mineral phases were confirmed by powder X-ray diffraction (XRD), Raman spectroscopy, and diffuse reflectance for the iron (hydr)oxides. Additional details can be seen on Silva et al. (2008).

2.2. Adsorption Isotherms. Batch experiments were carried out to obtain adsorption isotherms at pH 5.0 ±0.2 and 25 ±0.1 ^{o}C. As(V) solutions were prepared dissolving in Milli-Q water analytical reagent grade di-sodium hydrogen arsenate heptahydrate (Na_2HAsO_4 $7H_2O$; Ajax Finechem). Solid samples (0.1000g) and 25 mL

Table 1 – Specific surface area, mean particle size, and maximum As(V) adsorption capacity of the adsorbent materials (Further details can be seen in Chapter 1 or in Silva et al., 2008)

Adsorbent	Specific surface area [a/]	Particle size	Al for Fe substitution
	------- $m^2\ g^{-1}$ -------	-------- μm -------	---$mol_{Al}\ mol_{Fe}^{-1}$ ---
Hematite	34.8	0.20 ± 0.001[b/]	
Goethite	20.6	0.97 ± 0.022	
Ferrihydrite	260.4	23.47 ± 0.311	
Gibbsite	45.7	21.01 ± 0.460	
Alum. Hydroxide	8.3	12.60 ± 1.313	
Al-Goethite 13	119.4	11.33 ± 3.866	13
Al-Goethite 20	124.7	3.25 ± 0.466	20
Al-Goethite 23	113.2	2.55 ± 2.712	23

[a/] Determined by N_2 adsorption, BET method;
[b/] number followed by ± symbol means the standard deviation.

of As solution (concentrations ranging from 0.534 up to 21.586 mmol L^{-1}) were placed into a 50 mL polypropylene centrifuge tubes with screw caps and conical base, and equilibrated for 24 hours on a rotary shaker. The pH was checked at the first four hours and corrected when necessary. The ionic strength was set at 10 mmol L^{-1} using $CaCl_2$. After 24 h the samples were then centrifuged and syringe filtered using 0.22 μm membrane filters (Millipore Millex-GV, USA). The filtered was acidified and stored for further As analyses.

2.3. As(V) Adsorption Kinetics. The As(V) adsorption kinetics were assessed at two different solid:solution ratios, i.e. 2.0 and 5.0 g L^{-1}, and at initial As(V) concentration corresponding to 0.100, 0.200, 0.250, 0.400, 1.200, and 1.500 mmol g^{-1} of Gt, Hm, Gb, AlGts, Fh, and $Al(OH)_3$, respectively. Preliminary test showed that these concentrations were close to maximum As(V) adsorption. An arsenate stock solution was prepared in 10 mmol L^{-1} $CaCl_2$ containing As concentration of 13.35 mmol L^{-1}. Adsorption kinetics were obtained at pH 5.0 ±0.2 by equilibrating the solid sample (0.0500 g or 0.1250 g) with 25 mL of doped solution for 96 h at 25 ±0.1 ^oC. Solutions with adequate As(V) concentration for each adsorbent were placed into a 50 mL polypropylene centrifuge tubes with screw caps and conical base, and equilibrated on a rotary shaker. During the first four hours, pH was checked and corrected when necessary with HNO_3 or NaOH. The ionic strength was set at 10 mmol L^{-1} using $CaCl_2$. Aliquots of the supernatants were periodically collected at 0.5, 2, 4, 6, 12, 24, 48, and 96 h of reaction, and immediately syringe filtered using 0.22 μm

membrane filters (Millipore Millex-GV, USA), acidified, and stored for further As analyses.

2.4. As(V) Adsorption Envelopes. Adsorption envelopes were obtained by adsorption isotherm at different pre-adjusted pH values ranging from 3 to 9. The pH was adjusted by adding HNO_3 or NaOH. The pH was measured and adjusted during the first four hours when necessary and at the end of the experiment. In addition, blank experiments containing only arsenic solution were used to measure the amount of arsenic adsorbed by the walls of the reaction vessels.

2.5. Analytical Techniques. Arsenic in the equilibrium solutions was measured by inductively coupled plasma optical emission spectroscopy (ICP-OES), using a Perkin Elmer Optima 3300 DV. Scandium was used as internal standard to correct for instrumental instabilities and matrix effect. Solution of this element was added to the solution to reach a final concentration of 2.0 mg L^{-1}. Typical detection limits (3σ) of 0.134 μmol L^{-1} As were obtained. All assays were carried out in triplicates.

3. RESULTS AND DISCUSSION

3.1. Adsorption Isotherms. The different arsenate concentration ranges added were sufficient to achieve the maximum adsorption for all adsorbents (Figure 1). Adsorption isotherm taking into account the whole data fitted well to Langmuir model. Nevertheless, different adsorption regions can be clearly visualised for Hm, Fh, Gb, and $AlGt_{20}$. It is determined that these are related to the affinity of arsenate for at least two distinct energetically reactive sites on their surface.

In order to obtain the maximum arsenate adsorption, the data were fitted to the linear form of the Langmuir equation [C/q = (1/*K*b) + (C/b)], where C is the equilibrium concentration of As(V) remaining in the solution (mmol L^{-1}), q is the amount of adsorbed arsenate by the sorbent (mmol g^{-1}), b is the maximum arsenic adsorption (mmol g^{-1}), and *K* is the constant related to the energy of adsorption (L $mmol^{-1}$). It was utilised the second region of adsorption as preconised by Muljadi et al. (1966) for phosphate. According to

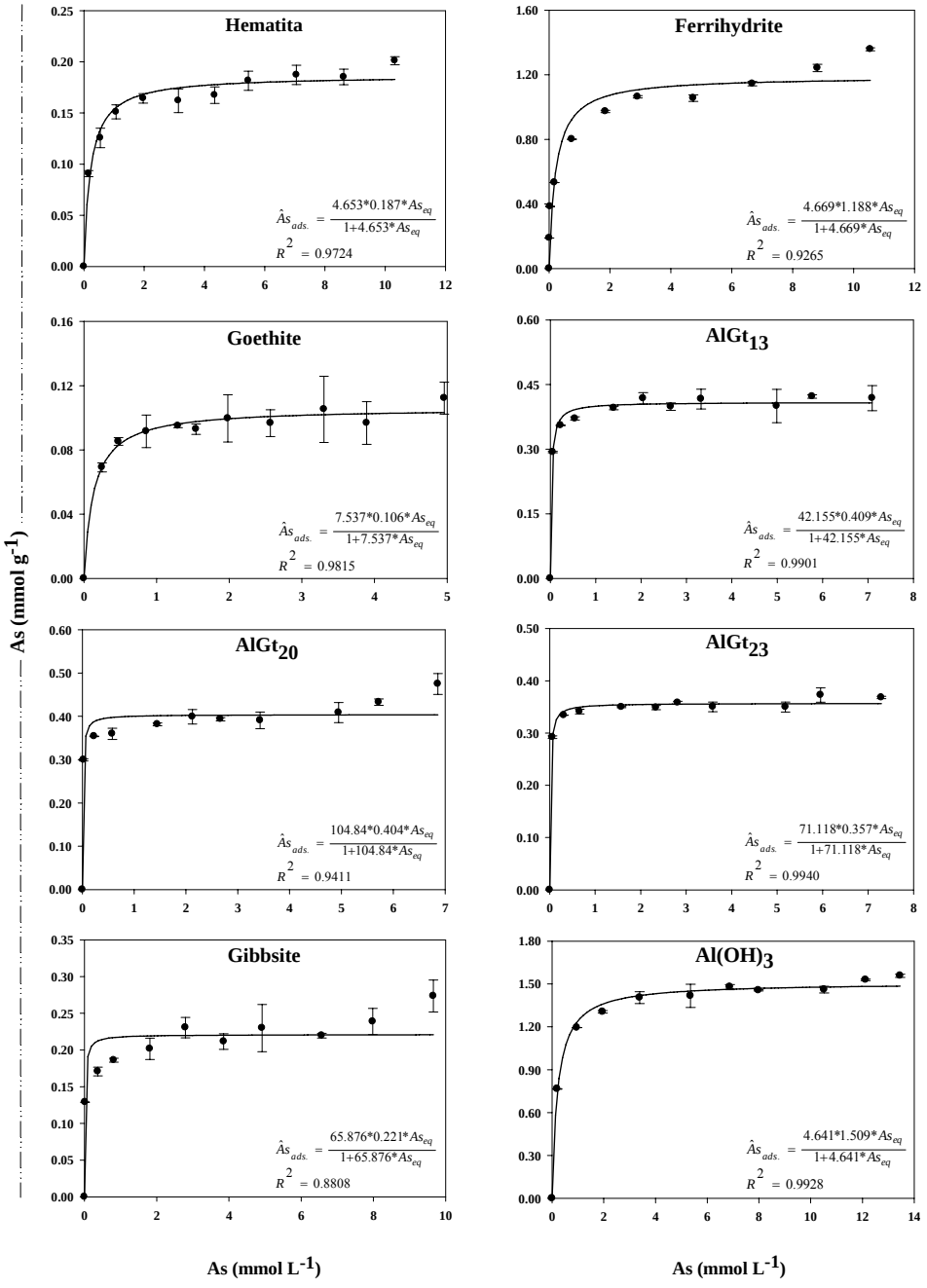

Figure 1 – Adsorption isotherm for synthetic Al and Fe (hydr)oxides. Solid line represents theoretical Langmuir model ($As_{ads} = K*b*As_{eq}/1+K*As_{eq}$) where As_{ads} is the maximum of adsorbed arsenate by the sorbent (mmol g^{-1}), K is the constant related to the energy of adsorption (L $mmol^{-1}$), b is the arsenate adsorption maximum (mmol g^{-1}), and As_{eq} is the equilibrium concentration of As(V) remaining in the solution (mmol L^{-1}). Data are represented as means ± standard error of the mean (n = 3); bars not visible are smaller than symbol.

these authors, the second region of the isotherm is the best suited to Langmuir's presupposition. Experimental data presented a good fit to the Langmuir equation, with correlation coefficient (r^2) values higher than 0.99 (Table 2).

Incorporation of Al in the goethite structure favoured the adsorption of As(V) in relation to pure goethite, and other crystalline phases, i.e. Hm and Gb. According to Schulze and Schwertmann (1987) goethite crystals become smaller as Al-substitution increases, changing its structure from polydomainic crystals to smaller monodomainic ones. Likewise, the incorporation of aluminium can also lead to structural defects with cation deficiency in the goethite framework (Gonzales et al. 2002) that contributes to increase the number of surface reactive sites, which is in agreement with their relatively large surface areas. Even though a large arsenate adsorption had been observed on AlGts, the Langmuir adsorption maxima (b) somewhat diminished with further increases in Al:Fe molar ratio (Table 2). This suggest a higher affinity between As and structural iron at the AlGts surface as reflected by the increase in As adsorbed per mol of iron. Decreasing of arsenate adsorption with the increase of structural Al was reported by Masue et al. (2007) to coprecipitated Al:Fe hydroxides. On the other hand, the lower As(V) adsorption capacity could be attributed to fewer surface reactive hydroxyls or water groups in well crystallised Hm, Gb, and pure Gt. Our results for maximum As(V) adsorptions agree well with the findings of previous work: poorly crystalline aluminium hydroxides of approximately 1.6 mmol g^{-1} at pH 5 (Anderson et al., 1976; Garcia-Sanchez et al., 2002), goethite ranging from 0.04 up to 0.186 mmol g^{-1} with maximum pH at 3.0 (Manning and Goldberg, 1996; Liu and Violante, 2001), and ferrihydrite from 1.0 to >2.6 mmol g^{-1} at pH 5 (Fuller et al., 1993; Raven et al., 1998; Garcia-Sanchez et al., 2002).

Spectroscopic investigations, i.e. FTIR, EXAFS, XANES, have shown that arsenate adsorption on ferric compounds occur via ligand exchange with OH and OH_2 groups forming inner-sphere mono or binuclear complexes (Manceau, 1995; Sun and Doner, 1996; Fendorf et al., 1997; Grossl et al., 1997; Sherman and Randall, 2003; Makris et al., 2007). EXAFS studies have shown that arsenate adsorption on ferrihydrite and goethite occurs predominantly as bidentate bridging complex and the formation of monodentate surface occurs to only at a limited extent and low surface coverage (Waychunas et al., 1993; Fendorf et al., 1997). The formation of stable complexes has been also reported for

Table 2 – Adsorption maxima (b), binding constant (*K*), and correlation coefficient (r^2) of the linear form of the Langmuir Isotherm for arsenate adsorption onto different Fe and Al compounds

Adsorbent	**b**			***K***	**R^2**
	--- mmol g^{-1} ---	**--- mmol m^{-2} ---**	**--- mmol mol^{-1} Fe ---**	**--- L $mmol^{-1}$ ---**	
Hm	0.193	0.0055	16.409	2.562	0.9949
Gb	0.228	0.0050	18.415[a/]	7.116	0.9964
Gt	0.101	0.0049	9.806	10.188	0.9988
$AlGt_{13}$	0.417	0.0035	51.010	22.301	0.9988
$AlGt_{20}$	0.395	0.0032	54.462	35.401	0.9996
$AlGt_{23}$	0.365	0.0032	53.5187	13.634	0.9975
Fh	1.258	0.0047	132.896	2.0408	0.9932
$Al(OH)_3$	1.498	0.1805	188.813[a/]	4.1620	0.9995

[a/] mmol mol^{-1} of Al.

aluminium hydroxides and gibbsite (Foster et al., 1998; Ladeira et al., 2001; Goldberg and Johnson, 2001; Arai and Sparks, 2002; Liu et al., 2006). Therefore, these complexes have likely been formed in our materials. However, further spectroscopic evidences are warranted to certificate the type of surface complexes preferentially formed at our conditions.

Calculated *K* values from the Langmuir function showed the following order: $AlGt_{20}$ > $AlGt_{13}$ > $AlGt_{23}$ > Gt > Gb > $Al(OH)_3$ > Hm ≥ Fh. Though the empirical *K* values has little or no significance as a theoretical chemical binding constant, this constant is rather useful for assessing comparative adsorption behaviour of different materials (Lafferty and Loeppert, 2005). In general, the crystalline adsorbents demonstrated higher arsenate retention capacity than poorly crystalline ones, except for Hm which *K* value laid close to Fh. Higher *K* values for Gt than Fh indicates its relative strong retention capacity for arsenate. Similar results were reported by Dixit and Hering (2003) and Lafferty and Loeppert (2005). Al-substituted goethites demonstrated higher affinity in adsorbing arsenic than pure Gt suggesting that incorporation of Al affect positively the interaction between arsenic and iron (hydr)oxides, however, no trend was observed between *K* value and Al content. Masue et al. (2007) also observed strong retention capacity of arsenate to coprecipitated Al:Fe hydroxides, but the affinity decreased as Al:Fe molar ratio was increased.

The maximum As(V) adsorption capacity decreased in the following order: $Al(OH)_3$ > Fh > $AlGt_{13}$ > $AlGt_{20}$ > $AlGt_{23}$ > Gb > Hm > Gt. The higher amount of arsenate adsorbed by poorly crystalline $Al(OH)_3$ and Fh could be attributed to their considerably larger specific surface area. The higher adsorption efficiency verified for $Al(OH)_3$ in comparison with Fh was also reported by Garcia-Sanchez et al. (2002). They attributed such results to different types of isotherm as classified by Giles et al (1960) (see also in Garcia-Sanchez et al., 2002). According to these authors adsorption isotherms for poorly crystalline aluminium hydroxides is H (high affinity) while for Fh is L (Langmuirian) type. This mean that aluminium hydroxides initially has such a strong affinity for As(V) that in short time the anions are almost completely adsorbed in diluted solutions. As the sites in aluminium hydroxides surface are occupied, it becomes increasingly more difficult for As(V) anions to react to empty active sites in the adsorbent. On the other hand, this adsorption pattern was not observed for Fh, being slower and likely taking place in two steps. Fuller et al. (1993) also observed an initial rapid adsorption rate of arsenate on ferrihydrite followed by a much slower kinetic due to a diffusion-controlled rate-determining step.

In general, the AlGts showed high As(V) loading capacity per mol of Fe being 3.2 and 5.4 times higher than Hm and pure Gt, respectively, but 2.5 times smaller than Fh (Table 2).

Normalized adsorption data by surface area demonstrated that the arsenate loading capacity was similar to Gb, Hm, and Gt followed by Fh and somewhat lower for AlGts (Figure 2). These results indicated that surface sites for Fh were not fully occupied by As(V) anions, as we obtained an adsorption density (≅ 0.13 mol mol^{-1} Fe) lower than the maximum stated to Fh by Dixit and Hering (2003) and reference therein, i.e. 0.25 mol mol^{-1} Fe at pH near to 4.6. This behaviour could be attributed to the relative short time frame adopted herein (24 h), therefore, our result is consistent with previous reported data, ranging from 0.11 up to 0.14 mol mol^{-1} Fe (Ferguson and Anderson, 1974; Raven et al., 1998; Pierce and Moore, 1982).

3.2. As(V) Adsorption kinetics. Adsorption kinetics of As(V) followed two different phase patterns (Figure 3). An initial fast phase corresponding to adsorption in the first couple of hours, and then, a slower phase from 2 to 92 hours. This finding is in line with

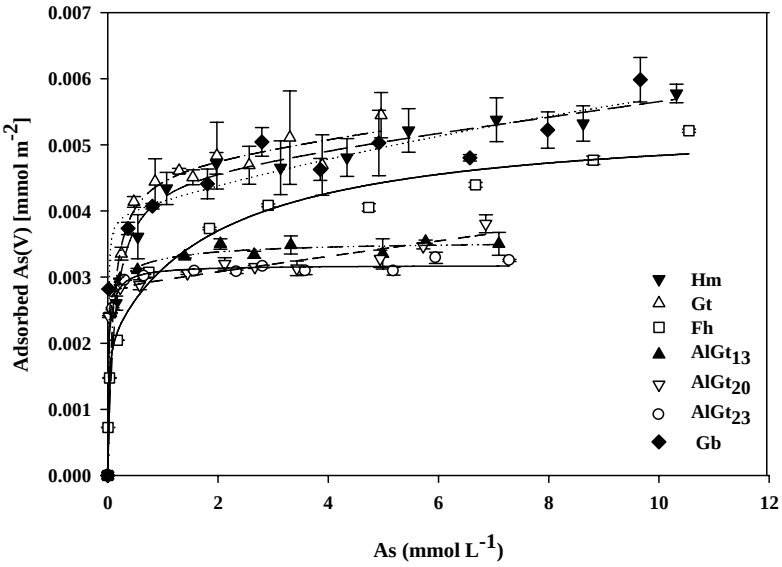

Figure 2 – Arsenate adsorption onto different Al and Fe (hydr)oxides normalized by specific surface area. Data are represented as means ± standard error of the mean (n = 3); bars not visible are smaller than symbol

those reported previously (Fuller et al., 1993; Hongshao and Stanforth, 2001). According to Hongshao and Stanforth (2001) adsorption in the first phase corresponds to irreversibly bound ion, while further slowly adsorbed ions are weakly bounded and easily exchanged by a competing anion, e.g. phosphate, silicate, and carbonate, etc. Many mechanisms are thought to be related to the second phase, such as precipitation on the surface, diffusion into surface pores or in the adsorbent matrix, formation of a solid-solution on the surface, or coagulation of the adsorbent particles. Though we have no spectroscopic evidence, we suppose that anion-induced dissolution (Hongshao and Stanforth, 2001) and diffusion-controlled (Raven et al., 1998; Fuller et al., 1993) mechanisms played the main role on As sequestration by the mineral surfaces over the time. Since an anion is adsorbed in a nonexchangeable form during initial phase, it can act as sorption sites for dissolved Al and, or, Fe. This causes a decrease in the dissolved concentration of these cations at the external solution, which along with the presence of anions in solution induce more aluminium and, or, iron to dissolve from the solid matrices. The attached Al or Fe in turns adsorbs more arsenate from external solution to form a surface precipitate. In addition, diffusion into

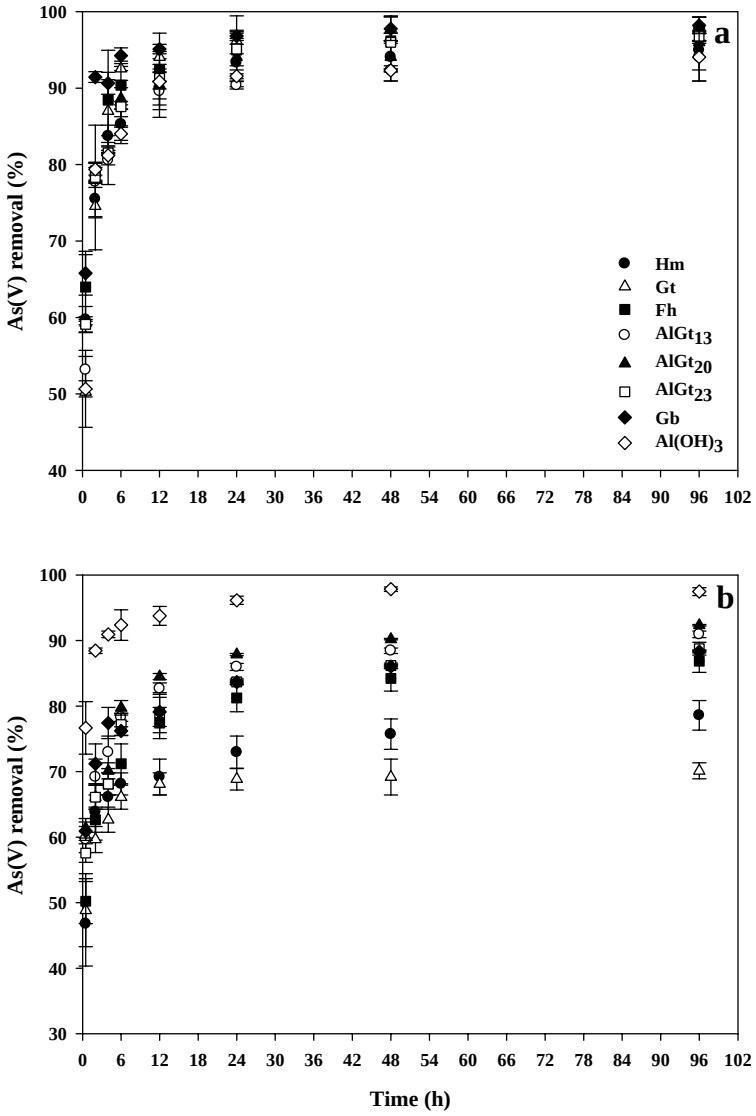

Figure 3 – As(V) adsorption kinetics by Al and Fe (hydr)oxides in a 2 g L^{-1} (a) and 5 g L^{-1} (b) suspension at pH 5.0 ±0.2. Data are represented as means ± standard error of the mean (n = 3); bars not visible are smaller than symbol

mineral particle should be also taking into account mainly for Fh and AlGts due to their elevated degree of structural disorder. This hypothesis is based upon the time dependence which is well characterised in our experiment, i.e. a rapid equilibrium being attained in the subset of surface sites located near the exterior of aggregates, as stated by Fuller et al. (1993). The ionic substitution of Al for Fe in the structure of goethite has a marked effect

on goethite properties. Variations in crystal size, shape and surface area, structural OH content, and dissolution behaviour were observed due to Al for Fe substitution in goethite structure (Murad and Schwertmann, 1983; Schwertmann, 1984; Schulze and Schwertmann, 1987; Torrent et al., 1987; Jeanroy et al., 1991).

For the smaller solid:solution ratio, 2.0 g L^{-1}, As(V) adsorption was over 94 % during the time frame. The increase in solid concentration affected arsenic removal by most adsorbents, especially, Gt and Hm, which efficiencies were depleted from ~98 and ~95 % to ~70 and ~78 %, respectively (Figures 1a and 1b). The decrease in adsorption density was consistent with visual observation that clearly indicated increasingly aggregation of goethite particles at higher solid concentrations. Although no visual aggregation was verified for the other adsorbents, we suppose that this phenomenon might have also happened, limiting As(V) adsorption at higher solid concentrations.

3.3. As(V) Adsorption Envelopes. Changes in the pH affected the sorption process of As(V) anions by Al and Fe (hydr)oxides (Figure 4), as widely reported in the literature (Anderson et al., 1976; Pierce and Moore, 1982; Manning and Goldberg, 1997; Lafferty and Loeppert, 2005; Garcia-Sanchez et al., 2002; Deschamps et al., 2003; Masue et al., 2007). In general maximum adsorption was obtained at pH range from 3.5 up to 5.5. Under such conditions, the monovalent anion ($H_2AsO_4^-$) is the dominant species. This implies that As(V) adsorption may be described by surface complexation models involving ligand exchange of surface hydroxyl groups, mainly with the surface OH_2 rather than surface OH groups. Low pH causes protonation of $–OH^{-1/2}$ groups to $OH_2^{+1/2}$, which facilitate the ligand exchange since H_2O is easier to detach from metal binding sites than OH (McBride, 1994). In this case the dissociation of H^+ from H_3AsO_4 also is considered to contribute to both, the protonation of surface OH groups and the increase of negatively charged adsorbate ($H_2AsO_4^-$). These effects, however, are counterbalanced by the decrease in the net positive charge as the pH increases to the point of zero charge (pH_{PZC}).

In general, the adsorption envelope followed a similar trend, indicating similar arsenate adsorption mechanism for all materials. It is worth of note, a more pronounced decrease in As(V) retention as the pH approaches to the second pK of the arsenic acid ($pK_{a2} = 6.9$). It is well known that specific adsorption affects the surface net charge,

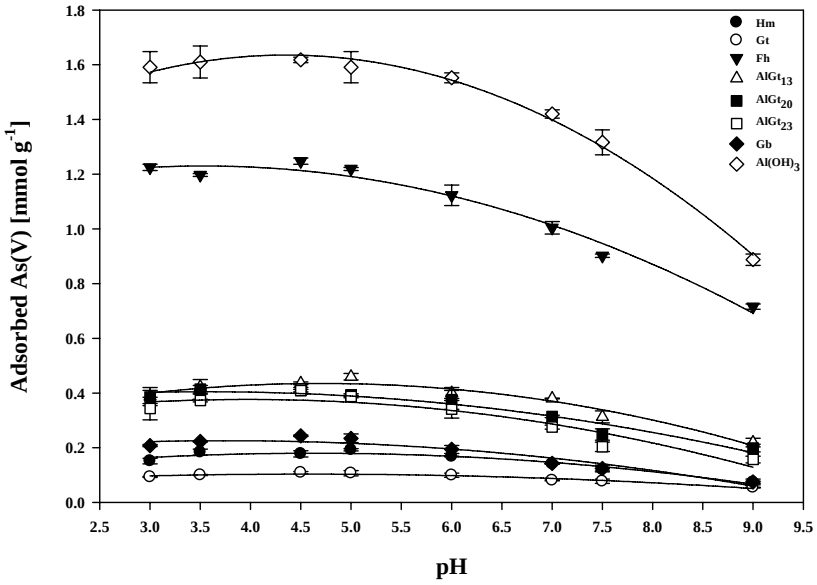

Figure 4 – Adsorption envelope for the reaction of arsenate with hematite, goethite, ferrihydrite, Al-substituted goethites, gibbsite, and aluminium hydroxides. Data are represented as means ± standard error of the mean (n = 3); bars not visible are smaller than symbol

conditioning the pH_{PZC} to a lower value. For example, Anderson et al. (1976) observed that the pH_{PZC} of aluminium hydroxides decreased from 8.5 to 4.6 after loaded with arsenate. For ferrihydrite, Jain et al. (1999) reported a decrease of 2.4 pH unit, from 8.5 to 6.1. A similar observation was reported by Ladeira and Ciminelli (2004) for goethite and gibbsite. This behaviour is also expected to other iron (hydr)oxides due to arsenate adsorption. Thereby, the decrease in arsenate adsorption as the pH rises can be due to two interacting factors: the decrease of positive net surface charge and the attachment of adsorbate which creates additional negative surface charges inducing repulsion of As(V) anions in the external solution and increasingly occupy available sites for adsorption.

4. **CONCLUSIONS**

The results clearly show that incorporation of structural Al into goethite minerals increases arsenate adsorption capacity. AlGts presented As(V) adsorption capacities almost

4 times higher than pure goethite. Arsenate adsorption onto Al and Fe (hydr)oxides is strongly influenced by pH, in a such way that maximum adsorption is achieved at slightly acidic conditions. Arsenate retention patterns suggested formation of stable, probably inner-sphere binuclear complexes, involving ligand exchange with the OH_2 groups. Notwithstanding, further spectroscopic studies are warranted to certificate the type of surface complexes are preferentially formed between As(V) and Al-substituted goethites.

In spite of the preference for iron in water treatment processes, aluminium (hydr)oxides revealed to be more efficient in adsorbing soluble As(V). Maximum adsorption of arsenate was higher on poorly crystalline $Al(OH)_3$ than on ferrihydrite. Similarly, gibbsite presented higher As(V) adsorption than hematite or goethite. Al-substituted goethites showed intermediate adsorption efficiency and can be considered promising materials to remove arsenic from contaminated water.

5. REFERENCE

Anderson, L.C.D., Bruland, K.W., 1991. Biogeochemistry of arsenic in natural waters: the importance of methylated species. Environ. Sci. Technol. 25: 420-427.

Anderson, M.A., Ferguson, J.F., Gavis, J., 1976. Arsenate adsorption on amorphous aluminum hydroxide. J. Colloid Interf. Sci. 54: 391-399.

Arai, Y., Sparks, D.L. 2002. Residence time effects on arsenate surface speciation at the aluminum oxide-water interface. Soil Sci. 167: 303-314.

Cornell, R.M., Schwertmann, U. 2003. The iron oxides: structure, properties, reactions, occurrences and uses, 2nd ed. ed. Wiley-VCH, Weinheim ; [Cambridge].

Cummings, D.E., Caccavo, J.F., Fendorf, S., and Rosenzweig, F., 1999. Arsenic mobilization by the dissimilatory Fe(III)-reducing bacterium Shewanella alga BrY. Environ. Sci. Technol. 33, 723-729.

Deschamps, E., Ciminelli, V.S.T., Frank, L.F.T., Matschullat, J., Rue, B., and Schmidt, H., 2002. Soil and sediment geochemistry of the Iron Quadrangle, Brazil: the case of arsenic. J. Soil Sed. 2, 216-222.

Deschamps, E., Ciminelli, V.S.T., Holl, W.H., 2005. Removal of As(III) and As(V) from water using a natural Fe and Mn enriched sample. Water Res. 39, 5212-5220.

Deschamps, E., Ciminelli, V.S.T., Weidler, P.G., and Ramos, A.Y., 2003. Arsenic sorption onto soils enriched in Mn and Fe minerals. Clays Clay Miner. 51, 197-204.

Dixit, S. and Hering, J.G., 2003. Comparison of arsenic(V) and arsenic(III) sorption onto iron oxide minerals: Implications for arsenic mobility. Environ. Sci. Technol. 37, 4182-4189.

Driehaus, W., Jekel, M., and Hildebrandt, U., 1998. Granular ferric hydroxide - a new adsorbent for the removal of arsenic from natural water. *J. Water Supply Res. Technol*. 47, 30 - 35.

Fendorf, S., Eick, M.J., Grossl, P., and Sparks, D.L., 1997. Arsenate and Chromate Retention Mechanisms on Goethite. 1. Surface Structure. Environ. Sci. Technol. 31, 315-320.

Ferguson, J.F., and Anderson, M.A., 1974. Chemical forms of arsenic in water supplies and their removal., in: Rubin, A.J. (Ed.), Chemistry of water supply, treatment, and distribution. Ann Arbor Science, Ann Arbor, MI, pp. 137-158.

Foster, A.L., Brown Jr., G.E., Tingle, T.N, and Parks, G.A., 1998. Quantitative arsenic speciation in mine tailings using X-ray absorption spectroscopy. Am. Miner. 83, 553-568.

Fuller, C.C., Davis, J.A., and Waychunas, G.A., 1993. Surface-Chemistry of Ferrihydrite .2. Kinetics of Arsenate Adsorption and Coprecipitation. Geochim. Cosmochim. Acta 57, 2271-2282.

Garcia-Sanchez, A., Alvarez-Ayuso, E., and Rodriguez-Martin, F., 2002. Sorption of As(V) by some oxyhydroxides and clay minerals. Application to its immobilization in two polluted mining soils. Clay Miner. 37, 187-194.

Goldberg, S., Johnston, C.T., 2001. Mechanisms of Arsenic Adsorption on Amorphous Oxides Evaluated Using Macroscopic Measurements, Vibrational Spectroscopy, and Surface Complexation Modeling. J. Colloid Interf. Sci. 234, 204-216.

Gonzalez, E., Ballesteros, M.C., and Rueda, E.H., 2002. Reductive dissolution kinetics of Al-substituted goethites. Clays Clay Miner. 50, 470-477.

Grossl, P.R., Eick, M., Sparks, D.L., Goldberg, S., and Ainsworth, C.C., 1997. Arsenate and Chromate Retention Mechanisms on Goethite. 2. Kinetic Evaluation Using a Pressure-Jump Relaxation Technique. Environ. Sci. Technol. 31, 321-326.

Hongshao, Z. and Stanforth, R., 2001. Competitive Adsorption of Phosphate and Arsenate on Goethite. Environ. Sci. Technol. 35, 4753-4757.

Jain, A., Raven, K.P., and Loeppert, R.H., 1999. Arsenite and Arsenate Adsorption on Ferrihydrite: Surface Charge Reduction and Net OH- Release Stoichiometry. Environ. Sci. Technol. 33, 1179-1184.

Jeanroy, E., Rajot, J.L., Pillon, P., and Herbillon, A.J., 1991. Differential Dissolution of Hematite and Goethite in Dithionite and Its Implication on Soil Yellowing. Geoderma 50, 79-94.

Jekel M. (1994). Arsenic removal in water treatment. In: Nriagu J. (ed.), Arsenic in the environment, 433-446.

Kyle J.H., Posner A.M., and Quirk J.P. (1975). Kinetics of isotopic exchange of phosphate adsorbed on gibbsite. J. Soil Sci. 26, 34-43.

Ladeira, A.C.Q. and Ciminelli, V.S.T., 2004. Adsorption and desorption of arsenic on an oxisol and its constituents. Water Research 38, 2087-2094.

Ladeira, A.C.Q., Ciminelli, V.S.T., Duarte, H.A., Alves, M.C.M., and Ramos, A.Y., 2001. Mechanism of anion retention from EXAFS and density functional calculations: Arsenic (V) adsorbed on gibbsite. Geochim. Cosmochim. Acta 65, 1211-1217.

Lafferty, B.J. and Loeppert, R.H., 2005. Methyl Arsenic Adsorption and Desorption Behavior on Iron Oxides. Environ. Sci. Technol. 39, 2120-2127.

Liu, F., De Cristofaro, A., and Violante, A., 2001. Effect of pH, phosphate and oxalate on the adsorption/desorption of arsenate on/from goethite. Soil Science 166, 197-208.

Liu, Y.T., Wang, M.K., Chen, T.Y., Chiang, P.N., Huang, P.M., and Lee, J.F., 2006. Arsenate Sorption on Lithium/Aluminum Layered Double Hydroxide Intercalated by Chloride and on Gibbsite: Sorption Isotherms, Envelopes, and Spectroscopic Studies. Environ. Sci. Technol. 40, 7784-7789.

Makris, K.C., Sarkar, D., Parsons, J.G., Datta, R., and Gardea-Torresdey, J.L., 2007. Surface arsenic speciation of a drinking-water treatment residual using X-ray absorption spectroscopy. J. Colloid Interf. Sci. 311, 544-550.

Manceau, A., 1995. The mechanism of anion adsorption on iron oxides: Evidence for the bonding of arsenate tetrahedra on free Fe(O, OH)6 edges. Geochim. Cosmochim. Acta 59, 3647-3653.

Manna, B.R., Dey, S., Debnath, S., and Ghosh, U.C., 2003. Removal of arsenic from groundwater using crystalline hydrous ferric oxide (CHFO). Water Qual. Res. J. Canada 38, 193-210.

Manning, B.A. and Goldberg, S., 1996. Modeling competitive adsorption of arsenate with phosphate and molybdate on oxide minerals. Soil Sci. Soc. Am. J. 60, 121-131.

Manning, B.A. and Goldberg, S., 1997. Adsorption and Stability of Arsenic(III) at the Clay Mineral-Water Interface. Environ. Sci. Technol. 31, 2005-2011.

Masue, Y., Loeppert, R.H., and Kramer, T.A., 2007. Arsenate and Arsenite Adsorption and Desorption Behavior on Coprecipitated Aluminum:Iron Hydroxides. Environ. Sci. Technol. 41, 837-842.

Matschullat, J., 2000. Arsenic in the geosphere - a review. The Sci. Total Environ. 249, 297-312.

Matschullat, J., Borba, R.P., Deschamps, E., Figueiredo, B.R., Gabrio, T., and Schwenk, M., 2000. Human and environmental contamination in the Iron Quadrangle, Brazil. App. Geochemi. 15, 181-190.

Maurice P.A., Lee Y.J., and Hersman L.E. (2000). Dissolution of Al-substituted goethites by an aerobic Pseudomonas mendocina var. bacteria. Geochim. Cosmochim. Acta 64, 1363–1374.

McBride, M.B., 1994. Environmental chemistry of soils. Oxford University Press, New York.

Mello, J., Roy, W., Talbott, J., and Stucki, J., 2006. Mineralogy and Arsenic Mobility in Arsenic-rich Brazilian Soils and Sediments. Journal of Soils and Sediments 6, 9-19.

Murad, E., Schwertmann, U., 1983. The Influence of Aluminum Substitution and Crystallinity on the Mossbauer-Spectra of Goethite. Clay Miner. 18, 301-312.

NHMRC & NRMMC, 2004. Australian drinking water guidelines. National Water Quality Management Strategy Paper No 6, National Health and Medical Research Council and Natural Resource Management Ministerial Council, Australian Government Publishing Service, Canberra.

Ona-Nguema, G., Morin, G., Juillot, F., Calas, G., and Brown, G.E., 2005. EXAFS analysis of arsenite adsorption onto two-line ferrihydrite, hematite, goethite, and lepidocrocite. Environ. Sci. Technol. 39, 9147-9155.

Pierce, M.L. and Moore, C.B., 1982. Adsorption of Arsenite and Arsenate on Amorphous Iron Hydroxide. Water Res. 16, 1247-1253.

Raven, K.P., Jain, A., and Loeppert, R.H., 1998. Arsenite and Arsenate Adsorption on Ferrihydrite: Kinetics, Equilibrium, and Adsorption Envelopes. Environ. Sci. Technol. 32, 344-349.

Schnoor, J.L., 1996. Environmental modeling : fate and transport of pollutants in water, air, and soil. J. Wiley, New York.

Schulze, D.G. and Schwertmann, U., 1987. The Influence of Aluminum on Iron-Oxides .13. Properties of Goethites Synthesized in 0.3-M Koh at 25-Degrees-C. Clay Miner. 22, 83-92.

Schwertmann, U., 1984. The Influence of Aluminum on Iron-Oxides .9. Dissolution of Al-Goethites in 6m HCl. Clay Miner. 19, 9-19.

Schwertmann, U., 1991. Solubility and Dissolution of Iron-Oxides. Plant and Soil 130, 1-25.

Schwertmann, U. and Cornell, R.M., 2000. Iron oxides in the laboratory : preparation and characterization, 2nd, completely rev. and extended ed. ed. Wiley-VCH, Weinheim; Chichester.

Sherman, D.M. and Randall, S.R., 2003. Surface complexation of arsenie(V) to iron(III) (hydr)oxides: Structural mechanism from ab initio molecular geometries and EXAFS spectroscopy. Geochim. Cosmochim. Acta 67, 4223-4230.

Sierra-Alvarez, R., Field, J.A., Cortinas, I., Feijoo, G., Teresa Moreira, M., Kopplin, M., and Jay Gandolfi, A., 2005. Anaerobic microbial mobilization and biotransformation of arsenate adsorbed onto activated alumina. Water Res. 39, 199-209.

Silva, J., Mello, J.W.V., Ciminelli, V.S.T., Dantas, M.S.S., Abrahao, W.A.P., and Gasparon, M., 2008. Raman spectroscopy of As(V) loaded Al and Fe (hydr)oxides. (To be submitted)

Singh, T.S. and Pant, K.K., 2004. Equilibrium, kinetics and thermodynamic studies for adsorption of As(III) on activated alumina. Sep. Pur. Technol. 36, 139-147.

Smedley, P.L. and Kinniburgh, D.G., 2002. A review of the source, behaviour and distribution of arsenic in natural waters. Appl. Geochem. 17, 517-568.

Smedley, P.L., Zhang, M., Zhang, G., and Luo, Z., 2003. Mobilisation of arsenic and other trace elements in fluviolacustrine aquifers of the Huhhot Basin, Inner Mongolia. Appl. Geochem. 18, 1453-1477.

Stumm, W. and Sulzberger, B., 1992. The Cycling of Iron in Natural Environments - Considerations Based on Laboratory Studies of Heterogeneous Redox Processes. Geochim. Cosmochim. Acta 56, 3233-3257.

Sun, X.H. and Doner, H.E., 1996. An investigation of arsenate and arsenite bonding structures on goethite by FTIR. Soil Sci. 161, 865-872.

Torrent, J., Schwertmann, U., and Barron, V., 1987. The Reductive Dissolution of Synthetic Goethite and Hematite in Dithionite. Clay Miner. 22, 329-337.

Torrent, J., Schwertmann, U., and Barron, V., 1992. Fast and slow phosphate sorption by goethite-rich natural materials. Clays and Clay Miner. 40, 14-21.

Waychunas, G.A., Rea, B.A., Fuller, C.C., and Davis, J.A., 1993. Surface-Chemistry of Ferrihydrite .1. Exafs Studies of the Geometry of Coprecipitated and Adsorbed Arsenate. Geochim. Cosmochim. Acta 57, 2251-2269.

Wickramasinghe, S.R., Han, B.B., Zimbron, J., Shen, Z., and Karim, M.N., 2004. Arsenic removal by coagulation and filtration: comparison of groundwaters from the United States and Bangladesh. Desalination 169, 231-244.

Wilkie, J.A. and Hering, J.G., 1996. Adsorption of arsenic onto hydrous ferric oxide: Effects of adsorbate/adsorbent ratios and co-occurring solutes. Colloids Surf. a-Physicochem. Engin. Asp. 107, 97-110.

Chapter 3

EFFECT OF BACTERIAL IRON REDUCTION AND COMPETING ION ON ARSENIC MOBILISATION

ABSTRACT

Arsenic mobility is controlled by iron and aluminium oxides in most environment, therefore, the use of these minerals in water treatment plants for removing arsenic has been investigated extensively. In anoxic environment dissimilatory iron reducing bacteria plays a fundamental role in catalysing the redox transformations that ultimately control the mobility of As in aquatic environment. Thus, we investigated the stability of arsenic retained by aluminium and iron (hydr)oxides under anoxic conditions in the presence of *Shawanella putrefaciens* cells, and phosphate or carbonate as competing anions. As(V) loaded samples of synthetic hematite (Hm), goethite (Gt), 2-line ferrihydrite (Fh), gibbsite (Gb), aluminium hydroxide [$Al(OH)_3$], and three Al-substituted goethites containing 13, 20, and 23 cmol mol^{-1} of Al ($AlGt_{13}$, $AlGt_{20}$, and $AlGt_{23}$, respectively) were anaerobically incubated under N_2 atmosphere and periodically sampled to evaluate the contents of soluble As in the supernatants. It was found that *S. putrefaciens* cells were able to bind on mineral surfaces and utilise both noncrystalline and crystalline iron (hydr)oxides as electron acceptor releasing arsenic into solution. Al-substituted goethites presented a decrease in the fraction of soluble iron and mobilised arsenic as structural Al increased. The expected relationship between specific surface area and reductive dissolution of Fe and As was also affected by the increment in structural Al. Phosphate and carbonate affected the kinetics of iron reduction due to precipitation of soluble iron as metastable mineral phases (e.g. vivianite and siderite). It seems that analogous mineral phases of phosphates served as a sink for As limiting its mobilisation. Phosphate competed strongly with arsenate and its efficiency seemed to be governed by the nature of the binding mechanism between As and adsorbent surface. Higher fraction of arsenic was desorbed by phosphate from gibbsite followed by AlGts. Conversely, only Gb showed significant amounts of arsenate displaced by carbonate. In spite of low crystallinity, $Al(OH)_3$ was the most efficient in retaining arsenate on its surface followed by Fh and Hm.

Keywords: biological reduction, arsenate, phosphate, carbonate, Al-substituted goethite, Al and Fe hydroxides.

1. INTRODUCTION

Arsenic contamination is an environmental, ecological and health concern. Due to new evidences of its carcinogenic effect, the World Health Organisation (WHO) has recommended to reduce the maximum arsenic level from 50 to 10 μg L^{-1} in drinking water. This regulatory limit has been adopted by many countries. Therefore, development of new technologies for arsenic removal from water has currently been a challenge to researchers worldwide. The input of arsenic in the environment is attributed to natural and anthropogenic sources which are related to weathering of As-bearing rocks, leakage of As-rich thermal waters to shallow aquifers, mining and smelting activity, pesticides and wood preservative uses, as well as its use as growth promoter for animals (Matschullat, 2000; Smedley and Kinniburg, 2002).

In aquatic environment arsenic can be found as inorganic and organic compounds, in several valence states, i.e. -3, -1, 0, +3, and +5. In natural water arsenic occurs mainly in inorganic forms as trivalent arsenite [As(III)] (as H_3AsO_3) or pentavalent arsenate [As(V)] (as $H_2AsO_4^-$ and $HAsO_4^{2-}$). In addition, in marine waters and lakes arsenic can undergo microbial methylation and both As(III) and As(V) can coexist with monomethilarsonic acid (MMA), and dimethilarsinic acid (DMA). Furthermore, redox potential (Eh) and pH control the distribution of arsenic species (e.g. $H_3AsO_4/H_2AsO_4^-$ $pK_{a1} = 2.2$; $H_2AsO_4^-/HAsO_4^{2-}$ $pK_{a2} = 6.9$; $HAsO_4^{2-}/AsO_4^{3-}$ $pK_{a3} = 11.4$). As(III) is expected to be the dominant species in anoxic conditions, but because of relatively slow transformation on the redox conditions, both species, As(III) or As(V), can be often found in either redox environment.

The aluminium and iron (hydr)oxides are ubiquitous reactive constituents of soil, sediments and aquifers. Due to high reactivity they play a fundamental role on the biogeochemical cycle of many elements (e.g. P, S, As, Pb, etc.). For this reason, the distribution of arsenic is mostly controlled by both, Al and Fe (hydr)oxides, in most oxidised environment, and the main technologies to remove arsenic from contaminated water are based on coagulation/precipitation or adsorption processes involving aluminium or ferric compounds. General experience has shown that aluminium salts are less efficient than ferric ones to remove arsenic from water. McNeil and Edwards (1997) reported that when ferric coagulants are added at water treatment plants, most of the Fe^{3+} precipitates as insoluble ferric hydroxide. In aluminium precipitation, however, a significant portion of the

added Al^{3+} remains as soluble complexes. Then, because only particulate metal hydroxides can mediate arsenic removal, alum plants must carefully consider aluminium solubility when arsenic removal is required in water treatment plants.

Although ferric compounds have lower solubility in relation to aluminium ones, they are unstable under low Eh conditions. In the absence of oxygen, Fe(III) minerals can be used as electron acceptor during microbial respiration (Lovley et al., 2004). In this process, bacteria coupled hydrogen and organic carbon oxidation to the reduction of Fe(III). Therefore, based on the association between many trace element and Fe(III) (hydr)oxides, and the tendency of these minerals to be dissolved under suboxic conditions, biological iron reduction can have a major impact on the persistence and mobility of toxic elements, radionuclides, and organic contaminants under such conditions (Lovley et al., 1993; Cummings et al., 1999; Zachara et al., 2001). Cummings et al. (1999) investigating the biological reduction of synthetic scorodite ($FeAsO_4 .2H_2O$), encountered that dissimilatory Fe reduction resulted in releasing of As(V) and Fe(II) into solution. Slower rate of reductive dissolution (chemical or microbiological) in the presence of Al substituting Fe in the iron (hydr)oxides structure was reported by Schwertmann (1984), Jeanroy et al. (1991), and reference therein. Torrent et al. (1987) observed that Al substitution depressed the reductive dissolution of synthetic goethite and hematite by dithionite/citrate/bicarbonate solution. Bousserrhine et al. (1999) also demonstrated that biological reduction of Al, Cr, Mn, and Co-substituted goethites was decreased as substitution increased. Al-goethite was more resistant to reductive dissolution than other substituted goethites.

Abiotic processes are also thought to be related to the decoupling of Al or Fe (hydr)oxides-associated arsenic. Natural attenuation of arsenic by adsorption on these minerals may be also limited due to competing oxyanions, in which one anion will normally be competing for the sorption sites (Hongshao and Stanforth, 2001; Sahai et al., 2007; Zang et al., 2008). Due to similar acid dissociation constants phosphate (pK_{a1} = 2.1, pK_{a2} = 7.2, pK_{a3} = 12.3) behaves much like arsenate (pK_{a1} = 2.2, pK_{a2} = 6.9, pK_{a3} = 11.4). In addition to phosphate, carbonate may also, to a lesser extent, limit the arsenate sorption reactions. The displacement of adsorbed As with dissolved carbonate was recently examined theoretically by Appelo et al. (2002), and this mechanism was proposed to be potentially one of the major reasons for high As concentrations in groundwater. Thus, it is

worthwhile to investigate the adsorption and replacement of one anion from mineral particles by another. In addition, investigations of the competition between the anions can provide insight into the reactions occurring on the surface (Hongshao and Stanforth, 2001).

By associating the higher binding affinity of Fe (hydr)oxides for arsenic and the higher stability of Al under anoxic conditions can be an advantageous alternative for removing arsenic from water. Few studies have focused on As sorption processes onto or As release by reductive dissolution of Al-substituted Fe (hydr)oxides. Masue et al. (2007) reported a decrease in both coprecipitated As(III) and As(V) adsorption onto aluminium:iron hydroxides as the Al:Fe molar ratio increased. Furthermore, desorption of As by phosphate competing ion was favoured by the increase of Al:Fe ratio. In view of these statement, the aim of this work was to investigate the decoupling of arsenate from Al-substituted goethites and other synthetic Al and Fe (hydr)oxides influenced by dissimilatory iron reduction and competing anions.

2. MATERIAL AND METHODS

2.1. Synthesis of Al and Fe (Hydr)oxides

Hematite (Hm), Goethite (Gt), and 2-line Ferrihydrite (Fh) were synthesised by neutralizing $Fe(NO_3)_3$ solution with KOH following the procedure outlined by Schwertmann and Cornell (2000). A series of aluminium substituted goethite with different Al:Fe ratios (15:50, 25:50, 35:50 v/v) was synthesised followed the methods therein. Al-substituted goethites were synthesized from ferrous and aluminium chloride solutions by precipitation with potassium hydroxides and aged in a plastic bottle during 90 days. Slow oxidation of Fe^{2+} to Fe^{3+} and incorporation of Al in the goethite structure were achieved by opening the bottle daily and stirring the suspensions vigorously during 5 minutes. In order to remove the excess of Al, precipitates were washed twice with 0.01 mol L^{-1} KOH solution, several times with Milli-Q water, centrifuged, and dried at 50 ^{o}C at an oven with air circulation. To remove the excess of electrolyte, precipitates of Fe (hydr)oxides were also washed several times with Milli-Q water until achieving minimum electrical conductivity. Samples were then centrifuged and dried at 50 ^{o}C at an oven with air circulation, except for Ferrihydrite which was freeze-dried.

Gibbsite (Gb) was prepared following the procedures outlined in Kyle et al. (1975). An $Al(NO_3)_3$ solution was titrated with 4 mol L^{-1} NaOH solution to a pH of 4.6 ± 0.2. The gelatinous precipitate was heated for two hours at 40 ^oC, then washed twice, dialyzed with Milli-Q water for 36 days and dried at 50 ^oC. The poorly crystalline aluminium hydroxide [$Al(OH)_3$] was also prepared from an aluminium nitrate solution by precipitation with 4 mol L^{-1} NaOH solution. The procedure was similar to that followed for the synthesis of gibbsite, but with the suppression of the heating step to preserve low crystallinity. Similarly to ferrihydrite, the aluminium hydroxide was freeze-dried in order to prevent its crystallization.

The specific surface area was determined by multipoint BET analyses with N_2 as adsorbent (Quantachrome model NOVA 1000). Particle size distribution was obtained from a laser analyser (Micromeritics Saturn Digisizer model 5200), respectively (Table 1).

2.2. As(V) Loaded Adsorbents. One gram of the adsorbents were loaded with arsenate from a 10 mmol L^{-1} $CaCl_2$ solution containing As(V) concentrations in a 250 mL polypropylene centrifuge tubes. Such concentrations were added to achieve the maximum adsorption capacity for each adsorbent, according to Silva et al. (2008). The pH was adjusted to 5.0 ±0.2 and the suspensions were equilibrated in a horizontal shaker during one week. The tubes were then centrifuged (3000 rpm, 30 min.), the supernatants filtered through 0.22 μm membrane filters (Millipore Millex-GV, USA), and storage for As analyses. The remaining solid phases were freeze-dried and stored for further incubation experiments. The amount of As(V) adsorbed was calculated by the difference between the initial and final As concentration in supernatants (Table 1). Checks containing arsenic in solution but no adsorbent material were used to measure the amount of arsenic adsorbed by the walls of the reaction vessels.

2.3. Bacterial Culture and Growth Medium. Cultures of *Shawanella putrefaciens* were obtained from Australian Collection of Microorganism at The University of Queensland. Bacteria were growth aerobically during 18 h to attain the log phase, and routinely cultured at 37 ^oC in sterile peptone yeast extract medium containing 10 g L^{-1} peptone, 5 g L^{-1} yeast, and 5 g L^{-1} NaCl at pH 7.2.

Table 1 – Surface area (SA), mean particle size (MPS), and adsorbed arsenic ($As_{adsorb.}$) of the different aluminium and ferric compounds. Data are represented as means ± standard error of the mean (n=3). (More details can be seen in Chapter 1)

Adsorbent	SSA	MPS	$As_{adsorb.}$ [a/]
	----- $m^2 g^{-1}$ -----	---------- μm ----------	---------- μmol g^{-1} ----------
Hm (α-Fe_2O_3)	34.8	0.20 ± 0.001	159.97 ± 2.68 [a/]
Fh ($Fe_5HO_8 . 4H_2O$)	260.4	23.47 ± 0.311	1,063.45 ± 45.10
Gt (α-FeOOH)	20.6	0.97 ± 0.022	77.92 ± 2.33
$AlGt_{13}$	119.4	11.33 ± 3.866	412.44 ± 1.90
$AlGt_{20}$	124.7	3.25 ± 0.466	407.75 ± 0.73
$AlGt_{23}$	113.2	2.55 ± 2.712	386.68 ± 3.02
Gb ($Al_2O_3 3H_2O$)	45.7	21.01 ± 0.460	215.88 ± 0.60
$Al(OH)_3$ [$Al(OH)_3 3H_2O$]	8.3	12.60 ± 1.313	1,541.22 ± 5.89

[a/] calculated by the difference between the initial and final As concentration in solution.

The composition of the basal medium used for reduction experiment was: 20 mmol L^{-1} NH_4Cl; 1.34 mmol L^{-1} KCl; 1.0 mmol L^{-1} $CaCl_2$; 0.34 mmol L^{-1} $MgCl_2$; and 20 mmol L^{-1} sodium lactate as the solo electron donor. The medium was extensively purged with high-purity N_2 and autoclaved at 121 ^oC during 20 min.

2.4. Incubation Experiments. In order to investigate the influence of dissimilatory iron reduction and the presence of competing anion on arsenic release from different As-loaded Al and Fe (hydr)oxides, a series of incubation experiments was carried out.

2.4.1. Dissimilatory Fe(III) reduction. As-loaded adsorbents (0.2000 g) were equilibrated with 96 mL of the sterile basal medium and 4.0 mL of *S. putrefaciens* cell suspension in a 125 mL screw cap plastic bottle. The mixture was buffered at pH 7.0 by adding 10 mmol L^{-1} 1,4-piperazinediethanesulfonic acid (PIPES). Then, the suspensions were purged with high-purity N_2 and anaerobically incubated in a glovebox for about 500 h. To investigate the possible influence of adsorbed arsenic in the bacterial activity, it was also carried out an assay with no As-loaded adsorbents.

2.4.2. Influence of competing anions. In order to investigate the effects of phosphate and carbonate on arsenic release under anaerobic conditions, two parallel experiments were carried out. Both were performed at the same conditions of the preceding experiment (section 2.4.1), with As-loaded adsorbents in the presence of *S putrefaciens*. The only difference was the addition of 5.0 mmol L^{-1} of phosphate (as KH_2PO_4) or 30 mmol L^{-1} of carbonate (as $NaHCO_3$) in the basal medium, as competing anions. In the latter experiment $NaHCO_3$ substituted the PIPES solution as pH buffer, lactate was supplied at 10 mmol L^{-1}, and As-loaded adsorbents at 1.0 g L^{-1}.

For all experiments checks were also carried out with no cell suspension. Aliquots were periodically taken, filtered through 0.22 μm membrane filters (Millipore Millex-GV, USA), acidified and stored for further analyses of Al, As, Fe, and P. The total volume of the aliquots did not exceed 10 % of the initial volume.

All chemical used were reagent grade and water was purified through a Milli-Q system. All cell additions, transferring, and culture samplings were performed with sterile syringe or pipette tips previously flushed with high-purity N_2. All assays were carried out in triplicates.

2.5. Analytical Techniques. Soluble Al, As, Fe, and P contents in the aliquots were measured by inductively coupled plasma optical emission spectroscopy (ICP-OES), using a Perkin Elmer Optima 3300 DV. Scandium was used as internal standard to correct for instrumental instabilities and matrix effect. Solution of this element was added to the aliquots to reach a final concentration of 44.5 μmol L^{-1}. Typical detection limits (3σ) of 0.42 μmol L^{-1} were obtained for As.

3. Results and Discussion.

3.1. Reduction of Fe(III) and Arsenic release. Contents of Al, As and Fe in solution were negligible in the control experiments, suggesting no As release due to Fe reduction at the absence of bacterial cell suspensions (data not shown). Initial low concentrations of Al (0.05 mmol L^{-1} and 0.075 mmol L^{-1} for gibbsite and poorly crystalline aluminium hydroxide, respectively) and As (< 1,6 μmol L^{-1}, for all of adsorbents) were ascribed to

dissolution-desorption equilibrium during the time period to set up the experiment (ca. 12 h). This result may be due to the relative high ionic strength (I=0.0252) of the basal medium, increasing the likelihood of the anion exchange. Thus, those initial concentrations were subtracted from further data to express solely effects associated to dissimilatory reduction.

Increases in soluble Fe was interpreted as dissimilatory reduction occurred for Fe(III) (hydr)oxides, indicating that they were able to support bacterial growth as electron acceptor, independent of the crystallinity or Al-substitution (Figure 1). All Fe(III) (hydr)oxides were partially reduced by bacteria, but the iron reduction rates were decreased for the As-loaded adsorbents (Figure 1b) in relation to no As-loaded ones (Figure 1a). For instance, higher percentages of reduced iron were obtained for $AlGt_{13}$, $AlGt_{20}$, and $AlGt_{23}$ without adsorbed arsenic which achieved respectively 12.8, 11.5, and 11.30 % in comparison with 8.1, 7.3, and 7.2 % observed in the presence of adsorbed arsenic. Additionally, Fe(II) production started earlier (< 48 h) in the absence of adsorbed As and just after 96 h of incubation time in its presence. These results indicate that adsorbed As not only delays, but also constrains the bacterial activity. The effect of arsenic on the bacterial activity can be better observed by the clear difference in iron reduction pattern for Fh (Figure 1a, and b). We evoked two hypotheses to explain this effect: (1) the toxicity of As *per se* to the bacterial cells; and (2) electrostatic repulsion between As-loaded (hydr)oxides and bacterial cells. The second hypothesis consider that *S. putrefaciens* cells present negative net charge at pH ≥ 4 (Claessens et al., 2004) and then they could easily attach to the positive surface of the iron (hydr)oxides at the conditions of this investigation (pH ≅ 7.0), as the point of zero charge (pH_{PZC}) is about 8-8.5 for most (hydr)oxides. Nevertheless, it is well known that specific adsorption of anions, e.g. phosphate or arsenate, modifies the mineral surfaces decreasing the pH_{PZC} up to four pH units (Arai and Sparks, 2001). Thus, by decreasing the pH_{PZC} adsorbed As would promote increases in the negative charge on the iron (hydr)oxide surfaces leading to electrostatic repulsion between bacterial cells and Fe(III) colloids.

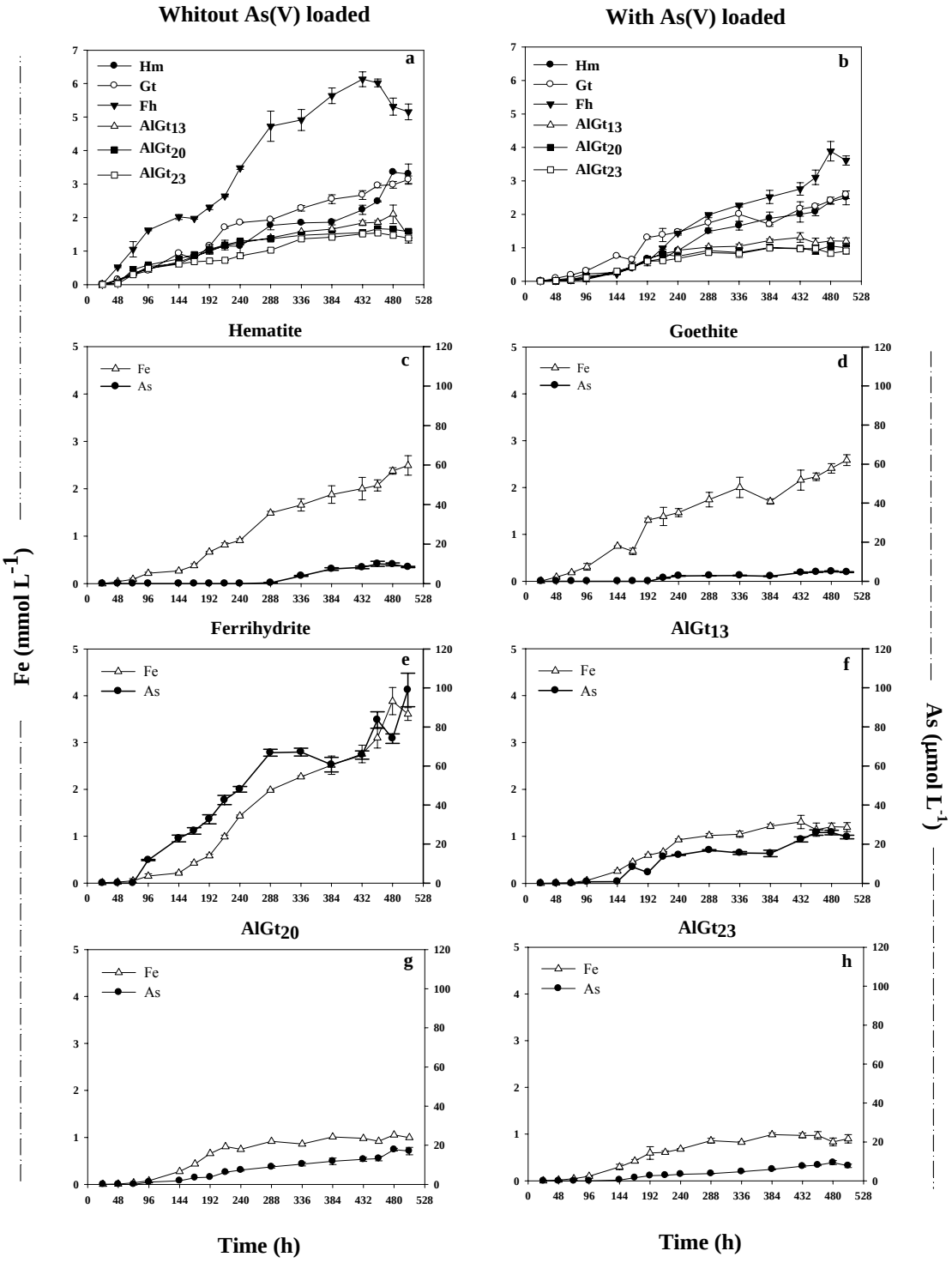

Figure 1 – Fe(III) reduction and As mobilisation from different Fe (hydr)oxides incubated with S. *putrefaciens*. Data are represented as means ± standard error of the mean (n=3); bars not visible are smaller than symbol

The presence of aluminium in the goethite structure limited the iron reduction rate, thereby, the Fe(II) concentrations were smaller as structural Al increased. This finding is in line with previous results (Schwertmann, 1984; Jeanroy et al., 1991; Boussarine et al., 1999), but diverges from data reported by Boussarine et al. (1999) concerning to Al solubilisation. According to these authors Al dissolution was congruent with Fe reduction from Al-substituted goethites which was not observed during the course of our experiment (data not shown). Such difference can be ascribed to distinct experimental conditions. The acidic medium (pH = 3.4) obviously conditioned Al solubilisation in the experiment performed by Boussarine et al. (1999). Under our experimental condition (pH ≅ 7.0) the Al^{3+} activity is rather low and $Al(OH)_3^{\circ}$ is expected to be the dominating soluble species, according to Lindsay (1979). Anyway, surface passivation can be ascribed to Al precipitates on the Al-goethite surfaces restraining its reductive dissolution as argued by Kakkudapu et al. (2001).

As a general observation it can be considered two different patterns for arsenic mobilisation: first, mobilisation of arsenic from well crystallized iron (hydr)oxides (Gt and Hm) was delayed in relation to Fe reduction (Figure 1c, and d). Second, a congruent release of As with Fe reduction from poorly crystallised Fh, and Al-substituted goethites (Figure 1e, f, g, and h). Such results suggest preferential mobilisation of Fe not associated with adsorbed As at the initial stages of the reductive dissolution of well crystallised Hm and Gt. On the other hand, iron dissolution from poorly crystallised Fh gave rise to a prompt As mobilisation which increased up to approximately 100 μmol L^{-1} during roughly 400 h of incubation time (Figure 1e). The amounts of arsenic mobilised from Al-substituted goethites were much lower than for Fh and decreased as the structural Al increased (Figure 1f, g, and h). This behaviour concurs and perhaps is associated with higher specific surface area and As adsorption capacity for Fh in relation to Hm and Gt (Table 1). Concerning to these aspects, Al-substituted goethites exhibited an intermediate behaviour between well and poorly crystalline Fe (hydr)oxides.

Although goethite and hematite had shown the lowest final concentrations of soluble arsenic, roughly 5 and 10 μmol L^{-1}, respectively, an opposite trend is depicted when the data are expressed as percentage of the initial content of Fe(III) and As in the solid phase. By considering the $As_{mobilised}/As_{total}$ ratio as a function of $Fe_{released}$ or $As_{mobilised}/As_{total}$ ratio

as a function of $Fe_{released}/Fe_{total}$ ratio (Figure 2a, and b), it can be observed that the lowest percentage of both Fe dissolution and arsenic mobilisation for $AlGt_{23}$, followed by $AlGt_{20}$. Hematite, Goethite, and $AlGt_{13}$ presented values quite similar, whilst Fh remained with the highest amount of iron and arsenic released, almost 20 % and 5 %, respectively. These results reflect that aluminium markedly enhanced the stability of the goethites face to dissimilatory iron reducing.

The expected relationship between surface area and Fe dissolution or arsenic mobilisation was not observed. When normalised to specific surface area, comparable fractions of $Fe_{released}/Fe_{total}$ were observed for Gt, Hm, and $AlGt_{13}$ (Figure 2c). Increment of structural aluminium reflected in lower fraction of reduced Fe, even though, Al-goethites present similar surface area. Thus, the difference in Fe solubilisation should be attributed to variations in crystal properties due to Al substitution, other than specific surface area. Additionally, as the direct contact between bacteria and (hydr)oxides surfaces is considered a rate determining step for iron reduction (Liu et al. 2001), the presence of Al sites on the crystal surfaces could have inhibited the electron shuttle between Al-goethite surfaces and cell membranes. This is based on fact that bacteria probably are not able to distinguish active Al or Fe charge sites, binding on either. Then, the likelihood of bacterial membrane to be bound with Al sites instated of Fe ones should be higher as structural Al increases.

The fraction of dissolved arsenic as a function of specific surface area mirrored the behaviour for iron, except to Al-substituted goethites (Figure 2c). Difference in the fractions of dissolved arsenic from Al-goethites was not observed, suggesting that mobilised arsenic could to a certain extent be readsorbed by Al reactive sites on the Al-goethite surfaces. This hypothesis is in line with the findings of Mello et al. (2006). These authors suggested that arsenic mobilised by reductive dissolution of iron (hydr)oxides may be readsorbed by gibbsite in As-rich soils submitted to anaerobic incubation.

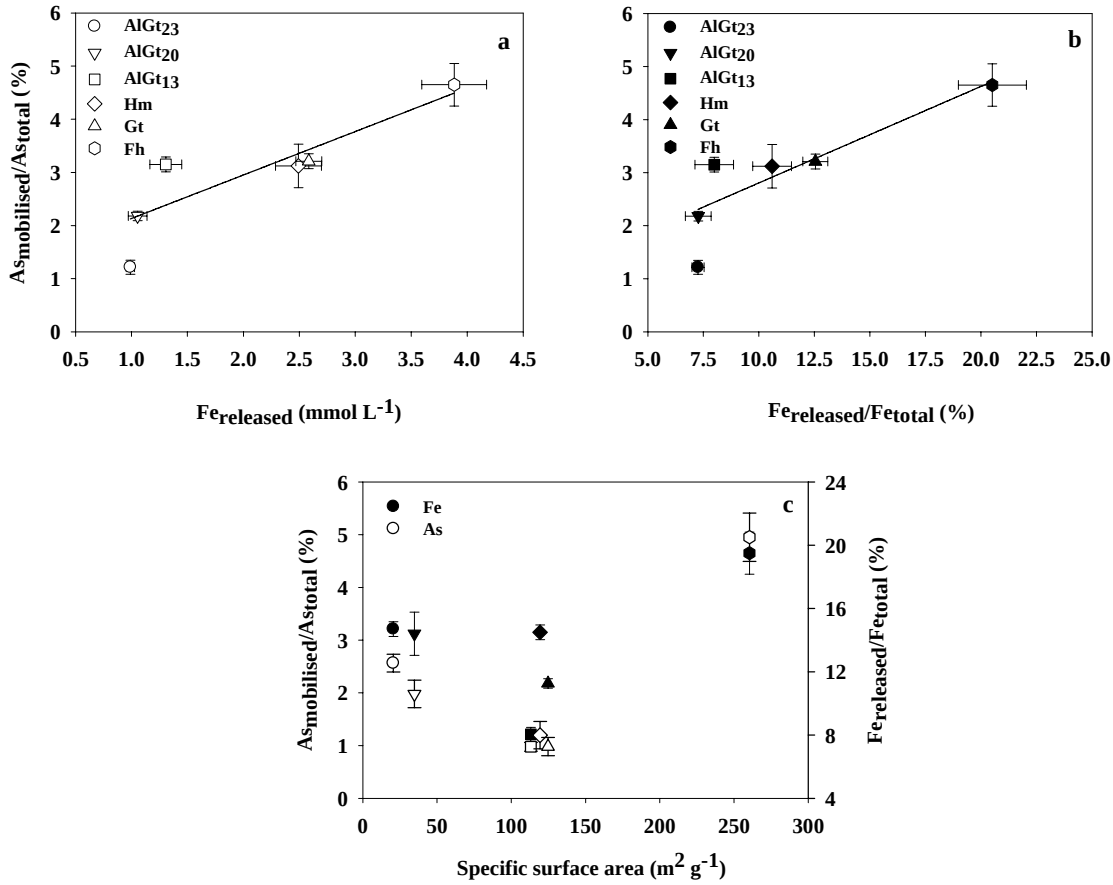

Figure 2 – Reduction of Fe(III) and mobilisation of arsenic from different Fe (hydr)oxides. a, relationship between the fraction of mobilised As and Fe release; b, relationship between the fraction of mobilised As and the fraction of Fe reduced; and c, the fraction of mobilised As and reduced Fe from Gt (●, ○), Hm (▼, ▽), AlGt23 (■, □), AlGt20 (▲, △), AlGt13 (◆, ◇), and Fh (◊, ♦) plotted against specific surface area. Data are represented as means ± standard error of the mean (n = 3); bars not visible are smaller than symbol

3.2. Influence of phosphate as competing anion. Dynamics of P under anaerobic conditions, at pH 7 ±0.2 and 37 ^{o}C, shows that phosphate readily displaced arsenate and promptly reacted with other ions in solution and solid matrixes (Figure 3). In general, more than 20 % of the added phosphate was immobilised after 4 h (first measurement) as a result of adsorption or precipitation equilibria. In fact, theoretical calculations support our statements, indicating formation of metastable phases. By running our data in the Visual Minteq® software (ver. 2.5), it was predicted saturation with respect to calcium phosphate phases, primarily hydroxyapatite. In addition, phosphate adsorption followed by As(V)

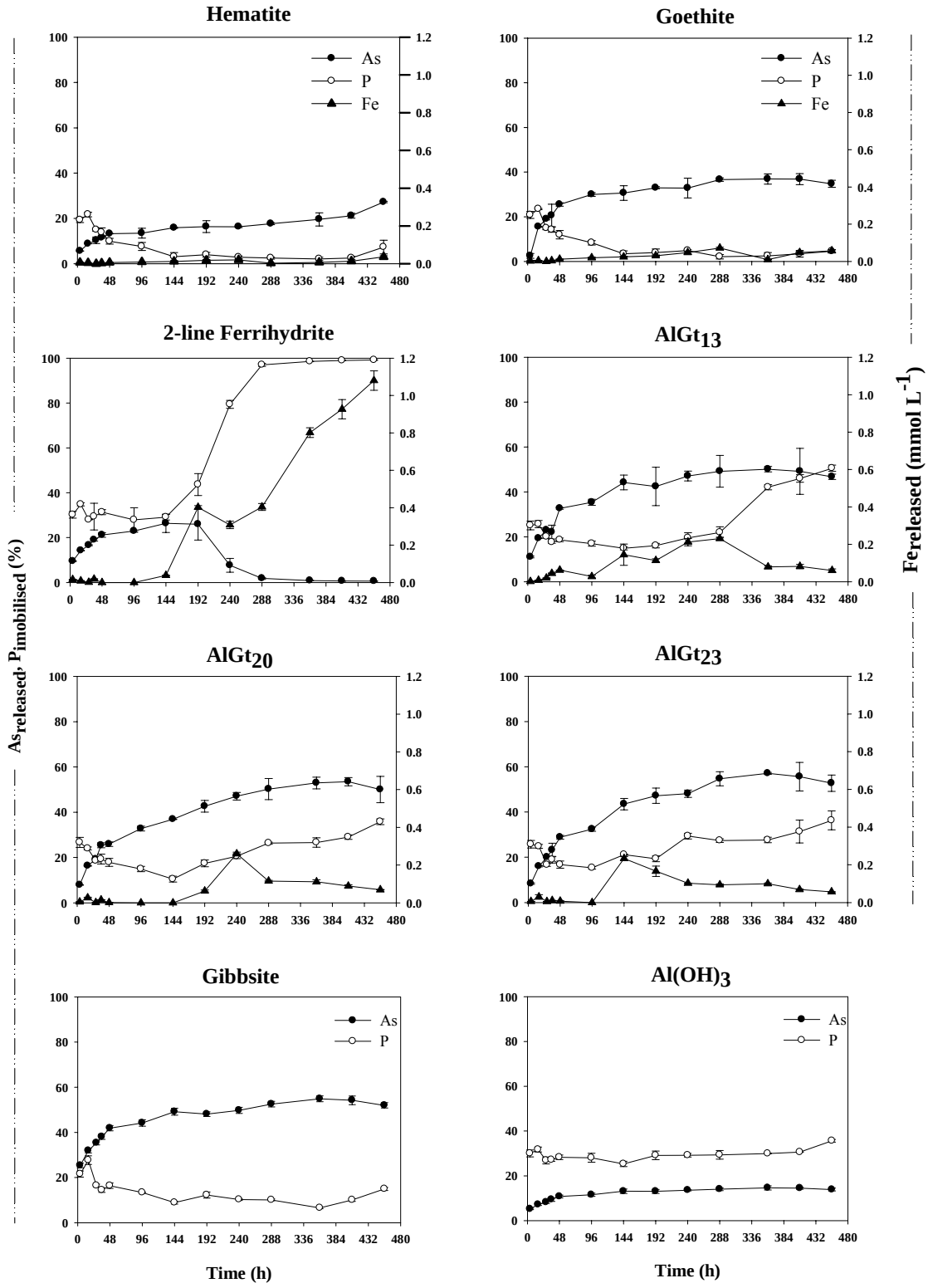

Figure 3 – Fe(III) reduction, As release, and P immobilisation from different Al and Fe suspension in the presence of *S. putrefaciens*. Inset in each panel represents the experiments without adsorbed arsenic. Data are represented as means ± standard error of the mean (n = 3); bars not visible are smaller than symbol

desorption can also be considered. By comparing these results with the data from the preceding section, it can be seem that As was early released here, at the start of the experiment. This initial release of As can be ascribed to exchange by competing phosphate equilibrium, as no Fe reduction is expected at the beginning of the experiment.

It is worth of note that initial P immobilisation was higher, almost 30 %, in the suspensions containing poorly crystalline (hydr)oxides [Fh and $Al(OH)_3$] and Al-substituted goethites. Taking into account that all adsorbents were submitted to similar experimental conditions, i.e. equal concentrations of Ca and P added to the medium, P immobilisation due to Ca-P precipitation should rigorously be the same for all adsorbents. Then, additional amount of P immobilised for Fh, $Al(OH)_3$, and AlGts in relation to well crystalline (hydr)oxides can be ascribed to P adsorption. It should also be considered that arsenic was loaded at near maximum adsorption capacity and that P was supplied at concentrations (5 mmol L^{-1}) sufficient to ensure a large excess with respect to total adsorbed arsenic. Anyway, amounts of desorbed As does not explain the excess of P immobilised in suspensions of poorly crystalline (hydr)oxides in relation to well crystalline ones. Therefore, it should be considered P adsorption at additional sites not occupied by As(V). In fact, previous investigations have shown that surface coverage in the competitive adsorption experiments is higher than the adsorption of the individual ions (Hongshao and Stanforth, 2001; Zhang and Selim, 2008) suggesting that there are some specific sites for each ion as well as other sites that can adsorb both ions (Manning and Goldberg, 1996b).

Later, after 12 h (second measurement), the fraction of phosphate immobilised decreased to achieve a steady-state by 144 h for those adsorbents to which no significant iron release was observed, i.e. hematite, goethite, gibbsite, and poorly crystalline $Al(OH)_3$. This indicates remobilisation of phosphate probably from those metastable precipitated phases previously referred. The late steady-state equilibrium, however, was not observed for poorly crystalline Fh and Al-substituted goethites (Figure 3). On the contrary, there is a clear increase in the fraction of immobilised phosphate for these minerals after 144 h which in general coincides with a peak of soluble iron, notably for Fh. This suggests further precipitation of $Fe^{(II)}$-P phases, as indicated by Visual Minteq® software. Theoretical equilibrium calculation revealed that vivianite [$Fe^{(II)}_3(PO_4)_2$ $8H_2O$] precipitates at Fe(II) concentration

higher than 10^{-3} mmol L^{-1} in the presence of phosphate at 5 mmol L^{-1}, under our experimental conditions.

Formation of vivianite can also be responsible for the surprisingly low concentration of soluble iron under anaerobic conditions, as also addressed by Burnol et al. (2007). Concentrations of soluble iron, as a result of biological reduction of the iron (hydr)oxides, were much lower in the experiment with phosphate (Figure 3) in relation to the previous experiment (section 3.1). Even for well crystalline Hm and Gt, precipitation of vivianite can be argued to explain the differences between experiments. Concentrations of soluble iron were about 0.02 mmol L^{-1} for Hm and 0.07 mmol L^{-1} for Gt that corresponds to respectively 140 and 40 times lesser than in the previous experiment, but still oversaturated with respected to vivianite. Alternatively, surface coverage of the adsorbents increased by P adsorption restricting the binding of (hydr)oxide surfaces on the *S. putrefaciens* cells can also be considered, as discussed earlier for arsenic.

The pattern of P immobilisation in the treatments without arsenate (Figure 4) was similar, but generally greater than in the treatments with loaded arsenic adsorbents. Differences should be attributed to higher adsorption of P at the absence of As(V). The greatest difference was verified to poorly crystalline Al hydroxides where P immobilisation increased from roughly 30 % in the presence of As(V) to almost 80 % in the absence of As(V). For Fh the initial difference was from nearly 30 to 50 %, and lower to AlGts followed by well crystalline Gb, Gt, and Hm, roughly corresponding to the amount of available adsorption sites, as measured by specific surface area or maximum As adsorption capacity.

Similar arsenic desorption trends were observed for all materials. The fraction of desorbed arsenic decreased in the following order: Gb ≥ AlGts > Gt > Hm > Fh > $Al(OH)_3$. The arsenic release initiated readily after the addition of phosphate (~4 h), increasing quickly up to 48 h and trended to slowed down thereafter (Figure 3). For example, nearly 70 % of the total of As solubilised from goethite was reached by 48 h. Considering that soluble iron was not detected during the initial interval (4 – 48 h), the arsenic displacement may be exclusively attributed to ligand exchange reactions with phosphate. Expressive amounts of As were released from gibbsite and Al-substituted goethites, in general more than 50 % within the time frame. This should integrally be attributed to exchange by phosphate

on Gb surface, but for AlGts part of the released amount must be attributed to biological iron reduction. Al-substituted goethites followed similar kinetics, and the fraction of mobilised arsenic was higher as the structural Al increased (Figure 3, $AlGt_{13}$, $AlGt_{20}$, and $AlGt_{23}$). Such weak retention of arsenic on the Al sites, except for poorly crystalline $Al(OH)_3$, suggest formation of unstable surface complex related to surface precipitation of arsenic on these adsorbents. Notwithstanding, spectroscopic investigation is warranted to further elucidate the type of surface complexes formed between As and these matrixes. Although less impressive, our data are in line with Masue et al. (2007) that reported increasingly As(V) desorption by phosphate from poorly crystalline Al-Fe hydroxides as the Al:Fe ratio increased, reaching to almost total arsenate desorption from pure Al hydroxide after 24 h. That difference can be ascribed to the much higher P:As (7500:1) ratio used by those authors.

The relatively low amounts of As desorbed by phosphate from crystalline iron (hydr)oxides that we observed agree with results from Hongshao and Stanforth (2001), and suggest that arsenate is adsorbed mainly as nonexchangeable ion, but there were a minor fraction exchangeable by phosphate. In fact, As(V) or P adsorption kinetics are considered a two-phase reaction, with a rapid initial step followed by a much slower reaction (Torrent et al., 1992; Hongshao and Stanforth, 2001). According to Hongshao and Stanforth (2001), the nonexchangeable fraction comprises the amount of ions initially adsorbed in the first step, and the exchangeable fraction corresponds to a surface precipitation on the adsorbed layer. Additionally, there is a fraction of the surface sites that are very rapidly occupied but which are not exchangeable once occupied. Phosphate and arsenate are adsorbed equally at low surface coverages, but arsenate forms a less soluble precipitate than does phosphate. Therefore, phosphate adsorption does not achieve the same surface coverage when added after arsenate.

The fraction of arsenic desorbed from Fh and Hm were quite similar, close to 26 %, but it reached almost 37 % from Gt. Nevertheless, it seems that exchange reactions not ceased after 456 h for Hm (Figure 3). A distinct behaviour was observed for Fh where the amount of arsenic released reached its maximum about 192 h and suddenly dropped off to almost zero. This depletion of soluble arsenic coincided to P immobilisation due to vivianite precipitation, as stated earlier. However, unlike P, As immobilisation can not be

ascribed to an $Fe^{(II)}$-As phase precipitation, as indicated by theoretical calculation. But, as phosphate behaves much like arsenate, it can be argued to As co-precipitation with vivianite. This hypothesis is feasible considering the structure of As(V) and P minerals, where typical tetrahedral anions $[XO_4]^{3-}$ are bound to octahedrally coordinated transition metal ions. Variations and multiples of this bonding pattern tend to create relatively open structures that allow for extensive substitution of cations, anions, anions groups, and water (O'Day, 2006). Consequently, the precipitation of $Fe^{(II)}$-P phases could act as sink for arsenic giving rise to a vivianite-like mineral $\{Fe^{(II)}_3[(As, P)O_4]_2.8H_2O\}$. This observation has a great environmental implication to the fate of As in eutrophic-reducing aquatic systems.

Aluminium hydroxide was by far the most efficient in retaining arsenic on its surface. Less than 15 % of the As_{total} were desorbed by phosphate. Arsenate adsorption kinetic data for $Al(OH)_3$ revealed that more than 92 % of the added arsenate was adsorbed in nearly 6 h (Silva et al., 2008). In addition, nearly 66 % of phosphate added to poorly crystalline $Al(OH)_3$ suspension was sorbed in 4 h (Figure 4), that corresponds to nearly 80 % of total P immobilised after 456 h. Phosphate adsorbed later (20%) is comparable to the fraction of As desorbed by competing P (15 %). Thus, considering that adsorption kinetic is related to exchangeability of P and As ions, as pointed out earlier, our data indicate comparable amounts of specific sites for adsorption of P and As in the initial phase. Then, it may be inferred that the majority of As is adsorbed on poorly crystalline $Al(OH)_3$ surface as a nonexchangeable phase, strongly attached and likely forming a very stable surface complex.

3.3. Influence of carbonate as competing anion. Desorption of arsenic by carbonate from Al and Fe (hydr)oxides, under dissimilatory iron reduction (Figure 5a), was in general inferior to that desorbed by phosphate (Figure 3). This indicates, a lower competitive effect for adsorption of carbonate on those surfaces, in relation to arsenate or phosphate, as previously reported (Ghosh et al., 2005; Radu et al., 2005; Burnol et al., 2007). Radu et al. (2007) observed that carbonate mobilised less adsorbed As(V) than was mobilized by phosphate, even when present in much higher concentrations than phosphate. Exceptions for Gb, Fh, and Gt can be ascribed to a weak surface binding mechanism of As(V) in Gb or

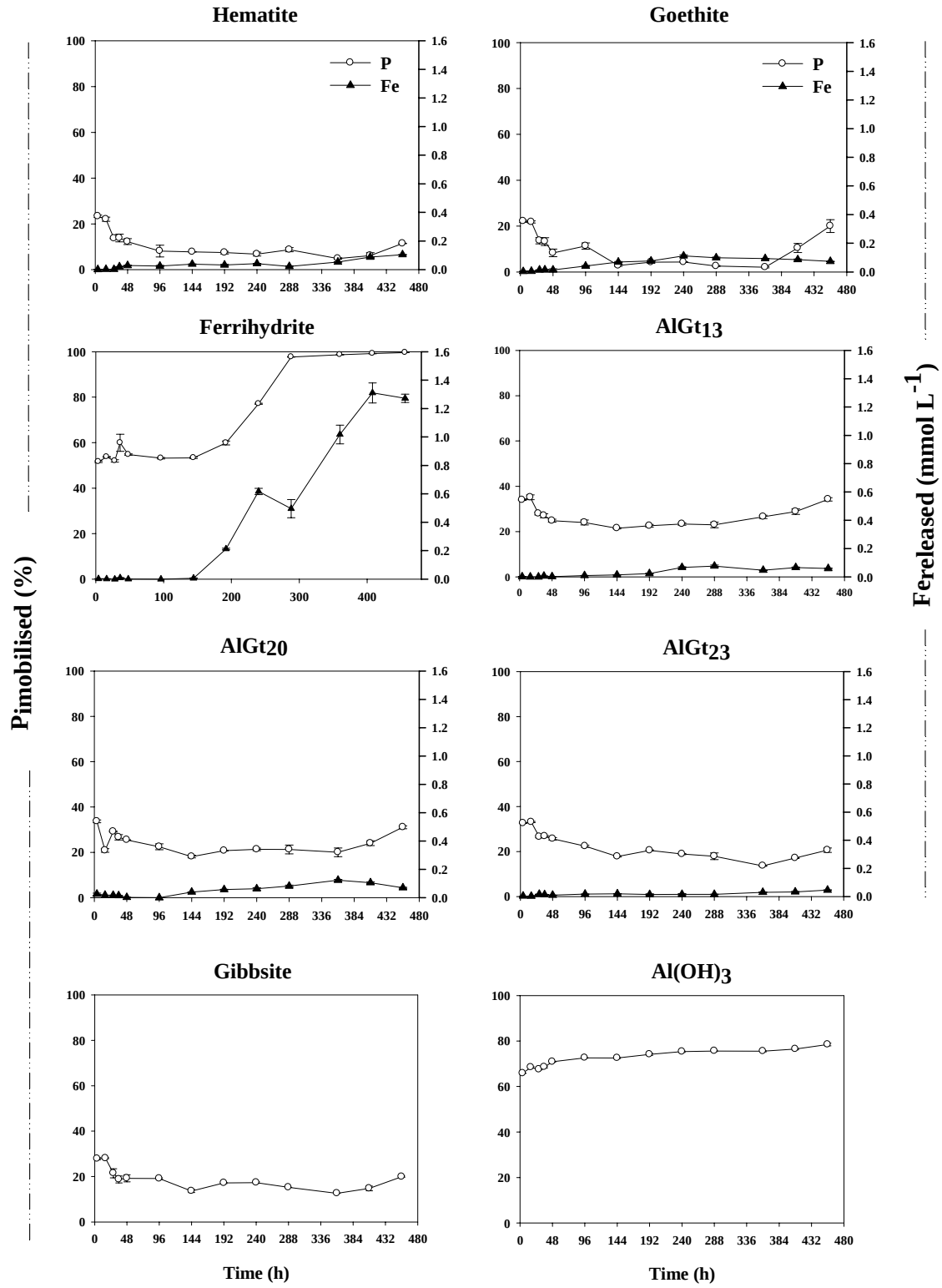

Figure 4 – Fe(III) reduction and P immobilisation from different Al and Fe suspension in the presence of S. *putrefaciens*. Data are represented as means ± standard error of the mean (n = 3); bars not visible are smaller than symbol

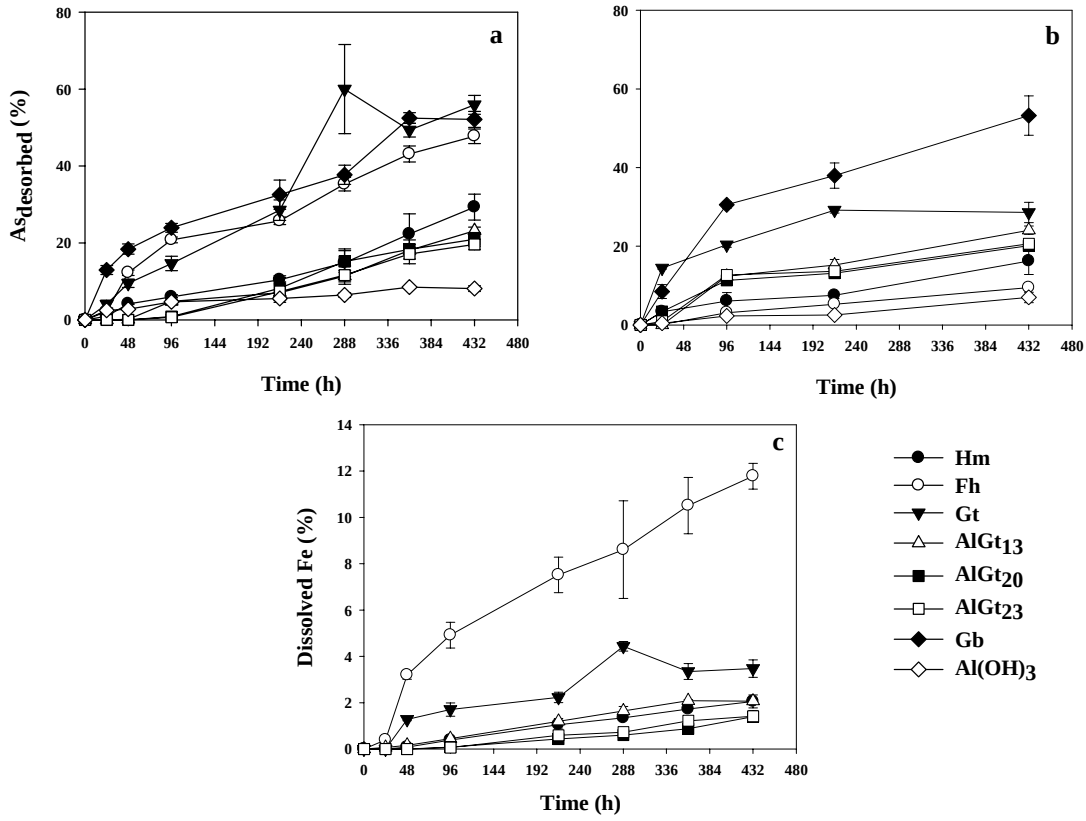

Figure 5 – Fraction of arsenic desorbed and Fe(III) reduced from different adsorbents by carbonate in the presence of S. *putraciens* cells. a, fraction of As mobilised in the presence of bacteria; b, fraction of As mobilised in the absence of bacteria, and; c. fraction of Fe dissolved by *S. putraciens* cells

to a mobilisation of As due to reductive iron dissolution in Fh and Gt, as will be discussed later.The fraction of arsenic desorbed by carbonate from Al-substituted goethites was almost the same in the presence (Figure 5a) and absence (Figure 5b) of iron reducing bacteria. Gibbsite also presented comparable fractions of arsenic desorbed in both presence and absence of *S. putrefaciens* cells, being quite similar to that removed by phosphate. This result confirm that As(V) adsorption onto Gb surface characterises a binding mechanism weaker than to other (hydr)oxides. It is also clear that arsenic mobilisation from Gb and AlGts is primarily due to desorption by exchange with carbonate rather than to reductive dissolution, as the fraction of iron dissolved from these adsorbents (Figuere 5c) was quite

low (< 2%). On the other hand, Fh, Gt, and in a lesser extent Hm presented higher arsenic release in the presence of bacteria in a such way that the differences can be ascribed to the reductive dissolution of iron. The highest difference was observed to Fh which presented less than 10 % of the adsorbed arsenic released in the absence of iron reducing bacteria. These results indicate that only 20 % of the arsenic release can be attributed to desorption by carbonate. For Gt, nearly 50 % of the arsenic release could be ascribed to that exchangeable mechanism.

Soluble Fe and Al concentrations were negligible in the absence of bacteria. Only for Fh and Gt, there were appreciable fractions of iron dissolved in the presence of bacteria. Thermodynamics calculations indicated precipitation of siderite [$Fe^{(II)}CO_3$] at Fe(II) concentration higher than 0.01 mmol L^{-1}, under our experimental conditions. Arsenic mobilisation from Gt and Fh under anaerobic conditions was congruent with biological iron reduction reaching nearly 60 and 50 %, respectively. These amounts of arsenic released by carbonate essay were superior to that observed to phosphate one. Although, theoretical calculations pointed out oversaturation with respect to siderite, unlike vivianite, apparently the metastable carbonate phases can not act as sink for soluble arsenic.

There is much spectroscopic evidence that adsorbed As forms inner-sphere binuclear surface complexes with aluminium (Arai and Sparks, 2002; Goldberg and Johnson, 2001; Ladeira et al., 2001; Foster et al., 1998) and iron (hydr)oxides (Makris et al., 2007; Sherman and Randall, 2003; Fendorf et al., 1997; Grossl et al., 1997; Sun and Doner, 1996; Manceau et al., 1995). These stable complexes can account for the generally low desorption of arsenic by carbonate and phosphate. Notwithstanding, our data suggest that these complexes are to a certain extent more stable for poorly crystalline $Al(OH)_3$ and Fh followed by Hm in relation to goethite and gibbsite.

4. ENVIRONMENTAL IMPLICATION

Our investigation presented insights related to arsenic mobilisation from Al-substituted goethites and other synthetic Al and Fe (hydr)oxides under anoxic conditions influenced by microbiological activity as well as by competing anions. Differences in Fe and As dissolution as affected by the nature of the (hydr)oxides were observed. In the

absence of competing ion, arsenic mobilisation from Gb and poorly crystalline $Al(OH)_3$ was negligible, since aluminium does not participate as electron acceptor for bacterial cells. In contrast, *S. putrefaciens* cells were able to reduce iron from both noncrystalline and crystalline iron (hydr)oxides. For Al-substituted goethites we observed a decrease in the fraction of soluble iron and arsenic mobilisation as structural Al increased. Structural Al affected the expected relationship between specific surface area and iron dissolution preventing arsenic mobilisation. In relation to arsenic desorption by phosphate and carbonate in the presence of *S. putrefaciens* cells, iron dissolution and arsenic mobilisation varied according to the competing anion. Both phosphate and carbonate were able to desorb great amounts of arsenic from Gb, but the fraction of As displaced by phosphate from Al-substituted goethites increased as structural Al increased. Then, we infer that the binding mechanism on the surface of these crystalline matrixes is governed to a certain extent by a weak binding complex. Poorly crystalline $Al(OH)_3$ was the most efficient in holding arsenate firmly on its surface followed by Fh and Hm. The poorly crystalline Al and Fe hydroxides proved to be most efficient phases in retaining arsenic, but aluminium hydroxide gains an advantage over Fh under reducing conditions. Arsenic released from poorly crystalline $Al(OH)_3$ was less than 8 % by carbonate in both presence and absence of iron reducing bacteria, and nearly 15 % by phosphate. Concerning to arsenic release under reducing condition, Fh showed to be more stable than poorly crystalline $Al(OH)_3$ only in a later incubation time after 240 hours in the presence of phosphate as competing anion. Once soluble iron increased to a certain level, it combined with phosphate or carbonate giving rise to new metastable vivianite and siderite phases, as predicted by thermodynamics calculations. Apparently, vivianite can act as a sink for soluble arsenic limiting its mobilisation, but the same can not be assumed for siderite. Therefore, poorly crystalline $Al(OH)_3$ can be considered the most effective adsorptive system to immobilise arsenic, because the presence of soluble carbonate is more common than phosphate in environmental conditions.

Aluminium and iron (hydr)oxides are ubiquitous in the environment, and goethite is one of the thermodynamically most stable iron oxides (Cornell and Schwertmann, 2003). Thus, the presence of goethite with high structural Al may contribute to not only to improve the As(V) adsorption capacity of soils and sediments, but also to diminish its

mobilisation under reducing conditions. In contrast, intense use of phosphate fertiliser and liming or carbonate produced via microbial metabolism may add further complication to potential arsenic desorption from soils and sediments with high content of Gb, a common mineral in many soils.

In water treatment, adsorptive process has been preferred due to its facility to handle the As-rich residues generated after adsorption process. Most investigations have suggested the use of hydrous ferric oxides to remove arsenic from drinking water due to their large surface area and consequently high efficiency. However, the disposal of the As-rich residues under reducing conditions, as might occur at a waste disposal sites (Masue et al., 2007), is a very concerning issue with regards to the redox transformations of Fe(III) to Fe(II) mediated by dissimilatory iron reducing bacteria leading to arsenic mobilisation. Hence, as Al is not redox sensitive, the use of a poorly crystalline $Al(OH)_3$ can be considered a good option for removing arsenic from contaminated water, since under our experimental conditions it showed to be the most efficient in retain arsenic. The use of Al-substituted goethites should also be taking into account as they presented high stability and As retention under anoxic conditions. Only in the presence of phosphate Al-substituted goethites were less effective than other iron (hydr)oxides, but environmental conditions presenting large P:As ratio as used herein is quite improbable.

Nevertheless, prediction of arsenic mobility is a very complex issue, and As sorption modelling requires a more detailed comprehension of the bonding mechanism and kinetics. Thus, investigations are warranted to further elucidate the binding mechanisms that play a key role on arsenic sorption on Al-substituted goethites surfaces.

5. REFERENCE

Appelo, C.A.J., Van der Weiden, M.J.J., Tournassat, C., Charlet, L., 2002. Surface complexation of ferrous iron and carbonate on ferrihydrite and the mobilization of arsenic. Environ. Sci. Technol. 36, 3096-3103.

Arai, Y. and Sparks, D.L., 2001. ATR-FTIR spectroscopic investigation on phosphate adsorption mechanisms at the ferrihydrite-water interface. J. Colloid Interf. Sc. 241, 317-326.

Arai, Y. and Sparks, D.L., 2002. Residence time effects on arsenate surface speciation at the aluminum oxide-water interface. Soil Sci. 167, 303-314.

Bousserrhine, N., Gesser U., Jeanroy E., and Berthelin J., 1999. Bacterial and chemical reductive dissolution of Mn-,Co-, Cr-, and Al-substituted goethites. Geomicrob. J. 16, 245-258.

Burnol, A., Garrido, F., Baranger, P., Joulian, C., Dictor, M.-C., Bodenan, F., Morin, G., and Charlet, L., 2007. Decoupling of arsenic and iron release from ferrihydrite suspension under reducing conditions: a biogeochemical model. Geochem. Trans. 8, 12.

Claessens, J., Behrends, T., and Van Cappellen, P., 2004. What do acid-base titrations of live bacteria tell us? A preliminary assessment. Aquatic Sci. - Research Across Boundaries 66, 19-26.

Cornell, R.M. and Schwertmann, U., 2003. The iron oxides: structure, properties, reactions, occurences and uses. Wiley-VCH, Weinheim ; [Cambridge].

Cummings D.E., Caccavo, J.F., Fendorf S., and Rosenzweig F., 1999. Arsenic mobilization by the dissimilatory Fe(III)-reducing bacterium Shewanella alga BrY. Environ. Sci. Technol 33, 723-729.

Deschamps, E., Ciminelli, V.S.T., and Holl, W.H., 2005. Removal of As(III) and As(V) from water using a natural Fe and Mn enriched sample. Water Res. 39, 5212-5220.

Deschamps, E., Ciminelli, V.S.T., Weidler, P.G., and Ramos, A.Y., 2003. Arsenic sorption onto soils enriched in Mn and Fe minerals. Clays Clay Miner. 51, 197-204.

Fendorf, S., Eick, M.J., Grossl, P., and Sparks, D.L., 1997. Arsenate and Chromate Retention Mechanisms on Goethite. 1. Surface Structure. Environ. Sci. Technol. 31, 315-320.

Foster, A.L. Brown Jr., G. E.; Tingle, T.N, and Parks, G. A., 1998. Quantitative arsenic speciation in mine tailings using X-ray absorption spectroscopy. Am. Miner. 83, 553-568.

Ghosh, A., Sáez, A.E., and Ela, W., 2006. Effect of pH, competitive anions and NOM on the leaching of arsenic from solid residuals. Sci. Total Environ. 363, 46-59.

Goldberg, S. and Johnston, C.T., 2001. Mechanisms of Arsenic Adsorption on Amorphous Oxides Evaluated Using Macroscopic Measurements, Vibrational Spectroscopy, and Surface Complexation Modeling. J. Colloid Interf. Sci. 234, 204-216.

Grossl, P.R., Eick, M., Sparks, D.L., Goldberg, S., and Ainsworth, C.C., 1997. Arsenate and Chromate Retention Mechanisms on Goethite. 2. Kinetic Evaluation Using a Pressure-Jump Relaxation Technique. Environ. Sci. Technol. 31, 321-326.

Hongshao, Z. and Stanforth, R., 2001. Competitive Adsorption of Phosphate and Arsenate on Goethite. Environ. Sci. Technol. 35, 4753-4757.

Jain, A., Raven, K.P., and Loeppert, R.H., 1999. Arsenite and Arsenate Adsorption on Ferrihydrite: Surface Charge Reduction and Net OH- Release Stoichiometry. Environ. Sci. Technol. 33, 1179-1184.

Jeanroy, E., Rajot, J.L., Pillon, P., and Herbillon, A.J., 1991. Differential Dissolution of Hematite and Goethite in Dithionite and Its Implication on Soil Yellowing. Geoderma 50, 79-94.

Kukkadapu, R.K., Zachara, J.M., Smith, S.C., Fredrickson, J.K., and Liu, C., 2001. Dissimilatory bacterial reduction of Al-substituted goethite in subsurface sediments. Geochim. Cosmochim. Acta 65, 2913-2924.

Kyle J.H., Posner. A. M., Quirk J.P., 1975. Kinetics of isotopic exchange of phosphate adsorbed on gibbsite. J. Soil Sci. 26, 34-43.

Ladeira, A.C.Q., Ciminelli, V.S.T., Duarte, H.A., Alves, M.C.M., and Ramos, A.Y., 2001. Mechanism of anion retention from EXAFS and density functional calculations: Arsenic (V) adsorbed on gibbsite. Geochim. Cosmochim. Acta 65, 1211-1217.

Lindsay, W. L., 1979. Chemical equilibria in soils. John Wiley & Sons, Inc, New York.

Liu, C., Kota, S., Zachara, J.M., Fredrickson, J.K., and Brinkman, C.K., 2001. Kinetic Analysis of the Bacterial Reduction of Goethite. Environ. Sci. Technol. 35, 2482-2490.

Lovley, D.R., Holmes, D.E., Nevin, K.P., Poole, 2004. Dissimilatory Fe(III) and Mn(IV) Reduction, Advances in Microbial Physiology. Academic Press, pp. 219-286.

Lovley, D.R., Roden, E.E., Phillips, E.J.P., and Woodward, J.C., 1993. Enzymatic iron and uranium reduction by sulfate-reducing bacteria. Marine Geology 113, 41-53.

Makris, K.C., Sarkar, D., Parsons, J.G., Datta, R., and Gardea-Torresdey, J.L., 2007. Surface arsenic speciation of a drinking-water treatment residual using X-ray absorption spectroscopy. J. Colloid Interf. Sc. 311, 544-550.

Manceau, A., 1995. The mechanism of anion adsorption on iron oxides: Evidence for the bonding of arsenate tetrahedra on free Fe(O, OH)6 edges. Geochim. Cosmochim. Acta 59, 3647-3653.

Manning, B.A. and Goldberg, S., 1996a. Modeling arsenate competitive adsorption on kaolinite, montmorillonite and illite. Clays Clay Miner. 44, 609-623.

Manning, B.A. and Goldberg, S., 1996b. Modeling competitive adsorption of arsenate with phosphate and molybdate on oxide minerals. Soil Sci. Soc. Am. J. 60, 121-131.

Manning, B.A. and Goldberg, S., 1997. Adsorption and stability of arsenic(III) at the clay mineral-water interface. Abstracts of Papers of the American Chemical Society 213, 221-GEOC.

Matschullat, J., 2000. Arsenic in the geosphere -- a review. Sci. Total Environ. 249, 297-312.

Masue, Y., Loeppert, R.H., and Kramer, T.A., 2007. Arsenate and Arsenite Adsorption and Desorption Behavior on Coprecipitated Aluminum:Iron Hydroxides. Environ. Sci. Technol. 41, 837-842.

McNeil L.S, and Eduard. M., 1997. Predicting As removal during metal hydroxide precipitation. J. Am. Water Works Assoc. 75-86.

Mello, J., Roy, W., Talbott, J., and Stucki, J., 2006. Mineralogy and Arsenic Mobility in Arsenic-rich Brazilian Soils and Sediments. J. Soils Sed. 6, 9-19.

O'Day, P. A., 2006. Chemistry and Mineralogy of Arsenic. Elements. 2, 77-83.

Radu, T., Subacz, J.L., Phillippi, J.M., and Barnett, M.O., 2005. Effects of Dissolved Carbonate on Arsenic Adsorption and Mobility. Environ. Sci. Technol. 39, 7875-7882.

Sahai, N., Lee, Y.J., Xu, H., Ciardelli, M., Gaillard, J.-F., 2007. Role of Fe(II) and phosphate in arsenic uptake by coprecipitation. Geochim. Cosmochim. Acta 71, 3193-3210.

Schwertmann, U., 1984. The Influence of Aluminum on Iron-Oxides .9. Dissolution of Al-Goethites in 6m Hcl. Clay Miner. 19, 9-19.

Schwertmann, U. and Cornell, R.M., 2000. Iron oxides in the laboratory : preparation and characterization. Wiley-VCH, Weinheim ; Chichester.

Sherman, D.M. and Randall, S.R., 2003. Surface complexation of arsenie(V) to iron(III) (hydr)oxides: Structural mechanism from ab initio molecular geometries and EXAFS spectroscopy. Geochim. Cosmochim. Acta 67, 4223-4230.

Silva, J., Mello, J.W.V., Gasparon, M., Abrahão, W.A.P., Ciminelli, V.S.T., and Jong, T. 2008. Arsenic adsorption onto aluminium and iron (hydr)oxides: kinetics, isotherm and envelope of adsorption. (To be submitted)

Smedley, P.L., Kinniburgh, D.G., 2002. A review of the source, behaviour and distribution of arsenic in natural waters. Appl. Geochem. 17, 517-568.

Sun, X.H. and Doner, H.E., 1996. An investigation of arsenate and arsenite bonding structures on goethite by FTIR. Soil Sci. 161, 865-872.

Torrent, J., Schwertmann, U., and Barron, V., 1987. The Reductive Dissolution of Synthetic Goethite and Hematite in Dithionite. Clay Miner. 22, 329-337.

Torrent, J., Schwertmann, U., and Barron, V., 1992. Fast and slow phosphate sorption by goethite-rich natural materials. Clays Clay Miner. 40, 14-21.

Vithanage, M., Senevirathna, W., Chandrajith, R., and Weerasooriya, R., 2007. Arsenic binding mechanisms on natural red earth: A potential substrate for pollution control. Sci. Total Environ. 379, 244-248.

Waychunas, G.A., Rea, B.A., Fuller, C.C., and Davis, J.A., 1993. Surface-Chemistry of Ferrihydrite .1. Exafs Studies of the Geometry of Coprecipitated and Adsorbed Arsenate. Geochim. Cosmochim. Acta 57, 2251-2269.

Zachara, J.M., Fredrickson, J.K., Smith, S.C., and Gassman, P.L., 2001. Solubilization of Fe(III) oxide-bound trace metals by a dissimilatory Fe(III) reducind bacterium. Geochim. Cosmochim. Acta 65, 75-93.

Zhang, J.S., Stanforth, R., and Pehkonen, S.O., 2008. Irreversible adsorption of methyl arsenic, arsenate, and phosphate onto goethite in arsenic and phosphate binary systems. J. Colloid Interf. Sc. 317, 35-43.

OUTLOOK AND CONCLUSIONS

In this study, we assessed the efficiency of different Al and Fe (hydr)oxides in removing arsenate from contaminated water as well as the stability of the As-rich residues. Different adsorbents were spectroscopically characterised, revealing spectral changes due to presence of structural Al and arsenate sorbed phases. Poorly crystalline $Al(OH)_3$ and ferrihydrite, presented higher arsenate adsorption efficiency, followed by Al-substitued goethites. The stability of the As-rich residue under reducing conditions was also higher to poorly crystalline $Al(OH)_3$ e Al-substituted goethites. In the presence of competing anions, phosphate and carbonate, the adsorbed arsenate on poorly crystalline $Al(OH)_3$ was stable, however, the same was not verified to Al-substituted goethites in the presence of phosphate. These results suggest the alternative use of Al to increase efficiency of water treatment methods. Use of poorly crystalline $Al(OH)_3$ would represent advantage in relation to disposal of sludge from water treatment plants under reducing conditions as well as in phosphate-rich eutrophic environments and in the presence of dissolved carbonates. In this sense, Al-substituted goethites are also promising alternatives, except when the As-rich residue needs to be disposed in unusually phosphate enriched environments.

REFERENCE

Anawar, H.M., Akai, J., Komaki, K., Terao, H., Yoshioka, T., Ishizuka, T., Safiullah, S., and Kato, K., 2003. Geochemical occurrence of arsenic in groundwater of Bangladesh: sources and mobilization processes. J. Geochem. Exp. 77, 109-131.

Anderson, M.A., Ferguson, J.F., and Gavis, J., 1976. Arsenate adsorption on amorphous aluminum hydroxide. J. Colloid Interf. Sc. 54, 391-399.

Appelo, C.A.J., Van der Weiden, M.J.J., Tournassat, C., and Charlet, L., 2002. Surface complexation of ferrous iron and carbonate on ferrihydrite and the mobilization of arsenic. Environ. Sci. Technol. 36, 3096-3103.

Banerjee, K., Amy, G.L., Prevost, M., Nour, S., Jekel, M., Gallagher, P.M., and Blumenschein, C.D. Kinetic and thermodynamic aspects of adsorption of arsenic onto granular ferric hydroxide (GFH). Water Res. In Press, Accepted Manuscript.

Bonneville, S., Behrends, T., Cappellen, P.V., Hyacinthe, C., and Roling, W.F.M., 2006. Reduction of Fe(III) colloids by Shewanella putrefaciens: A kinetic model. Geochim. Cosmochim. Acta 70, 5842-5854.

Bousserrhine N.,G.U.G., Jeanroy E., Berthelin J., 1999. Bacterial and chemical reductive dissolution of Mn-,Co-, Cr-, and Al-substituted goethites. Geomicrob. J. 16, 245-258.

Burnol, A., Garrido, F., Baranger, P., Joulian, C., Dictor, M.-C., Bodenan, F., Morin, G., and Charlet, L., 2007. Decoupling of arsenic and iron release from ferrihydrite suspension under reducing conditions: a biogeochemical model. Geochem. Tran. 8, 12.

Catalano, J.G., Park, C., Fenter, P., and Zhang, Z., 2008. Simultaneous inner- and outer-sphere arsenate adsorption on corundum and hematite. Geochim. Cosmochim. Acta 72, 1986-2004.

Cornell, R.M. and Schwertmann, U., 2003. The iron oxides : structure, properties, reactions, occurences and uses. Wiley-VCH, Weinheim ; [Cambridge].

Cummings D.E., Caccavo, J.F., Fendorf S., and Rosenzweig F., 1999. Arsenic mobilization by the dissimilatory Fe(III)-reducing bacterium Shewanella alga BrY. Environ. Sci. Technol 33, 723-729.

Deschamps, E., Ciminelli, V.S.T., and Holl, W.H., 2005. Removal of As(III) and As(V) from water using a natural Fe and Mn enriched sample. Water Res.39, 5212-5220.

Deschamps, E., Ciminelli, V.S.T., Weidler, P.G., and Ramos, A.Y., 2003. Arsenic sorption onto soils enriched in Mn and Fe minerals. Clays Clay Miner. 51, 197-204.

Driehaus, W., Jekel, M., Hildebrandt, U., 1998. Granular ferric hydroxide - a new adsorbent for the removal of arsenic from natural water. J. Water Sup. Res. Technol. 47, 30 - 35.

Frost, R.L. and Kloprogge, J.T., 2003. Raman spectroscopy of some complex arsenate minerals - implications for soil remediation. Spectrochim. Acta Part a-Mol. Biomol. Spec. 59, 2797-2804.

Frost, R.L., Kloprogge, T., Weier, M.L., Martens, W.N., Ding, Z., and Edwards, H.G.H., 2003. Raman spectroscopy of selected arsenates - implications for soil remediation. Spectrochim. Acta Part a-Mol. and Biomol. Spectroscopy 59, 2241-2246.

Frost, R.L., Weier, M., and Martens, W., 2006. Using Raman spectroscopy to identify mixite minerals. Spectrochim. Acta Part a-Mol. and Biomol. Spectroscopy 63, 60-65.

Garcia-Sanchez-, A., Alvarez-Ayuso, E., and Rodriguez-Martin, F., 2002. Sorption of As(V) by some oxyhydroxides and clay minerals. Application to its immobilization in two polluted mining soils. Clay Miner. 37, 187-194.

Gimenez, J., Martinez, M., de Pablo, J., Rovira, M., and Duro, L., 2007. Arsenic sorption onto natural hematite, magnetite, and goethite. J. Haz. Mat. 141, 575-580.

Goldberg, S., Lebron, I., Suarez, D.L., and Hinedi, Z.R., 2001. Surface Characterization of Amorphous Aluminum Oxides. Soil Sci. Soc. Am. J. 65, 78-86.

Grossl, P.R., Eick, M., Sparks, D.L., Goldberg, S., and Ainsworth, C.C., 1997. Arsenate and Chromate Retention Mechanisms on Goethite. 2. Kinetic Evaluation Using a Pressure-Jump Relaxation Technique. Environ. Sci. Technol. 31, 321-326.

Hongshao, Z. and Stanforth, R., 2001. Competitive Adsorption of Phosphate and Arsenate on Goethite. Environ. Sci. Technol. 35, 4753-4757.

Hope, G.A., Woods, R., and Munce, C.G., 2001. Raman microprobe mineral identification. Miner. Eng. 14, 1565-1577.

Islam, F.S., Gault, A.G., Boothman, C., Polya, D.A., Charnock, J.M., Chatterjee, D., Lloyd, J.R., 2004. Role of metal-reducing bacteria in arsenic release from Bengal delta sediments. Nature 430, 68-71.

Jain, A., Raven, K.P., and Loeppert, R.H., 1999. Arsenite and Arsenate Adsorption on Ferrihydrite: Surface Charge Reduction and Net OH- Release Stoichiometry. Environ. Sci. Technol. 33, 1179-1184.

Jeanroy, E., Rajot, J.L., Pillon, P., and Herbillon, A.J., 1991. Differential Dissolution of Hematite and Goethite in Dithionite and Its Implication on Soil Yellowing. Geoderma 50, 79-94.

Jia, Y. and Demopoulos, G.P., 2005. Adsorption of Arsenate onto Ferrihydrite from Aqueous Solution: Influence of Media (Sulfate vs Nitrate), Added Gypsum, and pH Alteration. Environ. Sci. Technol. 39, 9523-9527.

Jia, Y.F., Xu, L.Y., Fang, Z., and Demopoulos, G.P., 2006. Observation of surface precipitation of arsenate on ferrihydrite. Environ.Sci. Technol. 40, 3248-3253.

Ladeira, A.C.Q., Ciminelli, V.S.T., Duarte, H.A., Alves, M.C.M., and Ramos, A.Y., 2001. Mechanism of anion retention from EXAFS and density functional calculations: Arsenic (V) adsorbed on gibbsite. Geochim. Cosmochim. Acta 65, 1211-1217.

Lindsay, W.L., 1979. Chemical equilibria in soils. John Wiley & Sons, Inc, New York.

Liu, F., De Cristofaro, A., and Violante, A., 2001. Effect of pH, phosphate and oxalate on the adsorption/desorption of arsenate on/from goethite. Soil Sci. 166, 197-208.

Lovley, D.R., Roden, E.E., Phillips, E.J.P., and Woodward, J.C., 1993. Enzymatic iron and uranium reduction by sulfate-reducing bacteria. Marine Geol. 113, 41-53.

Makris, K.C., Sarkar, D., Parsons, J.G., Datta, R., and Gardea-Torresdey, J.L., 2007. Surface arsenic speciation of a drinking-water treatment residual using X-ray absorption spectroscopy. J. Colloid . Interf. Sci. 311, 544-550.

Manning, B.A., Fendorf, S. E., and Goldberg, S., 1998. Surface Structures and Stability of Arsenic(III) on Goethite: Spectroscopic Evidence for Inner-Sphere Complexes. Environ. Sci. Technol. 32, 2383-2388.

Manning, B.A. and Goldberg, S., 1996. Modeling arsenate competitive adsorption on kaolinite, montmorillonite and illite. Clays Clay Miner. 44, 609-623.

Manning, B.A. and Goldberg, S., 1997. Adsorption and stability of arsenic(III) at the clay mineral-water interface. Abstracts of Papers of the Am. Chem. Soc. 213, 221-GEOC.

Matschullat, J., 2000. Arsenic in the geosphere -- a review. The Science of The Total Environment 249, 297-312.

Mortazavi, S., Tezel, F.H., Tremblay, A.Y., and Volchek, K., 1999. Effect of pH on the uptake of arsenic from contaminated water by activated alumina. Adv. Environ. Res. 3, U9-118.

Myneni, S.C.B., Traina, S.J., Waychunas, G.A., and Logan, T.J., 1998. Experimental and theoretical vibrational spectroscopic evaluation of arsenate coordination in aqueous solutions, solids, and at mineral-water interfaces. Geochim. Cosmochim. Acta 62, 3285-3300.

O'Day, P.A., 2006. Chemistry and Mineralogy of Arsenic. Elements, 2, 77 - 83

Ona-Nguema, G., Morin, G., Juillot, F., Calas, G., and Brown, G.E., 2005. EXAFS analysis of arsenite adsorption onto two-line ferrihydrite, hematite, goethite, and lepidocrocite. Environ. Sci. Technol. 39, 9147-9155.

Sahai, N., Lee, Y.J., Xu, H., Ciardelli, M., and Gaillard, J.-F., 2007. Role of Fe(II) and phosphate in arsenic uptake by coprecipitation. Geochim. Cosmochim. Acta 71, 3193-3210.

Schwertmann, U., 1984. The Influence of Aluminum on Iron-Oxides .9. Dissolution of Al-Goethites in 6m Hcl. Clay Miner. 19, 9-19.

Smedley, P.L. and Kinniburgh, D.G., 2002. A review of the source, behaviour and distribution of arsenic in natural waters. Appl.Geochem. 17, 517-568.

Vithanage, M., Senevirathna, W., Chandrajith, R., and Weerasooriya, R., 2007. Arsenic binding mechanisms on natural red earth: A potential substrate for pollution control. Sci. Total Environ. 379, 244-248.

Waychunas, G.A., Rea, B.A., Fuller, C.C., and Davis, J.A., 1993. Surface-Chemistry of Ferrihydrite .1. Exafs Studies of the Geometry of Coprecipitated and Adsorbed Arsenate. Geochim. Cosmochim. Acta 57, 2251-2269.

Wilkie, J.A. and Hering, J.G., 1996. Adsorption of arsenic onto hydrous ferric oxide: Effects of adsorbate/adsorbent ratios and co-occurring solutes. Colloids Surf. a-Physicochem. Eng. Aspects 107, 97-110.

Zachara J.M., Fredrickson, J.K., Smith S.C., Gassman P.L., 2001. Solubilization of Fe(III) oxide-bound trace metals by a dissimilatory Fe(III) reducind bacterium. Geochim. Cosmochim. Acta 65, 75-93.

Zhang, H. and Selim, H.M., 2008. Competitive sorption-desorption kinetics of arsenate and phosphate in soils. Soil Sci. 173, 3-12.

Zobrist, J., Dowdle, P.R., Davis, J.A., and Oremland, R.S., 2000. Mobilization of Arsenite by Dissimilatory Reduction of Adsorbed Arsenate. Environ. Sci. Technol. 34, 4747 - 4753.